Spatio-Temporal and Multisensory Integration

Yoshiyuki Onuki

The research described in this thesis were performed at the Netherlands Institute of Neuroscience, Amsterdam, The Netherlands.

Research in this thesis was supported in part by grant, the Programmes for Excellence “Brain & Cognition: an Integrated Approach” number 433-09-245, from the Netherlands Organization for Scientific Research (NWO).

Cover design: Yoshiyuki Onuki
Word clouds in each chapter were generated by www.wordle.net
Printed by: ProefschriftMaken || www.proefschriftmaken.nl
ISBN: 978-94-6295-889-0

Spatio-Temporal and Multisensory Integration: The relationship between sleep and the cerebellum

Spatio-Temporele en Multisensorische Integratie: de relatie tussen slaap en het cerebellum

Proefschrift

ter verkrijging van de graad van doctor aan de
Erasmus Universiteit Rotterdam
op gezag van de
rector magnificus

Prof.dr. H.A.P. Pols

en volgens besluit van het College voor Promoties.

De openbare verdediging zal plaatsvinden op
woensdag 25 april 2018 om 13.30 uur
door

Yoshiyuki Onuki
geboren te Saitama, Japan

Erasmus University Rotterdam

Promotiecommissie:

Promotor:	**Prof. dr. C.I. De Zeeuw**
	Prof. dr. E.J.W. Van Someren
Overige leden:	**Prof. dr. J. Van der Steen**
	Prof. dr. G. P. Krestin
	Prof. dr. P. Lewis
Copromotor:	**dr. Y.D. Van der Werf**

Contents

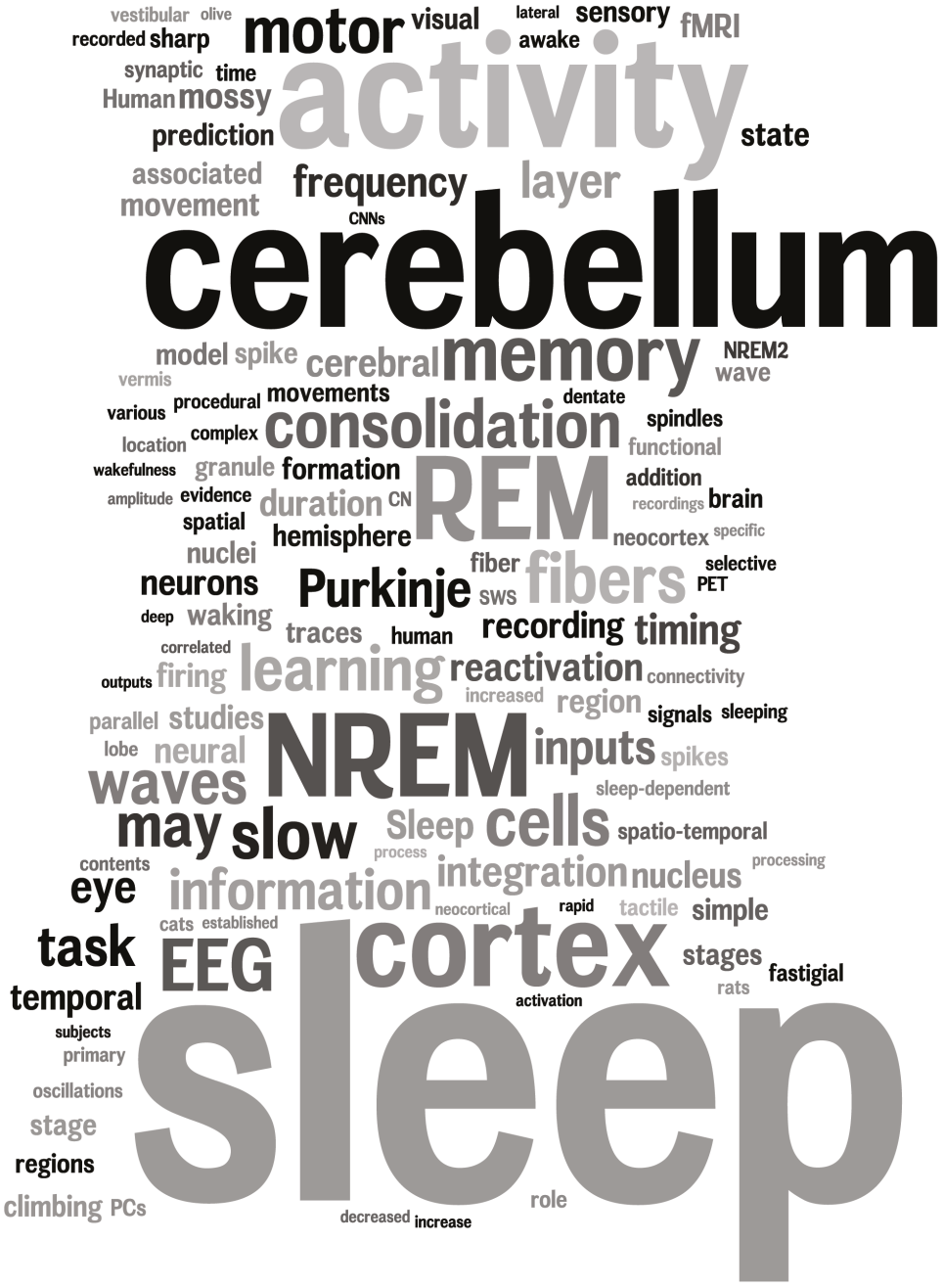
vestibular
olive
motor
visual
lateral
sensory
fMRI
recorded
sharp
awake
synaptic
time
activity
Human
mossy
prediction
state
associated
movement
frequency
layer
CNNs
cerebellum
model
spike
cerebral
memory
NREM2
wave
vermis
various
procedural
movements
dentate
consolidation
spindles
location
complex
functional
wakefulness
granule
formation
REM
addition
amplitude
evidence
duration
CN
recordings
brain
spatial
hemisphere
neocortex
specific
nuclei
fiber
selective
neurons
Purkinje
SWS
fibers
PET
deep
waking
traces
human
recording
timing
correlated
learning
reactivation
outputs
firing
connectivity
increased
region
parallel
studies
signals
sleeping
lobe
neural
NREM
inputs
spikes
waves
sleep-dependent
may
slow
Sleep
cells
spatio-temporal
process
contents
integration
nucleus
processing
eye
information
neocortical
rapid
tactile
simple
cats
established
task
EEG
cortex
stages
fastigial
temporal
rats
activation
subjects
sleep
primary
oscillations
stage
regions
climbing
PCs
role
decreased
increase

Chapter 1. Introduction

Parts of this introduction adapted from Cathrin B. Canto[‡], Yoshiyuki Onuki[‡], Bastiaan Bruinsma, Ysbrand D. Van der Werf[#], and Chris I. De Zeeuw[#]

[‡#] These authors contributed equally.

Published in:
Trends in Neurosciences, 2017
DOI: 10.1016/j.tins.2017.03.001

1.1. Sleep and the cerebellum

1.1.1. General sleep physiology

Sleep is an essential physiological phenomenon for many species[1]. Sleep disturbances are commonly associated with somatic, neuropsychological, and psychiatric symptoms[2–4]. The neuronal circuitries and cellular mechanisms that underlie the transitions between wakefulness and sleep have been investigated thoroughly and have led to models about how state-transitions occur[5,6].

With innovations in the neuroimaging technology for monitoring sleeping brains, sleep states can be categorized based using polysomnography. Polysomnography consists of an electroencephalogram (EEG) for recording the electrical neural activity, an electromyogram (EMG) for recording chin-muscle movements, and an electrooculogram (EOG) for the recording eye movements. Using polysomnography, sleep is classified into non-rapid eye movement (NREM) sleep and rapid eye movement (REM) sleep[7]. Sleep has an approximately 90-minute cycle of alternating NREM sleep and REM sleep. The cycle repeats 4-5 times when sleeping a full night, with NREM sleep dominating in the initial sleep cycles while REM sleep dominates at the later phases[8].

NREM sleep comprises three stages (NREM 1-3, Figure 1A)[7]. NREM stage 1 typically appears at both sleep onset and the beginning of each REM-NREM cycle in the human brain. The EEG characteristics of the NREM1 stage are the diminished 8-13 Hz activity (alpha activity) and the predominantly low amplitude 2-7 Hz activity accompanied by slow eye movement[7]. In addition, high-amplitude waves of 500 milliseconds or less in duration, the vertex sharp waves, appear over the central head region[7]. As sleep deepens to reach NREM stage 2, sleep spindles and the K-complex emerge on the sleep EEG. The sleep spindle is characterized as 11-16 Hz frequency activity of a 500 millisecond or more in duration[7]. It can be categorized into two types based on the frequency, and predominantly observed region: slow (11-13 Hz) spindles over the frontal area, and fast (13-16 Hz) spindles over the centro-parietal area[9,10]. The K-complex

is characterized as the combination of a negative high-amplitude sharp wave of a peak frequency of less than 1 Hz followed by a slower positive amplitude wave, of 500 milliseconds or more in duration[7]. K-complexes are single slow waves occurring typically in NREM2 that start to occur more frequently and continuously in the NREM stage 3. During the deepest sleep stage, NREM stage 3, the slow wave activity dominates the sleep EEG. The slow wave is defined as a 0.5-2 Hz frequency activity with an amplitude of 75 -140 μV; in addition, so-called delta waves with a frequency range from 0.5 to 4 Hz appear in sleep EEG of NREM stage 3[7]. The slow and delta waves are caused by large groups of neurons simultaneously alternating between a hyperpolarized down state in which the neurons are inactive, and a depolarized up-state with irregular neuronal firing that may resemble the waking state. These slow waves appear to be a cortically generated phenomenon, as isolated cerebral cortex still produces slow waves. They can occur in separate cortical areas but may also involve multiple cortical regions simultaneously.

Subsequent to the three stages of NREM sleep, REM sleep appears. The characteristics of REM sleep can be determined with composite criteria based on EEG, EOG, and EMG. In EEG, REM sleep is characterized by noncontinuous theta activity. The frequency is similar to that of wake-like EEG activity, but sawtooth waves sometimes appear. Sawtooth waves are defined as maximum 2-6 Hz frequency serrated activities lasting less than 500-millisecond duration[7,11]. Moreover, the rapid eye movements and minimal muscle tone with inconstant momentary muscle twitches can be observed in EOG and EMG, respectively. Particularly in animal experiments, ponto-geniculo-occipital waves occur, coinciding with the eye movements[12,13]. The ponto-geniculo-occipital (PGO) wave is a prominent sharp wave identified commonly from the pons, lateral geniculate nucleus of the thalamus, and the occipital cortex, across mammalian species from rodents to non-human primates[14–18].

Up to this point, sleep research has mainly focused on how states correlate in the neocortex and subcortical structures, whereas cerebellar activity has been largely

ignored. Cumulative evidence, however, suggests that the cerebellum contributes to the sleep physiology, i.e., the cerebellum is well connected with the neuronal circuitry underlying sleep-wake regulation, and many cerebellar neurons express clock-genes associated with control of the circadian rhythm. Malfunctions of the cerebellum may lead to changes in the sleep-wake cycle[19,20] and even cause sleep disorders[21]. Here, we introduce the anatomy of the cerebellum as background knowledge and also provide the evidence of the cerebellar involvements in the sleep physiology and connectivity between the cerebral cortex and subcortical regions from the perspective of electrophysiology and neuroimaging. Afterward, we present the main theme of this thesis, i.e., sleep's contributions to the consolidation of the cerebellar-dependent integration of spatial and temporal information, and the selective enhancement of learning during subsequent sleep through cerebellar-related multisensory information.

1.1.2. Macro- and microscopical anatomy of the cerebellum

The cerebellum is the brain part located under the cerebral cortex and dorsal to the pons and medulla. The midline of the cerebellum is called "vermis" and the folded lateral structures of the cerebellum are called the "hemispheres". The cerebellum has numerous folds extending sideways and the nomenclature of the human cerebellum (Lobule I-X) can be determined based on the fissures[22]. The deepest fissure slightly anterior to the center of the cerebellum is called the primary fissure where it reaches almost from the deep white matter to the outermost part of the cerebellar hemisphere. When seen in a sagittal plane, the lobule I-V of the vermis and the lobule III-V of the hemisphere are located in the anterior lobe, the region rostral to the primary fissure, while the lobule VI-X at both vermis and hemisphere is located in the posterior lobe, the caudal region to the primary fissure. In addition, the cerebellum body and flocculonodular lobe can be segmented by the posterolateral fissure located on the ventral side of the cerebellum.

The local neural circuit in the cerebellar cortex is uniform, from which it is estimated that the cerebellum performs a similar computational process on inputs of any brain region[23,24]. There are two main types of input fibers directly to the cerebellar cortex, the climbing fibers from the inferior olive and the mossy fibers from mainly the pontine nucleus[25]. The single output fibers from the cerebellar cortex to the cerebellar nucleus are the axons of the Purkinje cells. They are distributed systematically in the three layers of the cerebellar cortex: the granular layer, the Purkinje cell layer, and the molecular layer. The granular layer placed over the cerebellar white matter is the input layer with approximates 100 billion granule cells. Mossy fibers, one of the two major afferent inputs to the cerebellum, terminate in the granular layer and transfer the inputs from the cerebral cortex, brain stem, vestibular nerve, and spinal cord to the granule cells. The Purkinje cell layer, the middle layer among three layers, is the output layer of the cerebellum. In this layer, the Purkinje cells extend dendrites toward the molecular layer to receive two excitatory inputs from the mossy fiber through the parallel fibers of the granule cells and the climbing fibers. The Purkinje cells also receive inhibitory inputs from interneurons (the cerebellar astrocytes and basket cells). The axon of Purkinje cells is the only output fiber of the cerebellum, and it projects on either a cerebellar nucleus or the vestibular nucleus. The outputs of the Purkinje cells are determined based on the balance of the excitatory and inhibitory inputs. The molecular layer, the outermost layer of the three layers, is the layer on which the cerebellar cortex performs information processing. This layer has not only dendrites of Purkinje cells, but also the parallel fibers from the granule cells. Sensory and motor information originates from the cerebral cortex, and the peripheral nerve system transfers the information via the mossy fibers and the climbing fibers. The climbing fibers and mossy fiber - parallel fiber system converge on Purkinje cells and cerebellar nuclei neurons, that form the output of the cerebellar cortex and cerebellum as a whole, respectively. The climbing fibers produce the complex spikes, spike firings with low firing rates (0.5-5 Hz) in Purkinje cells, whereas the mossy fiber inputs through the parallel fibers produce the simple spikes, a spike firing with high frequency (30-120 Hz) in Purkinje cells[25]. The synchronous occurrence of a complex spike and a simple spike induces long-term depression (LTD) in the synapse

between parallel fibers and Purkinje cells whereas continuous simple spikes induce long-term potentiation (LTP)[26]. Both neural mechanisms contribute to cerebellum-related memory formation.

From the viewpoint of the input/output configuration in the cerebellum, the cerebellum can be divided into three regions: vestibulocerebellum (flocculonodular lobe), spinocerebellum (vermis and intermediate parts of the hemisphere), and cerebrocerebellum (the lateral parts of the hemisphere). Vestibulocerebellum receives the vestibular and visual inputs about the position and movement of head and eye and sends the outputs to the vestibular nucleus of the brain stem. The spinocerebellum receives inputs of the somatosensory information such as skin, muscle, and joints from the spinal cord, and transfers the outputs to the ciliary body nucleus and vestibular nucleus of the brain stem for controlling the eye movements, body posture, and locomotion. The cerebrocerebellum receives extensive inputs from the cerebral cortex and mainly project outputs to premotor, motor, and pre-frontal cortex through the thalamus for mediating an effect on motor and cognitive processes.

1.1.3. Sleep-stage dependent cerebellar activity

Cerebellar activity during sleep was already recorded in the early 1970s. This activity does not only reflect the intrinsic activity of its neurons but also the activity of its afferents including the climbing fibers and mossy fibers[25,27,28]. Compared to the awake state, both climbing fibers and mossy fibers in cats show relatively low and high levels of activity during NREM and REM, respectively[27,28], highlighting the existence of sleep-stage dependent cerebellar activity. Human cerebellar local field potentials (LFP) during sleep have also been recorded. The fastigial and dentate nuclei of epileptic patients implanted with electrodes in their cerebellar nuclei region show synchronous spike discharges during NREM and minor sharp potentials during REM activity[29] (Figure 1B). Yet, such invasive recordings of the cerebellum in humans can only be done during and/or after neurosurgery[30–32], while EEG measurements are contaminated with visual cortical and

muscle activity, that are difficult to segregate from cerebellum-related-EEG activity[33]. Furthermore, cerebellar signaling on the basis of EEG and magnetic encephalographic (MEG) data is also difficult to define due to the central location of the cerebellum and solving the inverse problem for estimating the current source of the EEG/MEG signals[34]. New approaches in the neurosciences involve combinations of techniques that will possibly solve the above issues, such as combined analyses of EEG and functional magnetic resonance imaging (fMRI), or positron emission tomography (PET) imaging. Despite the advances in human imaging technologies, animal studies render feasible the simultaneous recording of LFP and units of single neurons at a high spatiotemporal resolution with invasive approaches that are essential to complement human studies and help us to better understand sleep-stage dependent cerebellar activity.

1.1.4. NREM-dependent cerebellar activity

NREM-dependent activity and its characteristics, such as bistability, have also been studied in the second half of the previous century[35]. Extracellular electrophysiological recordings of individual neurons in the cerebellar cortex and cerebellar nuclei have been performed in naturally sleeping macaques and cats. The firing frequency of interpositus and fastigial cerebellar nucleus neurons and Purkinje cells do not show a difference in firing frequeny between wakefulness and superficial NREM (Figure 1C)[36]. During deep NREM3 however, the percentage of short interspike-intervals (< 10 ms) decreased at the cost of that of longer intervals (> 50 ms)[35,37]. Given that baseline simple spike activity of Purkinje cells is determined by intrinsic properties[38], the presence of long interspike-intervals during deep NREM is consistent with prevailing down-states following application of anesthetics[36]. The activity of climbing fibers and/or that of downstream interneurons may promote the alternation between the upstate and downstate of Purkinje cells [39,40]. Since the inferior olive, in turn, may well be modulated by neocortical up- and down-states[41], the cerebral cortex might impose its NREM state upon the cerebellum at least in part via the olive. However, general level setting systems, like the mono-aminergic inputs to the cerebellum, are also likely to contribute.

Given that cerebellar fMRI signals during NREM1 in humans are lower compared to those during wakefulness and that cerebellar fMRI signals largely reflect mossy and parallel fiber activity[42,43], mossy fibers derived from the pons may also contribute to cerebellar NREM sleep stages. Likewise, the results of PET studies indicate decreased cerebellar activity during the transition from pre-sleep wakefulness to slow wave sleep[44–48]. Interestingly, during NREM2 cerebellar fMRI signals can be associated with the occurrence of K-complexes[49] and sleep spindles[9] as measured with EEG from the neocortex, while during NREM3 cerebellar fMRI signals can be associated with slow-waves detected at the neocortex[43] (for details of slow-wave sleep (SWS) in neocortex, see Figure 1A as well as[50]). The level of slow-wave density associated with fMRI BOLD signals in the cerebellum may be positively correlated with its gray matter volume as measured with voxel-based morphometry (VBM)[50,51], providing possible explanations for intersubject variability of sleep EEG features as well as for interlobular differences within the cerebellum of individuals. Indeed, in both fMRI and PET studies, the reported changes in cerebellar activation were mainly localized in the larger lobules IV, V, VI and VII[9,43–46,48,50] (Figure 2).

1.1.5. REM-dependent cerebellar activity

In humans, increased cerebellar activity related to REM has been shown in the cerebellar hemispheres and vermis with the use of PET[44] and fMRI[52,53], highlighting an increase in activity in their mossy fiber - parallel fiber pathways during this sleep stage. In addition, REM-dependent cerebellar activity has been recorded in naturally sleeping cats and macaques. For example, large-amplitude ponto-geniculo-occipital-like waves have been recorded in various cerebellar nuclei during REM with the use of chronically implanted electrodes[54]. Given the increased oculomotor activity during REM, it is not surprising that the simple spike firing frequency of Purkinje cells can increase during this sleep stage compared to wakefulness or NREM sleep[55]. However, not all neurons, neither in the cerebellar cortex nor in the nuclei, show eye movement related activity and not all changes in neuronal or field activity are purely motor-related[54,56] (Figure 1C).

Interestingly, movements as those that occur during REM sleep might promote cerebellar development[57,58]. In the first two postnatal weeks, the firing of Purkinje cells and cerebellar nuclei neurons in rats correlate with their myoclonic twitch activity during active sleep, a form of REM sleep. Rhythmicity of spikes diminishes after postnatal day 8[57], highlighting the possibility that myoclonic twitches during active sleep support synapse maturation during early postnatal development. Taken together, the current data indicate that, in contrast to that during NREM, cerebellar activity increases during REM, and that one or more level setting systems are likely to control the activity of the cerebellar cortex and cerebellar nuclei in a concerted action (Figure 1).

1.1.6. Sleep-stage dependent cortico-cerebellar connectivity

The cerebellum is strongly and reciprocally connected with the cerebral cortex via the thalamus, pons, mesodiencephalic junction and inferior olive, and the reverberating activity in this loop will be heavily subject to the sleep - wake state[59]. For example, at the onset of natural sleep cerebellar nuclei neurons in cats show irregular, long bursts of spikes that are coherent with slow waves in the ventral lateral nuclei of the thalamus[60,61]. Additionally, during anesthesia activity in the inferior olive and that of crus II in the cerebellar cortex of rats reveal LFPs and multi-unit activity that are coherent with slow oscillations in the somatosensory neocortex, and cerebellar up-states and down-states in rats can be associated with an increase and decrease in multi-unit activity in the cerebral cortex, respectively[41]. Direct pharmaceutical and optogenetic manipulation of the activity of cerebellar nuclei neurons in awake mice can modify the oscillatory activity in the cerebral cortex under both physiological and pathological circumstances[31]. Coherence between oscillations and interactions between cerebellum and cerebrum also exists during natural spontaneous behavior and/or sensorimotor tasks in awake mice, rats and monkeys[41,62,63]**.** Still, it remains to be elucidated which parts of the cortico-cerebellar loop provides the most dominant impact on the reverberating activity in the awake state as well as during various sleeping stages. Lesion studies in anesthetized rats suggest that the cerebral cortex has a larger role than the cerebellar

cortex, in that abolishment of neocortical oscillations causes a cessation of cerebellar slow oscillations, whereas bilateral removal of the cerebellar cortex does not significantly alter LFP or multi-unit activity in the neocortex[41]. Connectivity analysis with the use of directed transfer functions in anesthetized rats indicates that the main flow of information during slow oscillations occurs from the neocortex to the cerebellum, with the somatosensory cortex having the strongest influence on cerebellar nuclei activity[64]. These data are in line with the fact that neocortical up-states can inhibit cerebellar nuclei neurons through activation of granule cells and Purkinje cells[64]. Some studies have also addressed the effect of sleep stages on the functional connectivity within the cortico-cerebellar network in human. Whereas during NREM2 the functional connectivity between cerebellum and cerebrum can be either increased or decreased, during NREM3 it is generally decreased[65]. This relation does not only hold for various parts of the neocortex, including somatosensory cortex, motor cortex, insular cortex, supramarginal gyrus, frontal and parietal lobes, but also the thalamus[66,67]. During REM stage, the left cerebellar lobule VI can show a negative correlation with the posterior cingulate cortex, while the right lobules IV and V can show a positive correlation with the thalamus[67], highlighting that cortico-cerebellar connectivity remains functionally intact during sleep but that its relevance depends on the sleep stage and brain region involved.

Together, the findings obtained in animals and humans suggest that the neocortex is able to entrain the cerebellum during slow oscillations, and conversely that the cerebellum may finetune neocortical forms of synchrony. Further pathophysiological studies, multivariate analysis and machine learning techniques may help to elucidate cerebro-cerebellar connectivity during sleep, especially REM sleep[65,68].

1.1.7. Sleep disorders can lead to cerebellar malfunction and vice versa

Patients suffering from primary sleep disorders can show signs of decreased activity in the cerebellum[21,69,70]. Patients with REM sleep behavior disorder (RBD), which generates dream-enacting motor activity during REM, can cause metabolic abnormalities[71–73] and a volumetric decrement in the anterior lobes of the cerebellar cortex as well as in the cerebellar nuclei [72,74]. Vice versa, patients suffering from primary malfunctions of the cerebellum can also have sleep disorders[21,75–79]. For example, patients with spinocerebellar ataxias (SCAs) [75,76,80,81], which are characterized by degeneration of the cerebellum and its afferent and efferent connections, can show increased daytime somnolence as well as NREM and REM-related parasomnias. These data underline that the cerebellum fine-tunes neocortical forms of sleep-related activity. Along the same line, lesions of the cerebellar cortex of the vermis and hemispheres in cats increase the mean duration of NREM and the total duration of REM periods, while decreasing the mean number of sleep periods throughout the sleep-wake cycle[20,82]. Moreover, lesions of the superior peduncle in cats, the sole output pathway of the cerebellum[25], result in a reduced mean duration and total time of NREM and REM sleep, respectively[19]. Thus, sleep disorders and cerebellar pathology are intricately involved with each other, and presumably due to the strong reciprocal projections between cerebellum and cerebral cortex, they co-exist relatively often.

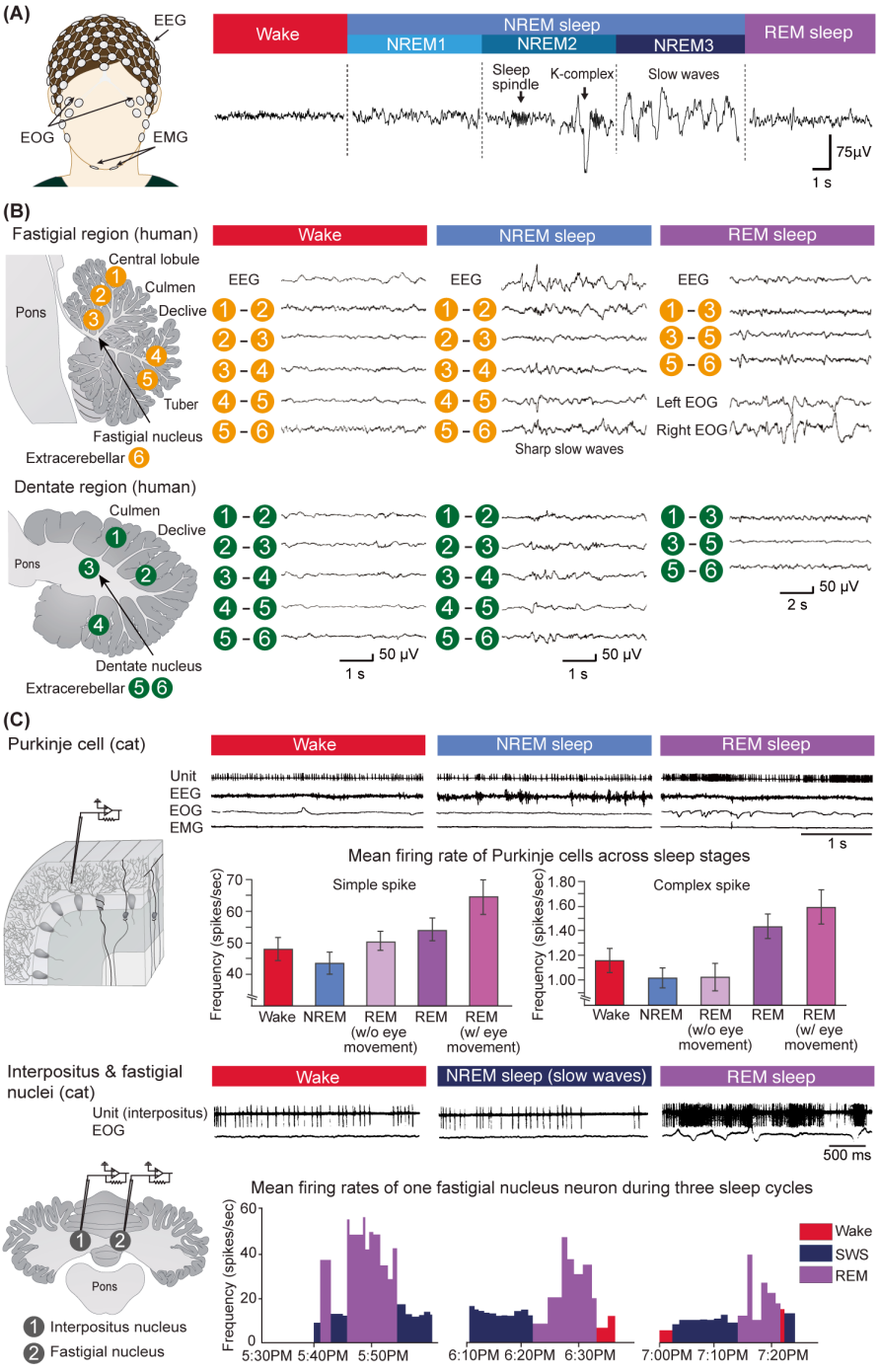
(A)
EEG
EOG
EMG
Wake
NREM sleep
NREM1
NREM2
NREM3
REM sleep
Sleep spindle
K-complex
Slow waves
75μV
1 s
(B)
Fastigial region (human)
Central lobule
Culmen
Declive
Pons
Tuber
Fastigial nucleus
Extracerebellar 6
Wake
NREM sleep
REM sleep
EEG
1 - 2
2 - 3
3 - 4
4 - 5
5 - 6
1 - 3
3 - 5
5 - 6
Left EOG
Right EOG
Sharp slow waves
Dentate region (human)
Culmen
Declive
Pons
Dentate nucleus
Extracerebellar 5 6
50 μV
1 s
2 s
(C)
Purkinje cell (cat)
Unit
EEG
EOG
EMG
Mean firing rate of Purkinje cells across sleep stages
Simple spike
Complex spike
Frequency (spikes/sec)
Wake
NREM
REM (w/o eye movement)
REM
REM (w/ eye movement)
Interpositus & fastigial nuclei (cat)
NREM sleep (slow waves)
Unit (interpositus)
500 ms
Pons
1 Interpositus nucleus
2 Fastigial nucleus
Mean firing rates of one fastigial nucleus neuron during three sleep cycles
Wake
SWS
REM
5:30PM 5:40PM 5:50PM
6:10PM 6:20PM 6:30PM
7:00PM 7:10PM 7:20PM

Figure 1. Human Scalp Electroencephalographic (EEG) Activity, Intracranial Recordings, and Extracellular Recordings of the Human and Cat Cerebellum during Different Sleep Stages. Neurophysiology of wake (red and left traces), nonrapid eye movement (NREM; blue and middle traces), and rapid eye movement (REM; right and purple traces) sleep. (A) Human scalp EEG recordings during waking, NREM1–3, and REM sleep. During waking the EEG is characterized by low-amplitude and high-frequency EEG. NREM sleep can be subdivided into lighter sleep stages NREM1–2 and deep slow-wave sleep (SWS). K-complexes are single slow waves occurring typically in NREM2. Spindles are short bursts of activity at a frequency of 11–16 Hz[7]. More continuous slow waves occur in what is considered deep sleep, NREM3, or SWS[83]. Slow waves are caused by large groups of neurons simultaneously alternating between a hyperpolarized down-state in which the neurons are inactive, and a depolarized up-state with irregular neuronal firing that may resemble the waking state[84]. Theta activity characterizes REM sleep, although not continuously. Particularly in animal experimental studies, striking so-called ponto-geniculo-occipital waves occur, coinciding with the eye movements. Human scalp EEG data were obtained from Eus J.W. van Someren (personal communication). (B) Human cerebellar nuclei show sleep activity during both NREM and REM sleep. (Top traces) Scalp EEG traces recorded during waking and sleep. (Lower traces) Human cerebellar local field potential recordings with the anatomical location of the recording sites drawn left. During NREM sleep, the fastigial trees show sharp slow wave-like activities, whereas the dentate trees show minor sharp slow waves. DuringREMsleep, the fastigial nucleus shows sharp slow waves, while the dentate nucleus shows less sharp slow waves. For the recordings of both the fastigial and dentate regions, each number denotes the location of the electrodes. Fastigial region: 1, rostral portion of central lobulus; 2, caudal (lower) portion of central lobulus; 3, culmen (5.5 mm dorsal to fastigial nucleus); 4, medullary substance between declive and tuber; 5, tuber; and 6, extracerebellar territory. Dentate region: 1, culmen; 2, declive; 3, dentate nucleus; 4, paramedian portion of biventer; 5 and 6, extra- cerebellar adjacent regions. The locations of the circles represent the locations of electrodes; as the authors did not specify the exact location or hemisphere of recording, this is an approximate location. The scales of the intracranialEEGused in the dentate region follow those in the fastigial region. Scalp EEG and intracranial recording images were adapted with permission from[29]. (C). Cat Purkinje cell and cerebellar nuclei neuron activity during waking and sleep. (Left) The recording locations. (Upper graphs) Cat Purkinje cell activity. To classify waking and sleep stages, the EEG, electro- oculogram (EOG), and electromyogram (EMG) are displayed together with the unit activity of simple and complex spikes of an extracellularly recorded Purkinje cell[55]. Below the traces, the histograms of the mean (± standard error of the mean) simple and complex spike firing rates of cat Purkinje cells (N = 39) under five behavioral conditions are presented (wake, NREM, REM without (w/o) eye movement, REM, and REM with (w/) eye movement). Spike frequency decreases slightly during NREM, while it increases during REM sleep. (Bottom traces and histograms) In addition, cat cerebellar nuclei neurons [interpositus (upper traces) and fastigial nuclei (bottom histograms)] show an increase in firing frequency during REM sleep. Each histogram bin represents the time of occurrence of successive groups of 500 interspike intervals. The image of the cat cerebellum and the extracellular recording results were adapted with permission from[55,56,85].

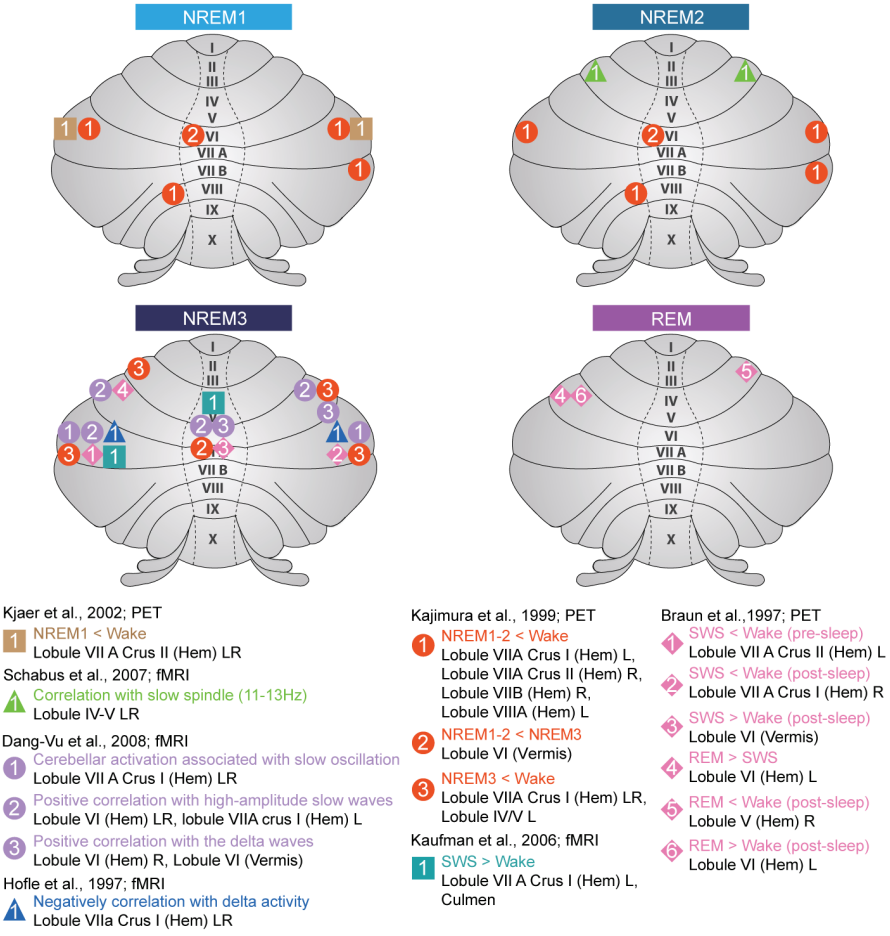

Figure 2. Human cerebellar activation map during various sleep stages (Stage NREM 1, NREM 2, NREM 3, and REM) based on PET and EEG-fMRI studies. Changes in cerebellar activation during NREM1 (light blue), NREM2 (blue), NREM3 (dark blue), and REM (purple). Changes in cerebellar activation have been mainly localized in the larger lobules IV, V, VI, and VII. The cerebellar label is redefined by a probabilistic atlas of the human cerebellum[86], referring to either Montreal Neurological Institute (MNI) or Talairach coordinations reported in[9,43–46,48,50]. Neither MNI nor Talairach coordinations in cerebellar regions are available in[47,49]. For display purposes, the locations of the circle labels do not correspond to the reported MNI or Talairach coordinates. If the awake period before and after sleep periods was analyzed and reported separately in an article, the additional labels, 'pre-sleep' and 'post-sleep', are mentioned after the term 'wake'. The recording modality (fMRI and PET) is mentioned after the reference. EEG, electroencephalographic; fMRI, functional magnetic resonance imaging; Hem, hemisphere; L, left hemisphere; NREM, nonrapid eyemovement; PET, positron emission tomography; R, right hemisphere; REM, rapid eye movement.

1.2. Sleep, the cerebellum, and cognition

1.2.1. Sleep's beneficial effects on cerebellum-dependent memory consolidation

Cumulative research evidence described above indicates that the cerebellum is associated with sleep physiology. Sleep also has an important role in the support of our cognitive processes such as memory retrieval, learning, attention, language-processing, decision-making, and even creativity[87,88]. The cerebellum has been known participate in procedural memory formation, e.g., malfunction of the cerebellum impairs the motor memory formation[25,26,89]. Procedural memory formation, which is known to be controlled at least in part by the cerebellum, is facilitated by sleep[90–96]. Sleep improves the speed of tapping by 10-20% in sleep-dependent sequence learning tasks, such as the sequence finger-tapping task and serial reaction time task[92]. The gain in performance of the finger-to-thumb opposition task can be correlated with the amplitude of sleep spindles and depth of REM sleep[97], while a reduction in sleep spindle duration as occurs during aging cannot only be associated with a decrease in gray matter volume of the cerebellum, but also with deficits in consolidation of motor memories[98]. The parts of the cerebellum that are activated during the execution of a serial reaction time task during wakefulness are significantly more active during the REM sleep in subjects previously trained on the task than in non-trained subjects[99–101].

How sleep promotes consolidation of cerebellum-dependent memories remains to be revealed. One of the interesting options is that new collaterals from mossy fibers, climbing fibers and/or nucleocortical afferents sprout in the cerebellar nuclei and cortex overnight and form massive new connections following procedural learning[89,102,103]. This could also explain why cerebellar learning may at first largely depend on rapid plasticity in the cerebellar cortex, and subsequently, as the memory stabilizes, on more gradual plasticity in the cerebellar and vestibular nuclei, downstream[104–108]. The role of sleep in consolidation of cerebellar memory formation is also supported by the precise sequence

of changes that occur over the course of long-term skill learning. For example, Fogel and colleagues showed that on the night that human subjects are first exposed to a procedural task, the density of fast spindles increases significantly during both NREM2 and SWS, whereas on the night that the subjects become experts, they show increased REM sleep duration while the spindles become larger in terms of amplitude and duration during SWS[109]. Re-exposure to the task one week later results in increased NREM sleep duration, and again, increased spindle density of fast spindles during SWS and NREM2, which can be correlated with overnight improvement in speed and precision of the task, highlighting putative cerebellar involvement. Interestingly, re-exposure to the actual task in the awake state may not even be required for enhancing consolidation.

To explain the underlying neural mechanisms for memory consolidation during sleep, there are two dominant explanatory models in the sleep research field: the reactivation and synaptic homeostasis model. The reactivation model proposes that the reactivation of learning-related neural patterns in sleep strengthens the neural network of acquired memory prior to sleep[110,111]. Both hippocampal place-cells and cells in the primary visual cortex V1 in rodents reactivate a sequential pattern of the learned route of a maze task during NREM sleep[112,113]. This pattern, which is especially prominent during SWS, is temporally compressed and accompanied by sharp-wave ripples. Such reactivations during NREM may even induce the formation of postsynaptic dendritic spines in pyramidal cells, highlighting structural phenomena that may provide a substrate for consolidation[114]. Importantly, although Yang et al show reduced synapse formation after sleep disturbance, the data do not exclude the possibility that improvement was driven by sleep facilitating intrasession learning or offline consolidation[115]: spine formation may also be related to bouts of waking. Nagai and colleagues used the same task and showed that improvement followed both sleep and sleep deprivation.

The synaptic homeostasis model states that the synaptic strengths saturated during cognitive processing are 'sheared off' during sleep, especially SWS, leaving task-relevant

synaptic connections intact and freeing up capacity for subsequent learning[116–118]. Reports in rodents and Drosophila support the possibility that net synaptic strength is increased during waking and decreased during SWS[119,120]. For example, the expression level of synaptic proteins is high in the awake state and low during sleep[121]. In the synaptic homeostasis model, the sleep-dependent consolidation is seen more or less as a 'by-product', as the preservation of task-relevant synapses and the removal of spurious synapses generates a neural representation with a higher signal-to-noise ratio[118].

Theoretical models developed to explain cerebellum-dependent learning have largely focused on the '**internal model**'[122,123]. This model describes a neural process estimating the future states of the motor system through the interpretation of the external sensory inputs at present ('forward model'), and allows this estimate in turn to be used to provide the commands to the motor system to shift the present state to the objected state ('inverse model'). Although sleep researchers have inferred that the underlying mechanism of sleep might help the development of an internal model[93,124], there is little direct evidence to support it. Recently, a theoretical model that integrates the reactivation model with cerebellar internal, forward and inverse, models has been proposed to optimize consolidation during sleep[125].

Sleep-dependent and cerebellum-related learning tasks often target smooth motor executions. Motor performance consisting of successive movements requires motor timing with prediction based on the integration of visual events (spatial information) and motor timing (temporal information)[126]. Indeed, the cerebellum is known to control temporal information processing on the time scale of tens of milliseconds to hundreds of milliseconds and is also involved in motor and perceptual tasks on the same time scale. However, little has been reported on the role of sleep in the consolidation of spatial-temporal integration. Sleep deprivation affects the acquisition of classical eyeblink conditioning[127], in which cerebellar LTD plays a role in the formation of the learning-dependent timing, rather than the formation of motor memory[128,129]. In addition, sleep deprivation affects the functional connectivity between the lateral

cerebellar nuclei and the neocortical superior temporal sulcus following learning of pursuit and rotation mouse tracking tasks[130]. Furthermore, the subsequent level of post-sleep activity in the cerebellar cortex correlated with the consolidation of the auditory-paced rhythmic motor learning while post-sleep hippocampal activity was related to the consolidation of temporal discrimination learning[131]. Indeed, the cerebellum is also involved in cognitive tasks on a time scale of several seconds to several tens of seconds in cooperation with other brain regions such as the frontal lobe and basal ganglia[132–134].

To test the hypothesis that the cerebellum invovles in the establishment of the spatio-temporal timing with possible collaboration of other subcortical area, **Chapter 2** investigates the functional interaction between these regions during spatiotemporal prediction, using a novel motor timing task and the functional magnetic resonance imaging. **Chapter 3** tests the hypothesis that the responsible region to establish cerebellar-hippocampal spatio-temporal prediction is the cerebellum by assigning the same motor timing task and neuropsychological assessments to patient with spinocerebellar ataxia type 6. To investigate a possible role of sleep in the integration of the spatial and temporal information, especially, timing of perceptual events, **Chapter 4** examines the hypothesis that sleep can facilitate sequential motor learning, on the basis of spatio-temporal prediction, using the same motor timing behavioral task in **Chapter 2 and 3**.

1.2.2. Establishing the contents of memory during sleep

Sleep may not only promote consolidation of procedural memories formed during the day, but it might even have impact on the first acquisition of very new memories and the selective enhancement of memory contents. Fifer and colleagues showed that new associative reflexes like conditioned eyeblink responses could be readily acquired in infants while sleeping[135]. It remains to be elucidated to what extent the putative up- and downstates of cerebellar neurons at the various sleeping stages directly affect

acquisition and consolidation of procedural memories[36], but the positive correlations provided above highlight the probability that sleep has an advantageous impact on both motor and cognitive forms of implicit learning, several of which may be mediated by the cerebellum.

A neural mechanism to stabilize our memory is through repetitive neural representations of experiences. A promising theoretical mechanism to induce the sleep-dependent memory consolidation is the reactivation phenomenon, described above. This phenomenon occurs spontaneously and uncontrollably, and it was thought to be difficult to direct reactivation to specific target memory contents. In recent years, however, sleep researchers have made a breakthrough to strengthen memory contents selectively, using so-called 'targeted memory reactivation'. Their experimental paradigms adopt the association learning to connect task contents with unrelated sensory cues such as odor or sound; and subsequently present these task-related sensory stimuli during sleep to artificially induce reactivation of the target-memory[136]. One study has shown, for instance, that selective reinforcement may occur in procedural memory upon such stimulus-driven reactivation[137]. In this experiment, subjects were trained to learn sequential finger movements that corresponded to the sequence of sounds. After letting the subjects learn three kinds of finger movement sequences and then presenting one of the learned sound sequences during sleep, they succeeded in improving the performance of specific finger movements. The approach proved so powerful that it was possible to enhance selective contents of declarative[136,138,139] and nondeclarative memory[137] and even beyond the memory consolidation such as the implicit elimination of sexual and racial discrimination[140]. As more direct evidence of the neural reactivation during human sleep, Van Dongen and colleagues initiated this reactivation process for specific memories on object - sound - location associations during slow-wave sleep and showed that post-sleep memory precision was positively correlated with sound-related fMRI signals during sleep in the thalamus, medial temporal lobe, and cerebellum[141].

All these targeted memory reactivation approaches focus on hippocampal-dependent learning during sleep, and only attempt to strengthen associations that were already established before sleep. It has, however, never been show that novel associations can be established during sleep.

The mammalian brain and particularly the cerebellum is exquisitely suited to integrate sensory information such as vision and tactile stimuli. A classical computational approach of the cerebellar information theory proposes that the granule cells that receive convergent multisensory inputs can generate outputs as synthesized sensory information only when multiple sensory signals were entered into the granule cells in a specific combination[142,143]. This perspective is supported by the recent studies of both in-vitro mapping and in-vivo patch-clamp recording to the granule cells in vivo[144,145]. We here wondered whether the sleep-dependent reactivation offered a window for such integration by timing it to stimuli of a different sensory modality.

Such multisensory integration that the cerebellum highly associated with was not attempted for the sleep-dependent selective enhancement of memory consolidation. **Chapter 5** assesses the hypothesis that cross-modal integration of visual and tactile information during sleep enhances visual motion learning by presenting directional tactile motion stimulation during sleep.

1.3. Scope of this thesis

Aiming at bridging a gap between sleep and cerebellum from the standpoint of cognitive functions, this thesis focuses on sleep's contributions to cerebellum-dependent spatio-temporal integration and cerebellum-related multisensory integration during sleep.

To investigate possible sleep-dependent cerebellar consolidation of the spatio-temporal integration, we first needed a cerebellar task; the cerebellum is reported to play a role in

spatial and temporal processing, especially when timing requirements are highly precise and spatial and temporal aspects need to be integrated. We therefore constructed a novel MRI-compatible task incorporating such demands in **Chapter 2** to allow us to investigate the underlying mechanism of the spatio-temporal prediction timing.

To obtain causal, rather than observational evidence for a cerebellar contribution to spatio-temporal prediction timing, **Chapter 3** compared the predictive and reactive behavioral properties in patients with spinocerebellar ataxia type 6, using the same behavioral task in **Chapter 2**. Finally, **Chapter 4** evaluated whether the spatial-temporal prediction timing for which the cerebellum is responsible can be enhanced through sleep.

Our next aim was to see if multisensory integration needs to be established before sleep in order to be strengthened, or whether the integration can in fact be established during sleep itself. In addition to the temporal processing, the cerebellum is known to involve in a cross-modal transfer between sensory information such as vision, auditory, and tactile. Indeed, tactile and visual information have similar spatial properties such as the occurrence of apparent motion[146] and can interacted to induce a conscious perception such as the motion after effect[147]. It is, however, not clear whether such multimodal interactive processes can be established during sleep. We therefore employed a targeted stimulus presentation procedure, not for reactivating an existing integrated memory, but aimed at actually initiating the integration during sleep: **Chapter 5** investigates a possible biasing effect by administering tactile inputs during the ongoing consolidation process of visual learning. Using a novel brain-computer interface to induce the specific spatial features of tactile stimulation during slow wave sleep, we demonstrate that we are able to direct visual perceptual learning in a directionally selective manner. Summarizing research findings in the proceeding chapters, i.e., the cerebellar interaction with the hippocampus during the spatial-temporal prediction, the cerebellar roles on various forms of the temporal prediction, the sleep dependency of the cerebellar-dependent learning, and the cross-modal effects of cerebellar-associated

sensory inputs on the memory consolidation process during sleep, **Chapter 6** discusses the perspectives of both sleep and cerebellum research agendas.

References

1. Cirelli, C. & Tononi, G. Is sleep essential? *PLoS Biology* **6,** 1605–1611 (2008).
2. Zhang, J. *et al.* Insomnia, sleep quality, pain, and somatic symptoms: Sex differences and shared genetic components. *Pain* **153,** 666–673 (2012).
3. Fortier-Brochu, É. & Morin, C. M. Cognitive Impairment in Individuals with Insomnia: Clinical Significance and Correlates. *Sleep* **37,** 1787–1798 (2014).
4. Ford, D. E. & Kamerow, D. B. Epidemiologic study of sleep disturbances and psychiatric disorders. An opportunity for prevention? *JAMA* **262,** 1479–84 (1989).
5. Saper, C. B., Fuller, P. M., Pedersen, N. P., Lu, J. & Scammell, T. E. Sleep State Switching. *Neuron* **68,** 1023–1042 (2010).
6. Brown, R. E., Basheer, R., McKenna, J. T., Strecker, R. E. & McCarley, R. W. Control of Sleep and Wakefulness. *Physiol. Rev.* **92,** 1087–1187 (2012).
7. Iber, C., Ancoli-Israel, S., Chesson, A. & Quan, S. *The AASM Manual for the Scoring of Sleep and Associates Events: Rules, Terminology and Technical Specifications*. *American Academy of Sleep Medicine* (American Academy of Sleep Medicine, 2007). doi:10.1002/ejoc.201200111
8. Dement, W. & Kleitman, N. Cyclic variations in EEG during sleep and their relation to eye movements, body motility, and dreaming. *Electroencephalogr. Clin. Neurophysiol.* **9,** 673–690 (1957).
9. Schabus, M. *et al.* Hemodynamic cerebral correlates of sleep spindles during human non-rapid eye movement sleep. *Proc. Natl. Acad. Sci. U. S. A.* **104,** 13164–13169 (2007).
10. Andrillon, T. *et al.* Sleep Spindles in Humans: Insights from Intracranial EEG and Unit Recordings. *J. Neurosci.* **31,** 17821–17834 (2011).
11. Pearl, P. L. *et al.* Sawtooth wave density analysis during REM sleep in normal volunteers. *Sleep Med.* **3,** 255–258 (2002).
12. Datta, S. & Hobson, J. A. Neuronal activity in the caudolateral peribrachial pons: relationship to PGO waves and rapid eye movements. *J. Neurophysiol* **71,** 95–109 (1994).
13. Gott, J. A., Liley, D. T. J. & Hobson, J. A. Towards a Functional Understanding of PGO Waves. *Front. Hum. Neurosci.* **11,** (2017).
14. Jouvet, M. & Michel, F. Electromyographic correlations of sleep in the chronic decorticate & mesencephalic cat. *C. R. Seances Soc. Biol. Fil.* **153,** 422–5 (1959).
15. Brooks, D. C. & Bizzi, E. Brain stem electrical activity during deep sleep. *Arch. Ital. Biol.* **101,** 648–665 (1963).
16. Mouret, J., Jeannerod, M. & Jouvet, M. Electrical activity of the visual system during the paradoxical phase of sleep in the cat. *J. Physiol. (Paris).* **55,** 305–6 (1963).
17. Vuillon-Cacciuttolo, G. & Seri, B. Effects of optic nerve section in baboons on the geniculate and cortical spike activity during various states of vigilance. *Electroencephalogr.Clin.Neurophysiol.* **44,** 754–768 (1978).
18. Kaufman, L. S. & Morrison, A. R. Spontaneous and elicited PGO spikes in rats. *Brain Res.* **214,** 61–72 (1981).
19. Cunchillos, J. . & De Andrés, I. Participation of the cerebellum in the regulation of the sleep-wakefulness cycle. Results in cerebellectomized cats. *Electroencephalogr. Clin. Neurophysiol.* **53,** 549–558 (1982).
20. de Andrés, I., Garzón, M. & Reinoso-Suárez, F. Functional Anatomy of Non-REM Sleep. *Front. Neurol.* **2,** 70 (2011).
21. DelRosso, L. M. & Hoque, R. The cerebellum and sleep. *Neurol. Clin.* **32,** 893–900 (2014).
22. Schmahmann, J. D. *et al.* Three-dimensional MRI atlas of the human cerebellum in proportional stereotaxic space. *Neuroimage* **10,** 233–260 (1999).
23. Voogd, J. & Glickstein, M. The anatomy of the cerebellum. *Trends Neurosci.* **21,** 370–5 (1998).
24. Kandel, E. R., Schwartz, J. H., Jessell, T. M., Siegelbaum, S. A. & Hudspeth, A. J. *Principles of Neural Science, Fifth Edition*. *The McGraw-Hill Companies, Inc.* (2013).
25. De Zeeuw, C. I. *et al.* Spatiotemporal firing patterns in the cerebellum. *Nat. Rev. Neurosci.* **12,** 327–344 (2011).
26. Gao, Z., Beugen, B. J. van & Zeeuw, C. I. De. Distributed synergistic plasticity and cerebellar learning. *Nat. Rev. Neurosci.* **13,** 619–635 (2012).

27. Marchesi, G. F. & Strata, P. Climbing fibers of cat cerebellum: modulation of activity during sleep. *Brain Res.* **17,** 145–148 (1970).
28. Marchesi, G. F. & Strata, P. Mossy and climbing fiber activity during phasic and tonic phenomena of sleep. *Pflügers Arch. Eur. J. Physiol.* **323,** 219–240 (1971).
29. Niedermeyer, E. & Uematsu, S. Electroencephalographic recordings from deep cerebellar structures in patients with uncontrolled epileptic seizures. *Electroencephalogr. Clin. Neurophysiol.* **37,** 355–365 (1974).
30. Teixeira, M. J. *et al.* Deep brain stimulation of the dentate nucleus improves cerebellar ataxia after cerebellar stroke. *Neurology* **85,** 2075–2076 (2015).
31. Kros, L., Rooda, O. H. J. E., Zeeuw, C. I. De & Hoebeek, F. E. Controlling Cerebellar Output to Treat Refractory Epilepsy. *Trends Neurosci.* **38,** 787–799 (2015).
32. Dalal, S. S., Osipova, D., Bertrand, O. & Jerbi, K. Oscillatory activity of the human cerebellum: The intracranial electrocerebellogram revisited. *Neurosci. Biobehav. Rev.* **37,** 585–593 (2013).
33. Muthukumaraswamy, S. D. High-frequency brain activity and muscle artifacts in MEG/EEG: a review and recommendations. *Front. Hum. Neurosci.* **7,** 138 (2013).
34. Grech, R. *et al.* Review on solving the inverse problem in EEG source analysis. *J Neuroeng Rehabil* **5,** 25 (2008).
35. Mano, N. Changes of simple and complex spike activity of cerebellar purkinje cells with sleep and waking. *Science (80-.).* **170,** 1325–7 (1970).
36. Schonewille, M. *et al.* Purkinje cells in awake behaving animals operate at the upstate membrane potential. *Nat. Neurosci.* **9,** 459–461 (2006).
37. McCarley, R. W. & Hobson, J. a. Simple spike firing patterns of cat cerebellar Purkinje cells in sleep and waking. *Electroencephalogr. Clin. Neurophysiol.* **33,** 471–483 (1972).
38. Zhou, H. *et al.* Cerebellar modules operate at different frequencies. *Elife* **2014,** 1–18 (2014).
39. Oldfield, C. S., Marty, A. & Stell, B. M. Interneurons of the cerebellar cortex toggle Purkinje cells between up and down states. *Proc. Natl. Acad. Sci. U. S. A.* **107,** 13153–8 (2010).
40. Loewenstein, Y. *et al.* Bistability of cerebellar Purkinje cells modulated by sensory stimulation. *Nat. Neurosci.* **8,** 202–11 (2005).
41. Ros, H., Sachdev, R. N. S., Yu, Y., Sestan, N. & McCormick, D. A. Neocortical networks entrain neuronal circuits in cerebellar cortex. *J. Neurosci.* **29,** 10309–20 (2009).
42. Diedrichsen, J., Verstynen, T., Schlerf, J. & Wiestler, T. Advances in functional imaging of the human cerebellum. *Curr. Opin. Neurol.* **23,** 382–387 (2010).
43. Kaufmann, C. *et al.* Brain activation and hypothalamic functional connectivity during human non-rapid eye movement sleep: An EEG/fMRI study. *Brain* **129,** 655–667 (2006).
44. Braun, A. Regional cerebral blood flow throughout the sleep-wake cycle. An H2(15)O PET study. *Brain* **120,** 1173–97 (1997).
45. Kajimura, N. *et al.* Activity of midbrain reticular formation and neocortex during the progression of human non-rapid eye movement sleep. *J. Neurosci.* **19,** 10065–73 (1999).
46. Hofle, N. *et al.* Regional cerebral blood flow changes as a function of delta and spindle activity during slow wave sleep in humans. *J. Neurosci.* **17,** 4800–4808 (1997).
47. Hiroki, M. Cerebral white matter blood flow is constant during human non-rapid eye movement sleep: a positron emission tomographic study. *J. Appl. Physiol.* **98,** 1846–1854 (2005).
48. Kjaer, T. W., Law, I., Wiltschiøtz, G., Paulson, O. B. & Madsen, P. L. Regional cerebral blood flow during light sleep--a H(2)(15)O-PET study. *J. Sleep Res.* **11,** 201–7 (2002).
49. Jahnke, K. *et al.* To wake or not to wake? The two-sided nature of the human K-complex. *Neuroimage* **59,** 1631–1638 (2012).
50. Dang-Vu, T. T. *et al.* Spontaneous neural activity during human slow wave sleep. *Proc. Natl. Acad. Sci. U. S. A.* **105,** 15160–15165 (2008).
51. Saletin, J. M., van der Helm, E. & Walker, M. P. Structural brain correlates of human sleep oscillations. *Neuroimage* **83,** 658–668 (2013).
52. Hong, C. C.-H. *et al.* fMRI evidence for multisensory recruitment associated with rapid eye movements during sleep. *Hum. Brain Mapp.* **30,** 1705–22 (2009).
53. Miyauchi, S., Misaki, M., Kan, S., Fukunaga, T. & Koike, T. Human brain activity time-locked to rapid eye movements during REM sleep. *Exp. Brain Res.* **192,** 657–667 (2009).
54. Velluti, R., Yamuy, J., Hadjez, J. & Monti, J. M. Spontaneous cerebellar nuclei PGO-like waves in natural paradoxical sleep and under reserpine. *Electroencephalogr. Clin. Neurophysiol.* **60,** 243–248 (1985).

55. Hobson, J. a & McCarley, R. W. Spontaneous discharge rates of cat cerebellar Purkinje cells in sleep and waking. *Electroencephalogr. Clin. Neurophysiol.* **33,** 457–469 (1972).
56. Palmer, C. Interpositus and fastigial unit activity during sleep and waking in the cat. *Electroencephalogr. Clin. Neurophysiol.* **46,** 357–70 (1979).
57. Sokoloff, G., Plumeau, A. M., Mukherjee, D. & Blumberg, M. S. Twitch-related and rhythmic activation of the developing cerebellar cortex. *J. Neurophysiol.* **114,** 1746–1756 (2015).
58. Del Rio-Bermudez, C., Plumeau, A. M., Sattler, N. J., Sokoloff, G. & Blumberg, M. S. Spontaneous activity and functional connectivity in the developing cerebellorubral system. *J. Neurophysiol.* **116,** 1316–27 (2016).
59. De Zeeuw, C. I., Hoebeek, F. E. & Schonewille, M. Causes and Consequences of Oscillations in the Cerebellar Cortex. *Neuron* **58,** 655–658 (2008).
60. Steriade, M., Apostol, V. & Oakson, G. Clustered firing in the cerebello-thalamic pathway during synchronized sleep. *Brain Res.* **26,** 425–432 (1971).
61. Steriade, M., Apostol, V. & Oakson, G. Control of unitary activities in cerebellothalamic pathway during wakefulness and synchronized sleep. *J. Neurophysiol.* **34,** 389–413 (1971).
62. Soteropoulos, D. S. & Baker, S. N. Cortico-cerebellar coherence during a precision grip task in the monkey. *J. Neurophysiol.* **95,** 1194–206 (2006).
63. Popa, D. *et al.* Functional role of the cerebellum in gamma-band synchronization of the sensory and motor cortices. *J. Neurosci.* **33,** 6552–6 (2013).
64. Rowland, N. C., Goldberg, J. A. & Jaeger, D. Cortico-cerebellar coherence and causal connectivity during slow-wave activity. *Neuroscience* **166,** 698–711 (2010).
65. Tagliazucchi, E. & Laufs, H. Decoding Wakefulness Levels from Typical fMRI Resting-State Data Reveals Reliable Drifts between Wakefulness and Sleep. *Neuron* **82,** 695–708 (2014).
66. Tagliazucchi, E. *et al.* Large-scale brain functional modularity is reflected in slow electroencephalographic rhythms across the human non-rapid eye movement sleep cycle. *Neuroimage* **70,** 327–339 (2013).
67. Chow, H. M. *et al.* Rhythmic alternating patterns of brain activity distinguish rapid eye movement sleep from other states of consciousness. *Proc. Natl. Acad. Sci. U. S. A.* **110,** 10300–5 (2013).
68. Altmann, A. *et al.* Validation of non-REM sleep stage decoding from resting state fMRI using linear support vector machines. *Neuroimage* **125,** 544–555 (2016).
69. Joo, E. Y. *et al.* Brain Gray Matter Deficits in Patients with Chronic Primary Insomnia. *Sleep* **36,** 999–1007 (2013).
70. Desseilles, M. *et al.* Neuroimaging insights into the pathophysiology of sleep disorders. *Sleep* **31,** 777–794 (2008).
71. Wu, P. *et al.* Consistent abnormalities in metabolic network activity in idiopathic rapid eye movement sleep behaviour disorder. *Brain* **137,** 3122–3128 (2014).
72. Hanyu, H. *et al.* Voxel-based magnetic resonance imaging study of structural brain changes in patients with idiopathic REM sleep behavior disorder. *Parkinsonism Relat. Disord.* **18,** 136–139 (2012).
73. Holtbernd, F. *et al.* Abnormal metabolic network activity in REM sleep behavior disorder. *Neurology* **82,** 620–7 (2014).
74. Boucetta, S. *et al.* Structural Brain Alterations Associated with Rapid Eye Movement Sleep Behavior Disorder in Parkinson's Disease. *Sci. Rep.* **6,** 26782 (2016).
75. Pedroso, J. L. *et al.* Sleep disorders in machado-joseph disease: frequency, discriminative thresholds, predictive values, and correlation with ataxia-related motor and non-motor features. *Cerebellum* **10,** 291–5 (2011).
76. Pedroso, J. L. *et al.* Sleep disorders in cerebellar ataxias. *Arq. Neuropsiquiatr.* **69,** 253–257 (2011).
77. Mehta, L. R. *et al.* Sporadic fatal insomnia masquerading as a paraneoplastic cerebellar syndrome. *Arch. Neurol.* **65,** 971–3 (2008).
78. Sonni, A., Kurdziel, L. B. F., Baran, B. & Spencer, R. M. C. The effects of sleep dysfunction on cognition, affect, and quality of life in individuals with cerebellar ataxia. *J. Clin. Sleep Med.* **10,** 535–43 (2014).
79. Garrido Zinn, C. *et al.* Major neurotransmitter systems in dorsal hippocampus and basolateral amygdala control social recognition memory. *Proc. Natl. Acad. Sci.* **113,** E4914–E4919 (2016).
80. Silva, G. M. F. *et al.* NREM-related parasomnias in Machado-Joseph disease: Clinical and polysomnographic evaluation. *J. Sleep Res.* **25,** 11–15 (2016).
81. Martinez, A. R. M. *et al.* Fatigue and Its Associated Factors in Spinocerebellar Ataxia Type 3/Machado-Joseph Disease. *Cerebellum* **16,** 118–121 (2017).

82. De Andres, I. & Reinoso-Suarez, F. Participation of the cerebellum in the regulation of the sleep-wakefulness cycle through the superior cerebellar peduncle. *Arch. Ital. Biol.* **117,** 140–163 (1979).
83. Riedner, B. A., Hulse, B. K., Murphy, M. J., Ferrarelli, F. & Tononi, G. Temporal dynamics of cortical sources underlying spontaneous and peripherally evoked slow waves. *Prog. Brain Res.* **193,** 201–18 (2011).
84. Steriade, M., Nuñez, A. & Amzica, F. A novel slow (< 1 Hz) oscillation of neocortical neurons in vivo: depolarizing and hyperpolarizing components. *J. Neurosci.* **13,** 3252–65 (1993).
85. Gray-edwards, H. L. *et al.* High resolution MRI anatomy of the cat brain at 3 Tesla. **227,** 10–17 (2014).
86. Diedrichsen, J., Balsters, J. H., Flavell, J., Cussans, E. & Ramnani, N. A probabilistic MR atlas of the human cerebellum. *Neuroimage* **46,** 39–46 (2009).
87. Diekelmann, S. & Born, J. The memory function of sleep. *Nat. Rev. Neurosci.* **11,** 114–26 (2010).
88. Diekelmann, S. Sleep for cognitive enhancement. *Front. Syst. Neurosci.* **8,** 46 (2014).
89. Krakauer, J. W. & Shadmehr, R. Consolidation of motor memory. *Trends Neurosci.* **29,** 58–64 (2006).
90. Diekelmann, S. & Born, J. The memory function of sleep. *Nat Rev Neurosci* **11,** 114–126 (2010).
91. Grube, M., Cooper, F. E., Chinnery, P. F. & Griffiths, T. D. Dissociation of duration-based and beat-based auditory timing in cerebellar degeneration. *Proc. Natl. Acad. Sci. U. S. A.* **107,** 11597–11601 (2010).
92. Walker, M. P., Brakefield, T., Morgan, A., Hobson, J. A. & Stickgold, R. Practice with sleep makes perfect: Sleep-dependent motor skill learning. *Neuron* **35,** 205–211 (2002).
93. Debas, K. *et al.* Brain plasticity related to the consolidation of motor sequence learning and motor adaptation. *Proc. Natl. Acad. Sci. U S A* **107,** 17839–17844 (2010).
94. Barakat, M. *et al.* Fast and slow spindle involvement in the consolidation of a new motor sequence. *Behav. Brain Res.* **217,** 117–21 (2011).
95. Stoodley, C. J. The cerebellum and cognition: Evidence from functional imaging studies. *Cerebellum* **11,** 352–365 (2012).
96. De Zeeuw, C. I. & Ten Brinke, M. M. Motor Learning and the Cerebellum. *Cold Spring Harb. Perspect. Biol.* **7,** a021683 (2015).
97. Barakat, M. *et al.* Sleep spindles predict neural and behavioral changes in motor sequence consolidation. *Hum. Brain Mapp.* **34,** 2918–2928 (2013).
98. Fogel, S. *et al.* Sleep spindles: a physiological marker of age-related changes in gray matter in brain regions supporting motor skill memory consolidation. *Neurobiol. Aging* **49,** 154–164 (2017).
99. Cousins, J. N., El-Deredy, W., Parkes, L. M., Hennies, N. & Lewis, P. A. Cued Reactivation of Motor Learning during Sleep Leads to Overnight Changes in Functional Brain Activity and Connectivity. *PLoS Biol.* **14,** e1002451 (2016).
100. Fischer, S., Hallschmid, M., Elsner, A. L. & Born, J. Sleep forms memory for finger skills. *Proc. Natl. Acad. Sci. U. S. A.* **99,** 11987–91 (2002).
101. Maquet, P. *et al.* Experience-dependent changes in cerebral activation during human REM sleep. *Nat. Neurosci.* **3,** 831–6 (2000).
102. Boele, H.-J., Koekkoek, S. K. E., De Zeeuw, C. I. & Ruigrok, T. J. H. Axonal sprouting and formation of terminals in the adult cerebellum during associative motor learning. *J. Neurosci.* **33,** 17897–907 (2013).
103. Gao, Z. *et al.* Excitatory Cerebellar Nucleocortical Circuit Provides Internal Amplification during Associative Conditioning. *Neuron* **89,** 645–657 (2016).
104. Yamazaki, T., Nagao, S., Lennon, W. & Tanaka, S. Modeling memory consolidation during posttraining periods in cerebellovestibular learning. *Proc. Natl. Acad. Sci. U. S. A.* **112,** 3541–6 (2015).
105. Kassardjian, C. D. *et al.* The site of a motor memory shifts with consolidation. *J. Neurosci.* **25,** 7979–85 (2005).
106. Shutoh, F., Ohki, M., Kitazawa, H., Itohara, S. & Nagao, S. Memory trace of motor learning shifts transsynaptically from cerebellar cortex to nuclei for consolidation. *Neuroscience* **139,** 767–77 (2006).
107. Anzai, M., Kitazawa, H. & Nagao, S. Effects of reversible pharmacological shutdown of cerebellar flocculus on the memory of long-term horizontal vestibulo-ocular reflex adaptation in monkeys. *Neurosci. Res.* **68,** 191–8 (2010).
108. Okamoto, T., Endo, S., Shirao, T. & Nagao, S. Role of Cerebellar Cortical Protein Synthesis in Transfer of Memory Trace of Cerebellum-Dependent Motor Learning. *J. Neurosci.* **31,** 8958–8966 (2011).

109. Fogel, S. M., Ray, L. B., Binnie, L. & Owen, A. M. How to become an expert: A new perspective on the role of sleep in the mastery of procedural skills. *Neurobiol. Learn. Mem.* **125,** 236–248 (2015).
110. Hasselmo, M. E. Neuromodulation: Acetylcholine and memory consolidation. *Trends Cogn. Sci.* **3,** 351–359 (1999).
111. Oudiette, D. & Paller, K. A. Upgrading the sleeping brain with targeted memory reactivation. *Trends Cogn. Sci.* **17,** 142–149 (2013).
112. Ji, D. & Wilson, M. a. Coordinated memory replay in the visual cortex and hippocampus during sleep. *Nat. Neurosci.* **10,** 100–107 (2007).
113. Nádasdy, Z., Hirase, H., Czurkó, A., Csicsvari, J. & Buzsáki, G. Replay and time compression of recurring spike sequences in the hippocampus. *J. Neurosci.* **19,** 9497–9507 (1999).
114. Yang, G. *et al.* Sleep promotes branch-specific formation of dendritic spines after learning. *Science* **344,** 1173–8 (2014).
115. Nagai, H. *et al.* Sleep Consolidates Motor Learning of Complex Movement Sequences in Mice. *Sleep* (2016). doi:10.1093/sleep/zsw059
116. Tononi, G. & Cirelli, C. Sleep function and synaptic homeostasis. *Sleep Med. Rev.* **10,** 49–62 (2006).
117. Nere, A., Hashmi, A., Cirelli, C. & Tononi, G. Sleep-dependent synaptic down-selection (I): modeling the benefits of sleep on memory consolidation and integration. *Front. Neurol.* **4,** 143 (2013).
118. Tononi, G. & Cirelli, C. Sleep and the Price of Plasticity: From Synaptic and Cellular Homeostasis to Memory Consolidation and Integration. *Neuron* **81,** 12–34 (2014).
119. Vyazovskiy, V. V, Cirelli, C., Pfister-Genskow, M., Faraguna, U. & Tononi, G. Molecular and electrophysiological evidence for net synaptic potentiation in wake and depression in sleep. *Nat. Neurosci.* **11,** 200–8 (2008).
120. de Vivo, L. *et al.* Ultrastructural evidence for synaptic scaling across the wake/sleep cycle. *Science (80-.).* **355,** 507–510 (2017).
121. Gilestro, G. F., Tononi, G. & Cirelli, C. Widespread changes in synaptic markers as a function of sleep and wakefulness in Drosophila. *Science (80-.).* **324,** 109–112 (2009).
122. Wolpert, D. M., Miall, R. C. & Kawato, M. Internal models in the cerebellum. *Trends Cogn. Sci.* **2,** 338–347 (1998).
123. Imamizu, H., Kawato, M. & Imamizu, H. Cerebellar internal models: Implications for the dexterous use of tools. *Cerebellum* **11,** 325–335 (2012).
124. Fischer, S. Motor Memory Consolidation in Sleep Shapes More Effective Neuronal Representations. *J. Neurosci.* **25,** 11248–11255 (2005).
125. Passot, J.-B., Luque, N. R. & Arleo, A. Coupling internal cerebellar models enhances online adaptation and supports offline consolidation in sensorimotor tasks. *Front. Comput. Neurosci.* **7,** 95 (2013).
126. Miyashita, K., Rand, M. K., Miyachi, S. & Hikosaka, O. Anticipatory saccades in sequential procedural learning in monkeys. *J. Neurophysiol.* **76,** 1361–1366 (1996).
127. Ohno, H., Urushihara, R., Sei, H. & Morita, Y. REM sleep deprivation suppresses acquisition of classical eyeblink conditioning. *Sleep* **25,** 877–881 (2002).
128. Koekkoek, S. K. E. *et al.* Cerebellar LTD and Learning-Dependent Timing of Conditioned Eyelid Responses. *Science (80-.).* **301,** 1736–1739 (2003).
129. Schonewille, M. *et al.* Reevaluating the Role of LTD in Cerebellar Motor Learning. *Neuron* **70,** 43–50 (2011).
130. Maquet, P., Schwartz, S., Passingham, R. & Frith, C. Sleep-related consolidation of a visuomotor skill: brain mechanisms as assessed by functional magnetic resonance imaging. *J. Neurosci.* **23,** 1432–40 (2003).
131. Lewis, P. A., Couch, T. J. & Walker, M. P. Keeping time in your sleep: Overnight consolidation of temporal rhythm. *Neuropsychologia* **49,** 115–123 (2011).
132. Mangels, J. A., Ivry, R. B. & Shimizu, N. Dissociable contributions of the prefrontal and neocerebellar cortex to time perception. *Cogn. Brain Res.* **7,** 15–39 (1998).
133. Dreher, J. C. & Grafman, J. The roles of the cerebellum and basal ganglia in timing and error prediction. *Eur. J. Neurosci.* **16,** 1609–1619 (2002).
134. Bueti, D. & Macaluso, E. Physiological correlates of subjective time: Evidence for the temporal accumulator hypothesis. *Neuroimage* **57,** 1251–1263 (2011).
135. Fifer, W. P. *et al.* Newborn infants learn during sleep. *Proc. Natl. Acad. Sci. U. S. A.* **107,** 10320–3 (2010).
136. Rudoy, J. D., Voss, J. L., Westerberg, C. E. & Paller, K. A. Strengthening individual memories by reactivating them during sleep. *Science* **326,** 1079 (2009).

137. Antony, J. W., Gobel, E. W., O'Hare, J. K., Reber, P. J. & Paller, K. A. Cued memory reactivation during sleep influences skill learning. *Nat. Neurosci.* **15,** 1114–1116 (2012).
138. Rasch, B., Büchel, C., Gais, S. & Born, J. Odor cues during slow-wave sleep prompt declarative memory consolidation. *Science* **315,** 1426–1429 (2007).
139. Diekelmann, S., Büchel, C., Born, J. & Rasch, B. Labile or stable: opposing consequences for memory when reactivated during waking and sleep. *Nat. Neurosci.* **14,** 381–6 (2011).
140. Hu, X. *et al.* Cognitive neuroscience. Unlearning implicit social biases during sleep. *Science (80-.).* **348,** 1013–1015 (2015).
141. van Dongen, E. V. *et al.* Memory stabilization with targeted reactivation during human slow-wave sleep. *Proc. Natl. Acad. Sci. U. S. A.* **109,** 10575–10580 (2012).
142. Albus, J. S. A theory of cerebellar function. *Math. Biosci.* **10,** 25–61 (1971).
143. Marr, D. A Theory of Cerebellar Cortex. *J. Physiol.* **202,** 437–470 (1996).
144. Huang, C. C. *et al.* Convergence of pontine and proprioceptive streams onto multimodal cerebellar granule cells. *Elife* **2013,** 1–17 (2013).
145. Ishikawa, T., Shimuta, M. & Häusser, M. Multimodal sensory integration in single cerebellar granule cells in vivo. *Elife* **4,** 1–10 (2015).
146. Carter, O., Konkle, T., Wang, Q., Hayward, V. & Moore, C. Tactile Rivalry Demonstrated with an Ambiguous Apparent-Motion Quartet. *Curr. Biol.* **18,** 1050–1054 (2008).
147. Konkle, T., Wang, Q., Hayward, V. & Moore, C. I. Motion Aftereffects Transfer between Touch and Vision. *Curr. Biol.* **19,** 745–750 (2009).


presses
corresponding
movements
conditions
VI
marker
PPI
temporal
activity
information
gyrus
predictive
performed
input
hemisphere
buttons
timing
Finger
images
studies
parietal
Spatial
side
one
fingers
uncorrected
analyses
hippocampal
cerebellum
overlapped
indicating
milliseconds
cortex
brain
correction
learning-dependent
time
markers
left
showed
requiring
average
threshold
based
imagery
functional
Flash
trial
execution
number
coordination
either
visual
target
sequence
Rest
flashes
seed
study
motor
perceptual
imagined
run
Observation
region
individual
main
integration
Four-Finger
effect
screen
activated
results
interval
prediction
averaged
tasks
Mental
moving
data
connectivity
button
cluster
finger
responses
times
basis
activation
variance
structural
distribution
motion
Rehearsal
spatio-temporal
ms
press
percentage
hippocampal-cerebellar
context
lobule
regions
level
flashing
movement
timed
stable
size
performance
contrast
spatial
correct
bilateral
different
requires
interaction
overlap
moment
navigation
right
Prediction
Marker
FWE
trials
control
reaction
Corresponding
fMRI
visuomotor
observed
Functional
show
extent
hippocampus

Chapter 2. Hippocampal-cerebellar interaction during spatio-temporal prediction

Yoshiyuki Onuki, Eus J.W. Van Someren, Chris I. De Zeeuw,
and Ysbrand D. Van der Werf

Published in:
Cerebral Cortex, 2015
DOI:10.1093/cercor/bht221

2.1 Abstract

The hippocampus and cerebellum play a role in the process of temporal memory formation. The interaction between these brain regions during the prediction of motor executions nevertheless remains unclear. Using fMRI we show here that the hippocampus and cerebellum are co-activated during a timing-dependent task that requires accurate prediction timing of finger movements following preceding visual cues, but not during two control tasks: a reaction task requiring identical coordination of individual and combined fingers without predicting the motor timing, or an imagery task. In addition, functional connectivity analyses revealed that the hippocampus showed increased functional connectivity with the bilateral hemispheres of the cerebellum. These results suggest that hippocampal-cerebellar interplay occurs during spatio-temporal prediction of movements on the basis of visuomotor integration.

2.2 Introduction

Predicting the timing of motor sequences on the basis of spatial information requires the precise execution of complex motor output, such as playing a musical instrument following the direction of a conductor. Spatio-temporal prediction, i.e. the anticipation of perceptual events for the execution of the timed motor responses (motor timing) or perceptual judgments, can be achieved by the use of temporal information (e.g. the velocity of an object) and spatial information (e.g. the location of an object) during a task[1–3].

The hippocampus and cerebellum underlie spatial and temporal coding in the formation of memories. Examples of spatial coding include spatial navigation and adaptation of goal-oriented behavior[4,5]. Specifically, Rochefort et al (2011) showed that the spatial coding of place cells was impaired only in the condition requiring egocentric navigation (spatio-temporal memory) of the maze task when protein kinase C-dependent plasticity was inhibited at the Purkinje cell level. In addition, lateralized regions within hippocampus and cerebellum interact during sequential route-based navigation and map-based navigation in humans[6,7]. For temporal coding, the hippocampus and cerebellum cooperate in controlling temporal aspects of learning-dependent motor output such as trace conditioning[8–12] and cued fear conditioning[13,14]. The interaction between the hippocampus and cerebellum during spatio-temporal prediction, however, is not yet fully understood.

We hypothesize that the hippocampus and cerebellum are co-activated and show significant functional connectivity during spatio-temporal prediction, but not during performance of coordinated movements only (i.e. without their predictive timing) or during motor imagery, even though these tasks may by themselves activate either the cerebellum[15–17] or the hippocampus[18–20].

We used functional Magnetic Resonance Imaging (fMRI) to measure the brain activity during a modified Serial Interception Sequence Learning (SISL) task[21] that allows to distinguish motor coordination from predictive and reactive timing functions. In addition, we included control conditions with imagined movements to investigate the involvement of the hippocampal and cerebellar systems in the planning of imagined versus executed motor actions. We hypothesized that the hippocampus interacts functionally with both hemispheres of the cerebellum to establish the spatio-temporal prediction of actual movements, but not reactive motor tasks and imagery.

2.3 Materials and Methods

2.3.1 Subjects

Sixteen healthy right-handed subjects (age 18-26, 3 females) participated in the experiments. None of the volunteers played musical instruments or rhythmic games on a regular basis. All subjects gave their informed consent prior to the study. The experiment was approved by the ethics committee of the Department of Psychology, the University of Amsterdam, The Netherlands.

2.3.2 Set-up, Conditions and experimental protocol

Setup. The subjects performed modified versions of the Serial Interception Sequence Learning (SISL) task[21], requiring precise timing of actual or imagined finger movements of the left non-dominant hand. The task was administered in the MRI scanner (Philips, 3.0-Tesla Achieva). Subjects had to actually press buttons, or imagine pressing buttons, exactly timed to the moment that upward moving black circles (referred to as moving markers) overlapped with corresponding fixed white circles in the top row (referred to as target markers) (Figure 1). The moving markers appeared at the bottom of the screen, moved upwards with constant velocity (2.8 milliseconds per pixel), overlapped with the target markers at the top row and kept moving up until they disappeared off the screen. The moving markers could appear either one by one or in pairs of two simultaneously.

The diameter of the target markers was 20% of the middle third of the display width. The diameter of moving markers was 20 pixels smaller than that of the target marker so as to fit completely inside the target markers and not to interfere with the moments of the complete overlap between markers observed by subjects. The task was programmed in Matlab (R2010a) using Psychtoolbox 3. The visual stimuli were provided by using LCD projection onto a screen that was visible through a mirror attached to the head coil. Finger responses of the left hand were acquired using a four-button box (from the little finger to the index finger) (Current Design, HHSC-1x4-CL).

Conditions. Each participant was presented six different task conditions, to distinguish spatio-temporal prediction, motor coordination and motor imagery in the main effect analysis of the fMRI data. The main experimental condition requiring spatio-temporal prediction was the Corresponding Finger condition (Figure 1a). Control conditions consisted of the Four-Finger condition (Figure 1b), Flash Marker condition (Figure 1c), Mental Rehearsal condition (Figure 1d), Observation condition (Figure 1e), and Rest condition (Figure 1f). In the Corresponding Finger condition (Figure 1a), subjects were asked to press the corresponding button or buttons at the moment when the moving markers overlapped with the target markers. In this condition, either a single or two simultaneously moving markers could overlap at a given moment. In the Four-Finger condition (Figure 1b), visual stimuli were exactly the same as those for the Corresponding Finger condition, but all four buttons had to be pressed simultaneously when any moving marker overlapped with any of the target markers. Thus it eliminated the coordination of individual finger movements while maintaining timing. In the Flash Marker condition (Figure 1c), the target markers flashed for 150 milliseconds at random time intervals from 480 - 1070 milliseconds (Average temporal interval: 770 milliseconds). The subjects were asked to respond to the white flashing target markers by pressing the corresponding buttons as soon as they detected them. The sequence of flashing of the target markers was exactly the same in as in the Corresponding Finger condition, but 1) its timing was independent of that of the sequence of upward streaming markers and hence could not be predicted from it, 2) the timing of marker

flashes was randomly jittered unlike the fixed timing of the sequence in the Corresponding Finger condition, and 3) used a larger range of stimulus intervals than in the Corresponding Finger condition. We thus maintained the same number of button presses between the Flash-Marker condition and the Corresponding Finger condition but eliminated spatio-temporal prediction only for the Flash Marker condition. In The Mental Rehearsal condition (Figure 1d), exactly the same visual stimuli were provided as in the Corresponding Finger condition, but now subjects were instructed to imagine pressing the buttons, rather than actually pressing them. In the Observation condition (Figure 1e), the identical moving markers were presented as in the Corresponding Finger condition, but the white target markers were not displayed, and the subjects were instructed to merely observe the flow of markers without any actual pressing or motor imagery. And finally in the Rest condition (Figure 1f), participants were instructed to stare at the crosshair fixation point in the middle of the black screen. All conditions were preceded by text-based cues, which appeared on the screen for a duration of 3 seconds. The sequence of appearance of moving markers followed the same order for all conditions (except the Rest condition during which no markers were shown): AC-B-AD-BC-CD-BD-C-A-AB-D (A: left-most trajectory, B: second trajectory, C: third trajectory, D: right-most trajectory). The average temporal interval between appearances was 600 milliseconds (range 500-660 milliseconds) for all conditions except the Flash Marker condition in which the intervals jittered differently, unpredictably and within a larger range to eliminate the timing aspect. The sequence appeared four times in one trial. No feedback to indicate the correct responses was given during the task.

Concertedly, the six conditions allowed us to assess different aspects of motor behavior including spatio-temporal prediction, motor coordination, and motor imagery. a) *Spatio-temporal prediction* (subtracting the Flash Marker condition (Figure 1c) from the Corresponding Finger condition (Figure 1a)); the Corresponding Finger condition and the Flash Marker condition were the same in terms of the visual input and the number of button presses made, but they differed with respect to the possibility to predict and plan the exact timing of the movements ahead, which was only possible in the

Corresponding Finger condition. b) *Motor coordination* (subtracting the Four-Finger condition (Figure 1b) from the Corresponding Finger condition (Figure 1a)); the Corresponding Finger condition and the Four-Finger condition were the same in terms of visual input, but they differed in that the fingers only had to be moved and coordinated separately in the Corresponding Finger condition (i.e. requiring visuomotor integration at the level of individual finger movements). c) *Motor imagery* (subtracting the Observation condition (Figure 1e) from the Mental Rehearsal condition (Figure 1d)); the Mental Rehearsal condition and the Observation condition were the same in terms of visual input and the number of button presses made (i.e. zero), but they differed in that brain activity related to imagined movements was evoked during the Mental Rehearsal condition, but not during the Observation condition.

Protocol. Participants performed 4 scanning runs. Each run contained 15 blocks (block duration = 33 seconds; 1 run = 8.25 minutes; total duration = 37 minutes) and in each run all conditions occurred twice except the Rest condition, which occurred five times. The order of the Four-Finger condition, Flash Marker condition, Mental Rehearsal condition, and Observation condition was pseudo-randomized within a run to counteract any order effect (Figure 1g).

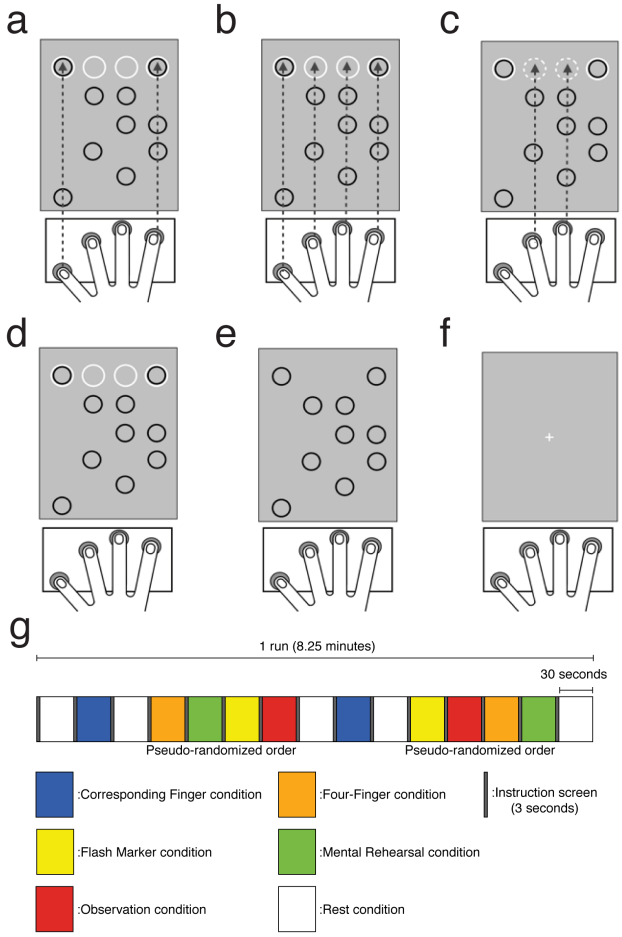

Figure 1. Experimental conditions and protocol. Subjects were subjected to 6 different conditions. (a) Corresponding finger movement condition. The subjects press assigned buttons when 1 or 2 moving markers overlap with the target markers. The purpose of the condition is to extract activity related to prediction timing and motor coordination. (b)Four-Finger movement condition. The subject presses all 4 buttons when any of the moving markers overlap with the target markers. Performance depends on timing of motor output. (c) Flash marker condition. Participants are instructed to press the buttons corresponding to the target markers as soon as the target markers flash. As the participants cannot anticipate the timing to press the buttons, the condition requires only finger coordination. (d) Mental rehearsal condition. The purpose of the condition is to imagine movements that require motor coordination and prediction timing. (e) Observation condition. This is the control condition of the mental rehearsal condition. (f) Rest condition. The subject stares at the fixation point. Colored dashed lines and arrows represent the expected locations to press buttons. (g) Experimental protocol. There are six conditions in one run: Corresponding Finger condition, Four-Finger condition, Flash marker condition, Mental Rehearsal condition, Observation condition, and Rest condition. The Four-finger condition, Flash marker condition, Mental rehearsal condition and Observation condition are pseudo-randomized to control for any order effect; the exact sequence presented here is thus an example. Each block took 33 seconds; a single run was 8.25 minutes. We conducted 4 runs; the total duration was 37 minutes.

2.3.3 Set-up, Quantification of behavioral performance

We calculated the average percentage of correctly timed responses (correct responses) for each trial during the Corresponding Finger condition and Four-Finger condition. A motor response was regarded correct if it was made within an interval of -150 to 150 milliseconds of the time of perfect overlap of target and moving marker; 150 milliseconds is the time needed for the center of the moving markers to move from the edge to the center of the target markers. Response time (Prediction time) is calculated based on the correct button responses only. For the Flash Marker condition responses are reactive rather than predictable and are made after observing the flashing stimulus; we quantified performance as the average reaction time of correct responses and as the number of correct responses, in the time window determined as the temporal interval from 100 milliseconds after the onset of one marker flash to the onset of another marker flash (average temporal interval 770 milliseconds, range $480 < t < 1070$ milliseconds). The button responses that were performed with the correct button but recorded within 100 milliseconds after the marker flashes were regarded as false alarms and disregarded; the false alarm rate in the time window from 0 to 100 milliseconds was 0.64 %, corresponding to 2.4 ± 1.9 (std) per block. We performed a one-way repeated measures analysis of variance (ANOVA) on the behavioral results, using condition as a within-subject variable.

2.3.4 Imaging parameters and acquisition

Functional and structural MR scans were recorded using a 3T scanner (Philips, 3.0-Tesla Achieva) at the Spinoza Center, University of Amsterdam. For functional MRI scans, whole-brain functional T2*-weight MRI data were acquired using a gradient-echo planar imaging (EPI) sequence (55 transverse slices with 0 mm gap, ascending slice acquisition; voxel size $2.5 \times 2.5 \times 2.5$ mm^3; repetition time (TR) 3179 ms, echo time (TE) 29.93 ms; flip angle 80°; field of view (FOV) 200×200 mm^2). For the structural MR scans, T1-weighted images were acquired (220 slices; TR 8.2 ms; TE 3.8 ms; inversion time 670.4ms; FOV 240

× 188 mm^2, matrix size 240 × 187; flip angle 8°; voxel size 1 × 1 × 1 mm^3). Head movements were minimized by restraining the subject's head using a sponge cushion inside the 32-channel head-coil.

2.3.5 fMRI data preprocessing

All data analyses were performed using SPM8 (Wellcome Trust Centre for Neuroimaging, University College London, UK). Images were realigned using iterative rigid body transformation, coregistered to the structural MRI images, normalized to the MNI standard brain template (the Montreal Neurological Institute), and smoothed with a 5-mm full-width at half maximum (FWHM) Gaussian kernel. A high pass filter (128 seconds) was applied.

To obtain accurate spatial normalization of the cerebellum, the spatial unbiased atlas template (SUIT) toolbox [22] was used, separate from and in parallel to the whole-brain analysis: specifically, after the functional images were realigned and coregistrered to the structural images, the cerebellum and brainstem in the structural image were isolated and warped into SUIT space. The functional images were resliced into the SUIT atlas space (resolution 1 mm isotropic) with the mask created by the isolation process of the structural scan to avoid contamination of BOLD signals outside of cerebellum such as the visual cortex. These functional images, dedicated to cerebellum-specific analysis, were then smoothed at 5mm FWHM, as those dedicated to the whole-brain analysis.

2.3.6 Task-dependent activation

Statistical testing was conducted to analyze data on an individual basis and across subjects. First-level analyses were computed using general linear models (GLM) and convolution with the canonical hemodynamic response function (HRF) for different experimental conditions. The following contrasts were calculated: spatio-temporal prediction (Corresponding Finger condition (Figure 1a) - Flash Marker condition (Figure

1c)), motor coordination (Corresponding Finger condition (Figure 1a) - Four-Finger condition (Figure 1b)), and motor imagery (Mental Rehearsal condition (Figure 1d) - Observation condition (Figure 1e)). To avoid any residual movement effects, the design matrix included the six head motion regressors (translations and rotations). In addition, to take into account learning effects of sequential finger movements in the Corresponding Finger condition, Flash Marker condition, and Four-Finger condition, we performed a parametric modulation analysis[23] based on the averaged performance rates, reaction times, and variance of reaction times. The parametric modulators and their temporal derivatives were added into the design matrix as parameters of no interest. Individual fixed-effects statistical parameter maps were generated from the linear contrasts. For the group analysis, each individual subject's first-level contrast images were entered into a second-level random-effect analysis. The contrasts were estimated at one sample t-test (uncorrected, $p < 0.0005$) with spatial extent threshold determined by family-wise error correction at cluster size at $p < 0.05$. The activated regions were identified on the basis of the anatomy toolbox containing probabilistic cyto-architectonic maps[24] and the spatially unbiased atlas for the cerebellum[25].

2.3.7 Functional connectivity analysis

Psychophysiological interaction (PPI) analyses[26] were used to evaluate functional connectivity between hippocampus or cerebellum (the seed area) with the rest of the brain including the cerebellum during spatio-temporal prediction, to exclude the possibility of independent co-activation of two different regions in the main effect analysis. To perform the analysis, we defined a linear model using three regressors: (1) the main effect for the Corresponding Finger condition versus Flash Marker condition (timing) as a context variable, (2) the activity of the seed, and (3) the psychophysiological interaction between the first regressor (context variable) and second regressor (the activity from the seed region). Seed regions were defined as the voxels within a 5 mm-radius sphere around the local maxima in the left hippocampus and cerebellar regions of the contrast (Corresponding Finger condition – Flash Marker

condition) in the group random effects analysis (uncorrected, $p < 0.0005$, spatial extent threshold using family-wise error (FWE) correction at cluster level at $p < 0.05$), excluding non-hippocampal and non-cerebellar regions on the basis of the anatomy toolbox[24]. The signal time courses within the seed regions were adjusted using the F-contrast of all conditions to exclude the possible effects explained by contrast columns and extracted as their first eigenvector. The parametric modulators, their temporal derivatives, and head motion regressors used in the main-effect were included in the model. The contrasts estimated from the individual PPI analysis were analyzed at a second-level one-sample t-test (uncorrected, $p < 0.0005$, spatial extent threshold using FWE correction at cluster level at $p < 0.05$).

As an additional analysis, to reveal possible hippocampal involvement during the motor imagery contrast, we tested functional connectivity from the coordinates of the cerebellar regions found in the main effect analysis of the motor imagery contrast, to examine the strength of the functional connectivity toward hippocampus during motor imagery. Following the extraction and F-contrast adjustment of the signal time course from the cerebellar seed regions during motor imagery, we conducted the same procedures as we described above for the PPI analysis of spatio-temporal prediction.

2.4 Results

2.4.1 Behavior

The percentage of correct responses gradually increased over the trials from 40% to 70%, showing learning of task-related visuomotor integration ($F_{(3.767,56.511)} = 8.828$, $p < 0.001$, one-way repeated measures ANOVA with a Greenhouse-Geisser correction) (Figure 2a). The distribution of the prediction-time for the correct button responses skewed towards negative (i.e. predictive) reaction times and its mean saturated at -55 ms before the exact moment when the moving marker overlapped with the target marker ($F_{(7,105)} = 10.741$, $p < 0.001$, one-way repeated measures ANOVA) (Figure 2b). Even if we restricted the analysis to single-finger responses only, thereby excluding the possibly confounding

effect of coordination of movements across fingers in the two-finger responses, we still observed that the prediction-time shifted slightly toward -60 ms ($F_{(3.880, 58.205)} = 8.720$, $p < 0.001$, one-way repeated measures ANOVA with a Greenhouse-Geisser correction), reflecting establishment of prediction timing. The averaged variance of the prediction time across trials slightly changed across trials ($F_{(7,105)} = 2.297$, $p < 0.05$, one-way repeated measures ANOVA). In the Four-Finger condition, the percentage of correct responses was slightly increased over the trials ($F_{(7,105)} = 2.30$, $p < 0.05$, one-way repeated measures ANOVA). Indeed, the percentage of correct responses started at a higher level at the first trial (approximately 57% as compared to ~40% in the Corresponding Finger condition) (Figure 3a). The prediction-time was approximately -50 ms at the start of the first trial and did not significantly change over the trials ($F_{(3.899,58.482)} = 1.401$, $p = 0.246$, one-way repeated measures ANOVA with a Greenhouse-Geisser correction) (Figure 3b). The averaged variance of the prediction time was stable across trials ($F_{(3.351, 50.259)} = 1.372$, $p = 0.261$, one-way repeated measures ANOVA with a Greenhouse-Geisser correction). In the Flash Marker condition, the percentage of correct responses increased from 63% to 84% ($F_{(2.530, 37.957)} = 9.928$, $p < 0.001$, one-way repeated measures ANOVA with a Greenhouse-Geisser correction), while the reaction time shifted from approximately 600 ms to 500 ms ($F_{(2.758,41.374)} = 16.247$, $p < 0.0001$, one-way repeated measures ANOVA with a Greenhouse-Geisser correction) (Figure 4a,b). The averaged variance of the reaction time in Flash Marker condition was significantly different across trials ($F_{(2.960,44.401)} = 2.992$, $p < 0.05$, one-way repeated measures ANOVA with a Greenhouse-Geisser correction). Overall, there were only few responses between 0 and 100 ms (false alarm rate: 0.64 %, corresponding to 2.4 ± 1.9 (std) per block).

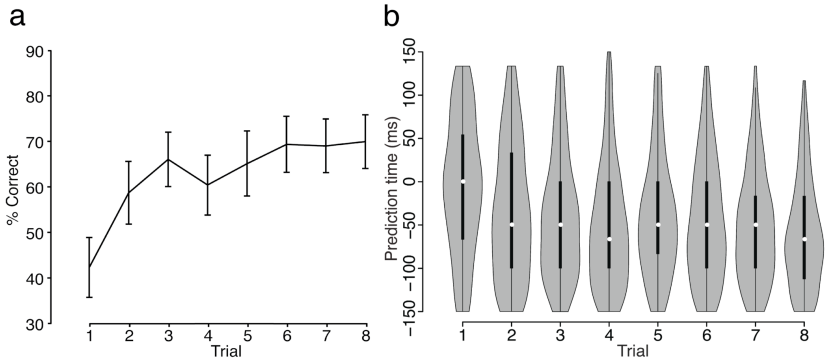

Figure 2. Behavioral results for the Corresponding Finger condition. (a) Percentage of correct responses. The average percentage of correct responses increases across trials indicating learning-dependent prediction timing of sequential motor responses ($F_{(3.767,56.511)} = 8.828$, $p < 0.001$, one-way repeated measures ANOVA with a Greenhouse-Geisser correction). Error bars indicate standard errors of the mean (SEM). **(b) Prediction time of movements.** The mean decrease and the probability distribution saturates at a value of 55 ms before the moment of marker overlap ($F_{(7,105)} = 10.741$, $p < 0.001$, one-way repeated measures ANOVA), indicating that spatio-temporal prediction for the motor execution occurs. Prediction time 0 represents the moment of complete overlap between target and motion markers. White dot: median. Black line: 25th–75th percentile. Gray-colored area: probability distribution of prediction time.

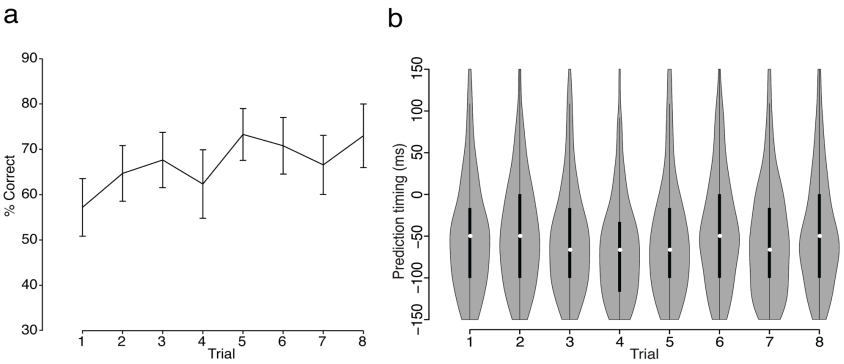

Figure 3. **Behavioral results for the Four-Finger condition. (a) Percentage of correct responses,** The performance rate is stable across trials ($F_{(7,105)} = 2.30$, $p < 0.05$, one-way repeated measures ANOVA). Error bars indicate standard errors of the mean (S.E.M.). **(b) Prediction-time of movements.** Prediction time remains stable across runs ($F_{(3.899,58.482)} = 1.401$, $p = 0.246$, one-way repeated measures ANOVA with a Greenhouse-Geisser correction). In this paradigm, the prediction time of about 55 milliseconds occurred immediately at the first trial, i.e. the responses were given before the moment that motion and target markers completely overlapped. The averaged variance of the reaction time across trials is stable ($F_{(3.351, 50.259)} = 1.372$, $p = 0.261$, one-way repeated measures ANOVA with a Greenhouse-Geisser correction). Reaction time 0 represents the moment of complete overlap between target and motion markers. White dot: median. Black line: 25^{th} – 75^{th} percentile. Gray colored area: probability distribution of prediction time.

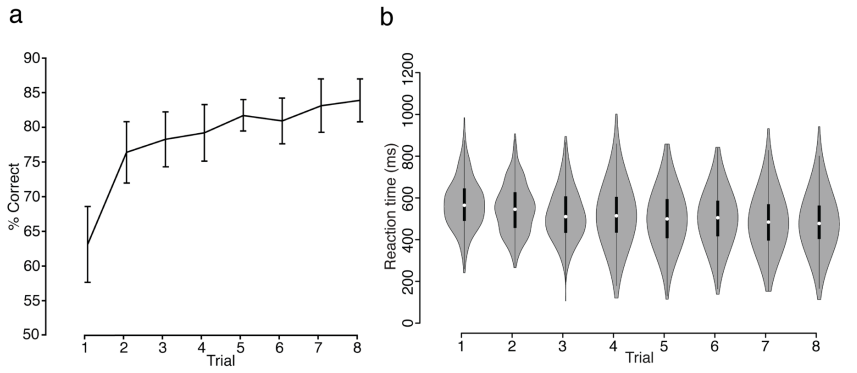

Figure 4. Behavioral results in the flash marker condition. (a) Percentage of correct responses. The number of correct reactions, displayed as averages +/- SEM, to the flashing markers increased across trials ($F_{(2.530, 37.957)} = 9.928$, $p < 0.001$, one-way repeated measures ANOVA with a Greenhouse-Geisser correction) **(b) Reaction time** The reaction time of responses becomes faster across trials ($F_{(2.758,41.374)} = 16.247$, $p < 0.0001$, one-way repeated measures ANOVA with a Greenhouse-Geisser correction). The averaged variance of the reaction time across trials is stable ($F_{(2.960,44.401)} = 2.992$, $p < 0.05$, one-way repeated measures ANOVA with a Greenhouse-Geisser correction). Reaction time 0 represents the moment of complete overlap between target and motion markers. White dot: median. Black line: 25th – 75th percentile. Gray colored area: probability distribution of reaction time.

2.4.2 Neuroimaging

To reveal increments in (co)activation related to spatio-temporal prediction, motor coordination, and motor imagery we compared the Corresponding Finger condition to the Flash Marker condition, the Corresponding Finger condition to the Four-Finger condition, and the Mental Rehearsal condition to the Observation condition, respectively. For the prediction-related increment of activity, Figure 5a presents a map of the hippocampal and cerebellar regions that were significantly more strongly activated in the Corresponding Finger condition as compared to the Flash Marker condition. It shows activation of the bilateral hemisphere and right vermis of cerebellar lobule VI, the left side of hippocampus, and visual cortex (V1, Cuneus, and V2) (for details, see Table 1). The right side of hippocampus was activated but failed to reach the threshold (FWE correction at cluster level at $p < 0.05$). The activity related to spatio-temporal prediction was not biased by the amount of motor execution, because

the total number of button presses between the Corresponding Finger condition and Flash Marker condition did not differ ($t_{(254)} = -1.84$, $p = 0.0664$, two-sample t test).

In contrast, the motor coordination-related and motor imagery-related increments of activity were only found in the cerebellum (motor coordination: bilateral hemisphere in cerebellar lobule VI, right vermis of central region of lobule V, and right hemisphere in cerebellar lobule VIIIa; motor imagery: bilateral hemisphere in lobule VI) (Figure 5b and 5c).

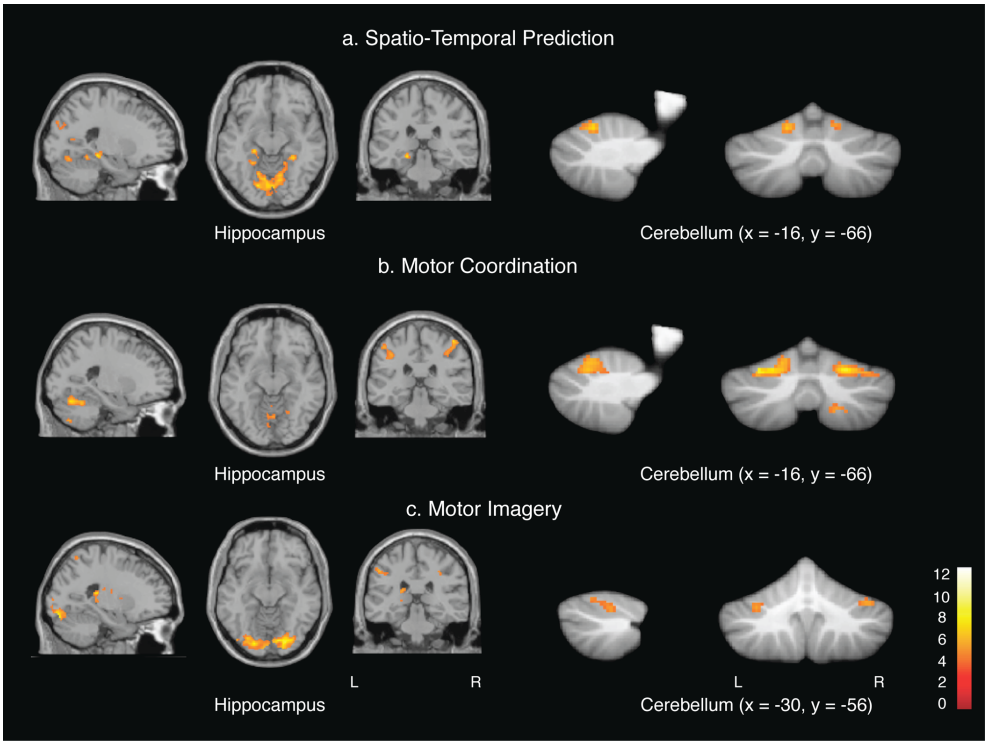

Figure 5. Functional MRI of hippocampal and cerebellar activity during spatio-temporal prediction, motor coordination, and motor imagery. Spatio-temporal prediction (a)was assessed by the contrast Corresponding Finger condition—flash marker condition, motor coordination (b) was assessed by the contrast Corresponding Finger condition—Four-Finger condition, and motor imagery (c) was assessed by the contrast mental rehearsal condition—observation condition. To allow comparison of hippocampal activation across the different contrasts, the x, y, and z planes are kept constant. The x and y coordination of cerebellar activations are displayed on the Figure. Note that the hippocampus was only activated during spatio-temporal prediction.

2.4.3 Functional connectivity

To test whether the left hippocampal regions activated in the spatio-temporal prediction contrast show functional connectivity with the cerebellar regions, we used psychophysiological interaction analysis (PPI analysis) using the clusters within the left hippocampus found for this contrast. We defined the hippocampal activity as the average of the activation in 5 mm radial spheres surrounding the peaks of activation of the left side ([-22, -32, -9]), masking out non-hippocampal tissue. After analyzing the connectivity at the level of individual subjects, we calculated the main effect at the group level using one-sample t-tests (uncorrected $p < 0.0005$, Spatial extent threshold: FWE correction at cluster level at $p < 0.05$). The cerebellar regions found in the PPI analysis from the left hippocampus seed region were the bilateral hemispheric lobules VI, right hemispheric region in lobule VIIa Crus I, left hemispheric region of lobule VIIIb (uncorrected $p < 0.0005$, Spatial extent treshold: FWE correction at cluster level, $p < 0.05$) (Figure 6). In addition to the cerebellar regions, functional connectivity was found for the Angular gyrus, Inferior occipital gyrus, Inferior parietal lobule, Inferior temporal gyrus, Middle frontal gyrus, Middle occipital gyrus, Premotor cortex, Primary visual cortex (V1), Ventral V4 (V4v), and Superior parietal lobule (see Table 2).

The common regions identified in both main effect analysis and PPI analysis were the bilateral cerebellar lobule VI and primary visual cortex (V1). For the inverse connectivity analyses, PPI analysis from the three cerebellar seed coordinates based on the main-effect analysis in the spatio-temporal prediction condition did not show any significant clusters in hippocampus (uncorrected $p < 0.0005$, Spatial extent: FWE correction at cluster level, $p < 0.05$). In addition, a seed voxel placed in the right side of cerebellum based on the motor imagery-related activation similarly yielded a functional connectivity in the left hippocampus that remained below threshold (uncorrected $p < 0.0005$, Spatial extent: FWE correction at cluster level, $p < 0.05$).

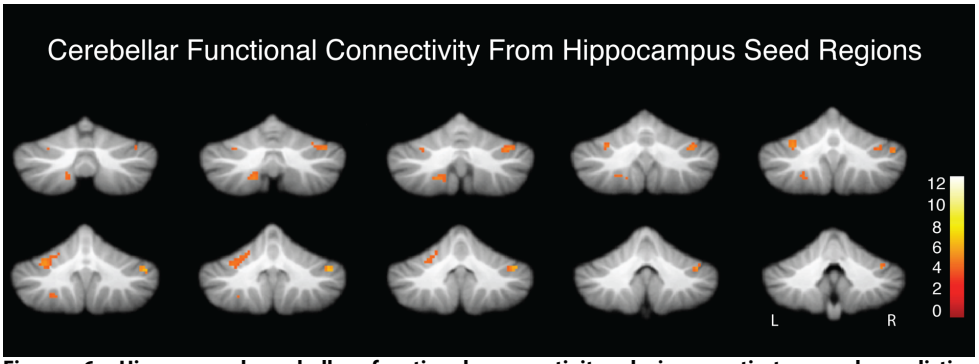

Figure 6. Hippocampal–cerebellar functional connectivity during spatio-temporal prediction. Activations represent the functional connectivity with the seed regions in the context of spatio-temporal prediction (Seed region: left hippocampus ([−22, −32, −9] (uncorrected P<0.0005, Cluster size threshold FWE correction at cluster level (P<0.05)).

2.5 Discussion

In this study, we have adapted a finger movement task to tease apart different aspects of motor control including spatio-temporal prediction, finger coordination and imagination of movements. We show that subjects display prediction and improved precision across trials and that the prediction-related contrast in the main effect analysis shows co-activation of hippocampus and cerebellum. Functional connectivity analyses reveal that the hippocampal activations significantly interact with specific cerebellar regions, only in the context of spatio-temporal prediction of fine motor skills.

2.5.1 Behavioral data

The increase in correct responses and the restricted distribution of the predictive response time in the Corresponding Finger condition reflect the improvement of motor control and establishment of spatio-temporal prediction with timed motor executions. The response probability shows that the motor timing of the button responses becomes stable following the initial trial and slightly antecedent to the moment of marker overlap, indicating establishment of the prediction. Establishment of spatio-temporal prediction in response to perceptual events during a task can be categorized as a type of learning-dependent timing (in this case “learning-dependent prediction timing”), as it

requires movements to be timed to ongoing visual input; i.e. the movement can be prepared or predicted, ahead of time.

A performance improvement and similar antecedent responding are not observed in the Four-Finger movement condition that requires prediction timing, but not individual control of fingers or finger combinations. In contrast, in the Flash Marker condition requiring reactive instead of predicted movements of individual and combined fingers, the performance improved across trials and the average reaction times became faster upon overlap of the moving markers with the target markers, but did not become predictive, i.e. antecedent, to the flashing, indicating absence of prediction learning based on timing aspects of the task. The changes may thus reflect simply improvement of reaction timing in the context of the task. Motor execution improvements based on temporal prediction of the motor executions in the Flash Marker condition cannot occur, owing to the randomized, jittered and larger interstimulus interval range between marker flashes, such that the timing of the flashes is unpredictable and the subjects passively react to, but cannot predict, the timing of flashes. Spatial prediction may still have occurred to a degree during the Flash Marker condition, as the sequence of responses was repeated, but since the temporal prediction is no longer possible, the integration of spatial and temporal prediction cannot occur. Also, the low percentage of correct button responses in the time window from 0 to 100 milliseconds after marker overlap (0.64 %) is consistent with a reactive rather than predictive timing in this condition.

2.5.2 Brain activation

We measured brain activation in the six variations of the task to extract the responsible regions during spatio-temporal prediction, motor coordination, and motor imagery. Previous research that addressed cerebellar regions involved in temporal processing has shown results partly overlapping with ours, i.e. lobule VI, VII, and superior vermis[27]. The differences may reflect the different demand of the task used in that study; some tasks

require explicit timing, i.e. the overt estimation or discrimination of the duration of perceptual events, while our task requires implicit timing, i.e. the indirect use of spatial-temporal information in responding to visual stimuli corresponding to each button. The difference in findings imply that different mechanisms may be recruited to process explicit vs. implicit timing within the cerebellum. We report here that both left posterior hippocampus and several cerebellar regions (i.e. the bilateral hemisphere and right vermis of cerebellar lobules VI) showed activity only during the spatio-temporal prediction aspect of the task. The activated regions found in lobule VI agree with part of the regions found in a previous study, which showed the neural correlate of motor and sensory timing[28–30] (Figure 5).

In contrast to prediction-related activation, the coordination of individual and combined fingers did not induce joint activation of the cerebellum and hippocampus, but solely of the cerebellum (bilateral hemisphere in cerebellar lobule VI, right vermis of central region of lobule V, and right hemisphere in cerebellar lobule VIIIa). Similarly, for imagined timed movements, the cerebellum, but not the hippocampus, was activated (bilateral hemisphere in lobule VI) although cortical areas (superior and inferior parietal areas supplementary motor cortex) observed during motor coordination contrast and motor imagery were consistent with previous neuroimaging research of complex motor coordination[31,32] and motor imagery[33–36]. Lobule V and VI have been observed as part of a sensorimotor network, with especially lobule V involved in arm and finger movements[37–39]. These data are in line with outcomes of fMRI studies employing imagery tasks involving specific timing and sequential finger coordination, such as imagery of playing a piano and a finger-tapping task[16,40]. Possibly, the cerebellum participates in motor imagery for forming and using internal models so as to facilitate predictions during cognitive control, regardless of actual performance[17]. The lack of hippocampal activation during our motor imagery timing task suggests that a hippocampal contribution is only needed for real as opposed to imagined timing of finger movements. Yet, the hippocampus appears to be activated during mental navigation and motor imagery of locomotion[18–20]. Future studies will have to elucidate

to what extent the difference in results reflects a difference in exact requirements of timing and/or motor domains. The different conditions of our task matched in terms of visual-temporal input and motor output, but differed only in terms of the demands placed on visuomotor integration, allowing us to extract brain activation relevant for spatio-temporal prediction, motor coordination or motor imagery separately. In addition, our finding that parts of lobule VI were activated during spatio-temporal prediction is in line with the notion that our task included not merely motor output but also a cognitive aspect of the prediction of a complex motor sequence[41].

To confirm whether the hippocampal and cerebellar activations observed in the main effect analysis interact with each other in spatio-temporal prediction, we conducted a psychophysiological interaction analysis[26]. As we hypothesized, the functional connectivity analyses in spatio-temporal prediction showed that the left hippocampus connect extensively to several cerebellar lobules in the hemispheres; the left hippocampus connects to the bilateral hemispheric lobules VI, right hemispheric region in lobule VIIa Crus I, right side of lobule VIIIa and left side of lobule VIIIb. Participation of lobule VII and VIII is consistent with previous research in the context of spatio-temporal prediction in the perceptual judgement task[3]. In addition to the cerebellar regions, functional connectivity in hippocampus was found for visuomotor system (the angular gyrus, inferior occipital gyrus, inferior parietal lobule, inferior temporal gyrus, middle frontal gyrus, middle occipital gyrus, primary visual cortex (V1), ventral V4 (V4v), premotor cortex, superior parietal lobule). The premotor and parietal cortices are reported to involve in the implicit timing with cerebellum[2]. Indeed, a recent cerebellar-patient study with the perceptual judgement task that demands spatio-temporal prediction shows that the cerebellum acts to recalibrate predictive models from perceptual cues[42].

The main effect analysis and the functional connectivity analysis share lobule VI as the common cerebellar regions, in addition to the primary visual cortex. Since cerebellar lobule VI is commonly found activated in both sensorimotor and cognitive

processes[39,43,44], our results may indicate that the hippocampus contributes to establish spatio-temporal prediction by integrating complex motor execution and specific timing onsets in a network of several brain regions responsible for spatio-temporal processing while the cerebellum may contribute to optimize the spatio-temporal prediction that is highly required for accomplishing the task. To our knowledge, our data are the first demonstration of a hippocampal-cerebellar interaction during spatio-temporal prediction.

2.5.3 Functional implications of hippocampal-cerebellar interaction

Information about hippocampal-cerebellar functional interaction is scant. In the spatial domain, cerebellar impairment leads to malfunction of the spatial code (as determined by place cells) in the hippocampus, causing disorientation in a maze in circumstances where self-motion information from the cerebellum is required to navigate in the maze[5]. Spatial processing recruits lateralized regions within hippocampus and cerebellum; when sequential route-based navigation is required, the right cerebellar lobule VIIa and left hippocampus appear to form a functional loop together with the prefrontal cortex, whereas when map-based navigation is required the left cerebellar lobule VIIa and right hippocampus form a circuit with the parietal cortex[6,7].

In the temporal domain, however, little direct physiological evidence for the interaction of hippocampus and cerebellum has been reported although many studies including animal and human patient studies show either hippocampal or cerebellar involvement in processes of temporal information[3,12,45,46]. A recent study reported the synchronization of theta oscillations between hippocampus (CA1) and cerebellum in eyeblink conditioning[9] indicating that the hippocampus modulates the function of the cerebellum. In addition, eye blink conditioning in an fMRI study in humans showed that hippocampal activation is identified only during trace conditioning (the temporal gap between off set of conditioned stimulus and onset of unconditioned stimulus) while the cerebellar lobule VI activates in both trace conditioning and delay conditioning (in the

latter, the termination of the conditioned and unconditioned stimulus occurs simultaneously)[47]. From a theoretical aspect, a computational model of learning of adaptive timing proposes the interaction between the internal clock of the hippocampus and that of the cerebellum; the neural circuits of the hippocampus may modulate attention of cues, while the timing circuit ("internal clock") of the olivocerebellar system may control timing of motor planning and execution[48,49]. The hippocampal clock may thus cooperate with the cerebellar clock and its forward modeling[50], i.e. the internal model of motor timing, to learn the interval between the moving markers and the timing of motor execution and to predict the upcoming perceptual events.

Like for spatial processing, we found a lateralization of the interaction between hippocampus and cerebellum as the left side of hippocampus, the region implicated in spatio-temporal memory formation[6,7], was more strongly and extensively activated than its right counterpart in the main effect analysis; anatomically, the cerebellum connects preferentially with cerebral regions in a contralateral manner. Our results reveal functional interaction using left hippocampal seeds each with both ipsi- and contralateral cerebellar regions. Although we found hippocampal-cerebellar interaction during spatio-temporal prediction in the PPI analysis, a directional information flow (causal relationship) about hippocampal-cerebellar functional interaction remains obscure because PPI analysis cannot infer causality[26,51]. Classical studies using animal experiments have reported a bi-directional projection between cerebellum and hippocampus[15,52–54], yet anatomical connectivity between these structures remains ill understood; at the least, it appears multisynaptic, offering possibility for widespread and bilateral functional connectivity. Future analyses will need to use methods for determining the directional causality between hippocampus and cerebellum during spatio-temporal prediction, such as dynamic causal modeling (DCM)[55] or Granger causality, neither of which was suited for the current study design; alternatively, intervention studies using transcranial magnetic stimulation may provide a means to

unravel causal relationships, although current tools allow only to stimulate relatively superficial cortical and cerebellar areas.

In conclusion, we have shown here an interaction between hippocampus and cerebellum in the performance of a novel task requiring spatio-temporal prediction, or learning-dependent prediction timing. Future experiments and analyses will need to reveal the nature of the lateralization (e.g. using tasks requiring one or both hands, comparing the activations of spatial, temporal, and spatio-temporal prediction task, conducting patient studies with selective lesions to either hippocampal or cerebellar subfields) and the direction of information flow between hippocampus and cerebellum.

Table 1. Activations for spatio-temporal prediction, motor coordination, and motor imagery

(1) Spatio-temporal prediction

Region	t-value	Cluster size (voxels)	MNI coordinate			z-score
			x	y	z	
Primary Visual Cortex (V1) L	11.81	5964	-2	-76	-1	5.84
Cuneus R	11.33		2	-82	31	5.74
Secondary Visual Cortex (V2) R	11.3		8	-78	13	5.73
Hippocampus (*Subiculum*) L	7.64	115	-22	-32	-9	4.81
Cerebellum Lobule VI (Hem) L	7.2	64	-18	-64	-17	4.67
Cerebellum Lobule VI (Vermis)	6.23	73	0	-72	-27	4.31
Cerebellum Lobule VI (Hem) R	5.27	45	18	-60	-19	3.9

(2) Motor coordination

Region	t-value	Cluster size (voxels)	MNI coordinate			z-score
			x	y	z	
Cerebellum Lobule VI (Hem) L	9.53	644	-26	-62	-23	5.34
Cerebellum Lobule VI (Hem) R	9.08	600	24	-68	-23	5.22
Supplementary Motor Cortex R	8.37	360	6	6	51	5.03
Primary Somatosensory Cortex L	8.29	705	-46	-38	57	5.01
Precuneus L	8.17	489	0	-66	55	4.97
Primary Somatosensory Cortex R	7.4	379	46	-30	61	4.73
Cuneus L	6.62	331	2	-78	31	4.46
Premotor Cortex R	6.61	110	30	-6	57	4.46
Cerebellum Lobule V (Vermis) R	6.41	30	2	-54	-7	4.38
Cerebellum Lobule VIIIa (Hem) R	6.32	64	22	-62	-49	4.35

(3) Motor imagery

Region	t-value	Cluster size (voxels)	MNI coordinate			z-score
			x	y	z	
Lingual Gyrus (hOC3v, V3v) R	10.65	2206	24	-84	-7	5.6
Primary Visual Cortex (V1) R	9.5		8	-86	-5	5.33
Thalamus R	9.41	152	20	-12	-1	5.31
Caudate L	7.35	296	-16	-26	21	4.72
Middle Occipital Gyrus R	7.04	92	40	-66	3	4.61
Inferior Parietal Lobule L	6.05	167	-52	-30	43	4.24
Supplementary Motor Area L	5.09	97	-2	2	55	3.82
Cerebellum Lobule VI (Hem) L	5.75	68	-32	-54	-29	4.12
Superior Parietal Lobule (7A) L	5.6	123	-26	-60	61	4.05
Cerebellum Lobule VI (Hem) R	5.56	63	38	-58	-25	4.03

* $p < 0.0005$, uncorrected, spatial extent threshold is determined by family-wise error (FWE) correction for the multiple comparison at cluster level ($p < 0.05$). L, Left; R, Right.

Table 2. Functional Connectivity from hippocampus in the Spatio-Temporal Prediction

Functional Connectivity in the Spatio-Temporal Prediction (Seed region: left hippocampus [-22, -32, -9])						
			MNI coordinate			
Region	t-value	Cluster size (voxels)	x	y	z	z-score
Angular Gyrus R	8.86	1004	28	-54	45	5.16
Superior Parietal Lobule (7A) R	7.33		30	-66	55	4.71
Superior Parietal Lobule (7A) R	7.12		30	-58	67	4.64
Superior Parietal Lobule (7A) L	7.93	309	-28	-68	55	4.9
Inferior Parietal Lobule L	6.82	398	-42	-40	45	4.53
Middle Occipital Gyrus L	6.8	173	-24	-72	25	4.53
Middle Frontal Gyrus R	6.67	148	40	0	59	4.48
Primary Visual Cortex (V1) R	6.53	513	14	-92	-1	4.43
Cerebellum Lobule VIIa Crus I (Hem) R	6.37	33	46	-56	-31	4.37
Inferior Occipital Gyrus L	6.18	104	-40	-56	-5	4.29
Inferior Temporal Gyrus R	6.17	96	42	-56	3	4.29
Primary Visual Cortex (V1) L	6.16	153	-8	-90	3	4.29
Middle Occipital Gyrus L	6.1	158	-34	-84	5	4.26
Superior Parietal Lobule (7A) L	6.02	50	-26	-54	69	4.23
Premotor Cortex L	5.77	70	-44	-2	51	4.12
Ventral V4 (V4v) L	5.53	151	-34	-80	-13	4.02
Premotor Cortex L	5.49	94	-30	-8	65	4
Cerebellum Lobule VI (Hem) L	5.34	69	-30	-56	-27	3.94
Cerebellum Lobule VI (Hem) R	5.13	35	36	-62	-27	3.84
Cerebellum Lobule VIIIb (Hem) L	4.87	38	-16	-62	-49	3.71

* $p < 0.0005$, uncorrected, cluster size is corrected by FWE correction for the multiple comparison at cluster level at $p < 0.05$. L, Left; R, Right.

References

1. Assmus, A. *et al.* Left inferior parietal cortex integrates time and space during collision judgments. *Neuroimage* **20,** 82–88 (2003).
2. Coull, J. T. & Nobre, A. C. Dissociating explicit timing from temporal expectation with fMRI. *Curr. Opin. Neurobiol.* **18,** 137–144 (2008).
3. O'Reilly, J. X., Mesulam, M. M. & Nobre, A. C. The cerebellum predicts the timing of perceptual events. *J. Neurosci.* **28,** 2252–2260 (2008).
4. Burguière, E. *et al.* Spatial navigation impairment in mice lacking cerebellar LTD: a motor adaptation deficit? *Nat. Neurosci.* **8,** 1292–1294 (2005).
5. Rochefort, C. *et al.* Cerebellum Shapes Hippocampal Spatial Code. *Science (80-.).* **311,** 385–390 (2011).
6. Iglói, K., Doeller, C. F., Berthoz, A., Rondi-Reig, L. & Burgess, N. Lateralized human hippocampal activity predicts navigation based on sequence or place memory. *Proc. Natl. Acad. Sci.* **107,** 14466–14471 (2010).
7. Iglói, K. *et al.* Interaction between hippocampus and cerebellum crus i in sequence-based but not place-based navigation. *Cereb. Cortex* **25,** 4146–4154 (2015).
8. Takehara, K., Kawahara, S. & Kirino, Y. Time-dependent reorganization of the brain components underlying memory retention in trace eyeblink conditioning. *J. Neurosci.* **23,** 9897–9905 (2003).
9. Hoffmann, L. C. & Berry, S. D. Cerebellar theta oscillations are synchronized during hippocampal theta-contingent trace conditioning. *Proc. Natl. Acad. Sci. U. S. A.* **106,** 21371–6 (2009).
10. Wikgren, J., Nokia, M. S. & Penttonen, M. Hippocampo-cerebellar theta band phase synchrony in rabbits. *Neuroscience* **165,** 1538–1545 (2010).
11. Koekkoek, S. K. E. *et al.* Cerebellar LTD and Learning-Dependent Timing of Conditioned Eyelid Responses. *Science (80-.).* **301,** 1736–1739 (2003).
12. MacDonald, C. J., Lepage, K. Q., Eden, U. T. & Eichenbaum, H. Hippocampal 'time cells' bridge the gap in memory for discontiguous events. *Neuron* **71,** 737–49 (2011).
13. Ruediger, S. *et al.* Learning-related feedforward inhibitory connectivity growth required for memory precision. *Nature* **473,** 514–518 (2011).
14. Scelfo, B., Sacchetti, B. & Strata, P. Learning-related long-term potentiation of inhibitory synapses in the cerebellar cortex. *Proc. Natl. Acad. Sci. U. S. A.* **105,** 769–774 (2008).
15. WHITESIDE, J. A. & SNIDER, R. S. Relation of cerebellum to upper brain stem. *J. Neurophysiol.* **16,** 397–413 (1953).
16. Meister, I. G. *et al.* Playing piano in the mind--an fMRI study on music imagery and performance in pianists. *Brain Res. Cogn. Brain Res.* **19,** 219–28 (2004).
17. Ito, M. Control of mental activities by internal models in the cerebellum. *Nat. Rev. Neurosci.* **9,** 304–313 (2008).
18. Bird, C. M., Capponi, C., King, J. a., Doeller, C. F. & Burgess, N. Establishing the Boundaries: The Hippocampal Contribution to Imagining Scenes. *J. Neurosci.* **30,** 11688–11695 (2010).
19. Ghaem, O. *et al.* Mental navigation along memorized routes activates the hippocampus, precuneus, and insula. *Neuroreport* **8,** 739–744 (1997).
20. Sacco, K. *et al.* Motor imagery of walking following training in locomotor attention. The effect of 'the tango lesson'. *Neuroimage* **32,** 1441–1449 (2006).
21. Gobel, E. W., Parrish, T. B. & Reber, P. J. Neural correlates of skill acquisition: Decreased cortical activity during a serial interception sequence learning task. *Neuroimage* **58,** 1150–1157 (2011).
22. Diedrichsen, J. A spatially unbiased atlas template of the human cerebellum. *Neuroimage* **33,** 127–138 (2006).
23. Kleinschmidt, A., Buchel, C., Zeki, S. & Frackowiak, R. S. Human brain activity during spontaneous reversing perception of ambiguous figures. *Proc. R. Soc. London B Biol. Sci.* **265,** 2427–2433 (1998).
24. Eickhoff, S. B. *et al.* A new SPM toolbox for combining probabilistic cytoarchitectonic maps and functional imaging data. *Neuroimage* **25,** 1325–1335 (2005).
25. Diedrichsen, J., Balsters, J. H., Flavell, J., Cussans, E. & Ramnani, N. A probabilistic MR atlas of the human cerebellum. *Neuroimage* **46,** 39–46 (2009).

26. Friston, K. J. *et al.* Psychophysiological and modulatory interactions in neuroimaging. *Neuroimage* **6,** 218–229 (1997).
27. Spencer, R. M. C. & Ivry, R. B. in *Handbook of the Cerebellum and Cerebellar Disorders* (eds. Manto, M., Schmahmann, J. D., Rossi, F., Gruol, D. L. & Koibuchi, N.) 1201–1219 (Springer Netherlands, 2013).
28. Aso, K., Hanakawa, T., Aso, T. & Fukuyama, H. Cerebro-cerebellar interactions underlying temporal information processing. *J. Cogn. Neurosci.* **22,** 2913–2925 (2010).
29. Bares, M. *et al.* Impaired predictive motor timing in patients with cerebellar disorders. *Exp. brain Res.* **180,** 355–65 (2007).
30. Bares, M. *et al.* The Neural Substrate of Predictive Motor Timing in Spinocerebellar Ataxia. *The Cerebellum* **10,** 233–244 (2011).
31. Sadato, N., Yonekura, Y., Waki, A., Yamada, H. & Ishii, Y. Role of the supplementary motor area and the right premotor cortex in the coordination of bimanual finger movements. *J Neurosci* **17,** 9667–9674 (1997).
32. Witt, S. T., Laird, A. R. & Meyerand, M. E. Functional neuroimaging correlates of finger-tapping task variations: An ALE meta-analysis. *Neuroimage* **42,** 343–356 (2008).
33. Gerardin, E. *et al.* Partially overlapping neural networks for real and imagined hand movements. *Cereb. Cortex* **10,** 1093–1104 (2000).
34. Thompson, W. L., Kosslyn, S. M., Sukel, K. E. & Alpert, N. M. Mental imagery of high- and low-resolution gratings activates area 17. *Neuroimage* **14,** 454–464 (2001).
35. Richter, W. *et al.* Motor Area Activity During Mental Rotation Studied by Time-Resolved Single-Trial fMRI. *J. Cogn. Neurosci.* **12,** 310–320 (2000).
36. Parsons, L. M. *et al.* Use of implicit motor imagery for visual shape discrimination as revealed by PET. *Nature* **375,** 54–58 (1995).
37. Grodd, W., Hülsmann, E., Lotze, M., Wildgruber, D. & Erb, M. Sensorimotor mapping of the human cerebellum: fMRI evidence of somatotopic organization. *Hum. Brain Mapp.* **13,** 55–73 (2001).
38. Habas, C. *et al.* Distinct Cerebellar Contributions to Intrinsic Connectivity Networks. *J. Neurosci.* **29,** 8586–8594 (2009).
39. Stoodley, C. J. & Schmahmann, J. D. Evidence for topographic organization in the cerebellum of motor control versus cognitive and affective processing. *Cortex* **46,** 831–844 (2010).
40. Hanakawa, T. *et al.* Functional Properties of Brain Areas Associated With Motor Execution and Imagery Functional Properties of Brain Areas Associated With Motor Execution and Imagery. 989–1002 (2013). doi:10.1152/jn.00132.2002
41. Cross, E. S., Stadler, W., Parkinson, J., Schütz-Bosbach, S. & Prinz, W. The influence of visual training on predicting complex action sequences. *Hum. Brain Mapp.* **34,** 467–486 (2013).
42. Roth, M. J., Synofzik, M. & Lindner, A. The cerebellum optimizes perceptual predictions about external sensory events. *Curr. Biol.* **23,** 930–935 (2013).
43. Kelly, R. M. & Strick, P. L. Cerebellar loops with motor cortex and prefrontal cortex of a nonhuman primate. *J. Neurosci.* **23,** 8432–8444 (2003).
44. Stoodley, C. J. & Schmahmann, J. D. Functional topography in the human cerebellum: A meta-analysis of neuroimaging studies. *Neuroimage* **44,** 489–501 (2009).
45. Grube, M., Cooper, F. E., Chinnery, P. F. & Griffiths, T. D. Dissociation of duration-based and beat-based auditory timing in cerebellar degeneration. *Proc. Natl. Acad. Sci. U. S. A.* **107,** 11597–11601 (2010).
46. Ivry, R. B. The representation of temporal information in perception and motor control. *Curr. Opin. Neurobiol.* **6,** 851–857 (1996).
47. Cheng, D. T., Disterhoft, J. F., Power, J. M., Ellis, D. A. & Desmond, J. E. Neural substrates underlying human delay and trace eyeblink conditioning. *Proc. Natl. Acad. Sci.* **105,** 8108–8113 (2008).
48. Grossberg, S. & Merrill, J. W. L. The hippocampus and cerebellum in adaptively timed learning, recognition, and movement. *J. Cogn. Neurosci.* **8,** 257–277 (1996).
49. De Zeeuw, C. I. *et al.* Spatiotemporal firing patterns in the cerebellum. *Nat. Rev. Neurosci.* **12,** 327–344 (2011).
50. Wolpert, D. M., Miall, R. C. & Kawato, M. Internal models in the cerebellum. *Trends Cogn. Sci.* **2,** 338–347 (1998).
51. O'Reilly, J. X., Woolrich, M. W., Behrens, T. E. J., Smith, S. M. & Johansen-Berg, H. Tools of the trade: Psychophysiological interactions and functional connectivity. *Soc. Cogn. Affect. Neurosci.* **7,** 604–609 (2012).

52. Heath, R. G. & Harper, J. W. Ascending projections of the cerebellar fastigial nucleus to the hippocampus, amygdala, and other temporal lobe sites: Evoked potential and histological studies in monkeys and cats. *Exp. Neurol.* **45,** 268–287 (1974).
53. Newman, P. P. & Reza, H. Functional relationships between the hippocampus and the cerebellum: an electrophysiological study of the cat. *J. Physiol.* **287,** 405–26 (1979).
54. Snider, R. S. & Maiti, A. Cerebellar contributions to the papez circuit. *J. Neurosci. Res.* **2,** 133–146 (1976).
55. Friston, K. J., Harrison, L. & Penny, W. Dynamic causal modelling. *Neuroimage* **19,** 1273–1302 (2003).

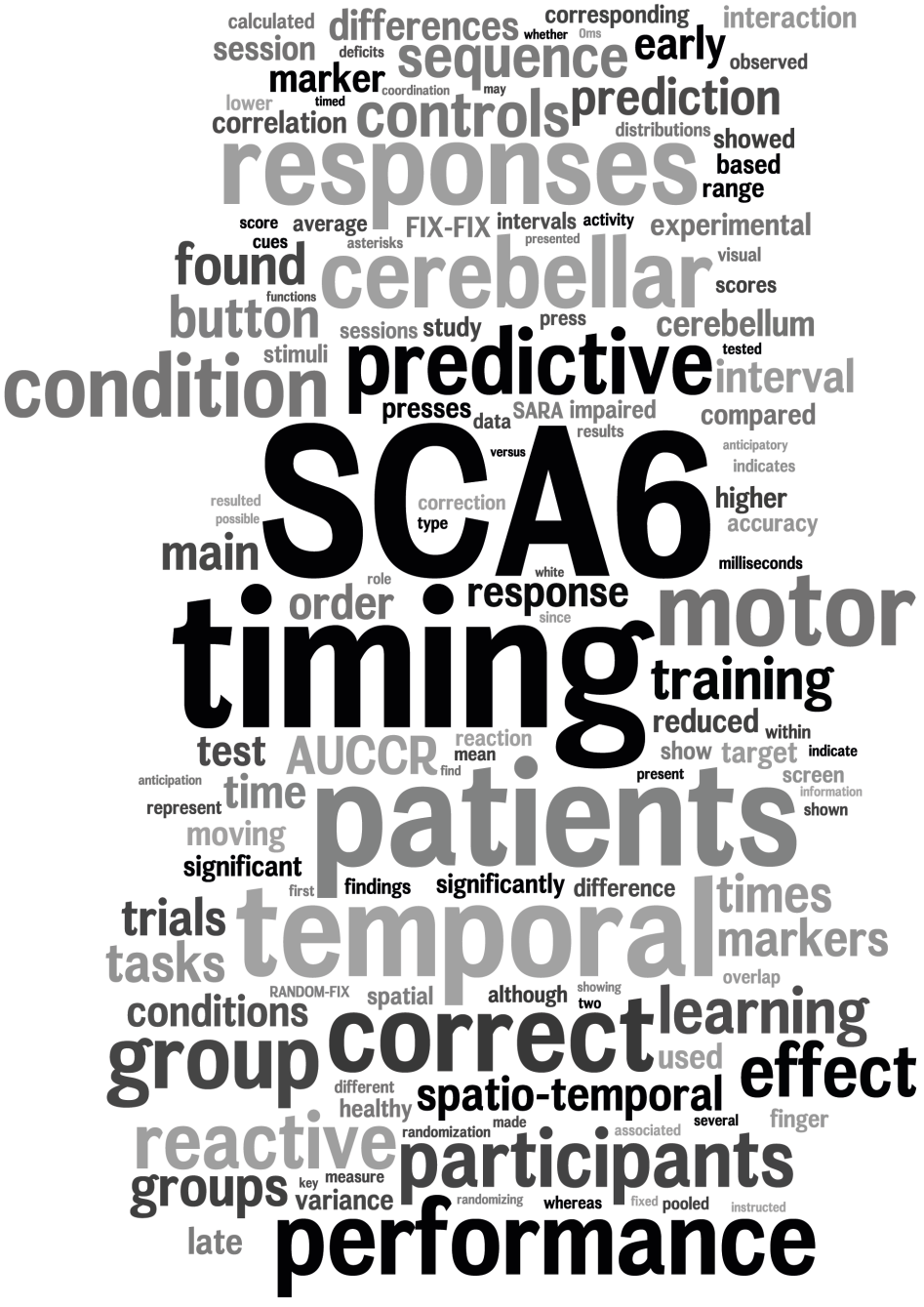
calculated
differences
corresponding
interaction
session
deficits
sequence
early
observed
marker
coordination
prediction
lower
timed
correlation
controls
distributions
showed
responses
based
range
score
average
FIX-FIX
intervals
activity
experimental
cues
asterisks
presented
found
cerebellar
visual
scores
functions
button
sessions
study
press
cerebellum
stimuli
predictive
tested
condition
interval
presses
data
SARA
impaired
compared
SCA6
results
anticipatory
versus
indicates
resulted
correction
higher
possible
type
accuracy
main
milliseconds
white
role
order
response
motor
timing
since
training
reduced
within
test
AUCCR
reaction
show
target
indicate
mean
find
present
screen
anticipation
time
information
represent
patients
shown
moving
significant
first
findings
significantly
difference
times
trials
temporal
markers
tasks
overlap
RANDOM-FIX
spatial
although
showing
conditions
two
learning
correct
group
used
effect
different
healthy
spatio-temporal
finger
reactive
randomization
made
associated
several
participants
groups
key
measure
variance
randomizing
whereas
fixed
pooled
instructed
late
performance

Chapter 3. Impaired spatio-temporal predictive motor timing associated with spinocerebellar ataxia type 6

Robin Broersen, Yoshiyuki Onuki, Abdel R. Abdelgabar, Cullen B. Owens, Samuel Picard, Jessica Willems, Henk-Jan Boele, Valeria Gazzola, Ysbrand D. Van der Werf, and Chris I. De Zeeuw

Published in:
PLOS ONE, 2016
DOI: 10.1371/journal.pone.0162

3.1 Abstract

Many daily-life activities demand precise integration of spatial and temporal information of sensory inputs followed by appropriate motor actions. This type of integration is carried out in part by the cerebellum, which has been postulated to play a central role in learning and timing of movements. Cerebellar damage due to atrophy or lesions may compromise forward-model processing, in which both spatial and temporal cues are used to achieve prediction for future motor states. In the present study, we sought to further investigate the cerebellar contribution to predictive and reactive motor timing, as well as to learning of sequential order and temporal intervals in these tasks. We tested patients with spinocerebellar ataxia type 6 (SCA6) and healthy controls for two related motor tasks; one requiring spatio-temporal prediction of dynamic visual stimuli and another one requiring reactive timing only. We found that healthy controls established spatio-temporal prediction in their responses with high temporal precision, which was absent in the cerebellar patients. SCA6 patients showed lower predictive motor timing, coinciding with a reduced number of correct responses during the 'anticipatory' period on the task. Moreover, on the task utilizing reactive motor timing functions, control participants showed both sequence order and temporal interval learning, whereas patients only showed sequence order learning. These results suggest that SCA6 affects predictive motor timing and temporal interval learning. Our results support and highlight cerebellar contribution to timing and argue for cerebellar engagement during spatio-temporal prediction of upcoming events.

3.2 Introduction

Many daily life activities demanding immediate timed motor responses require integration of spatial and temporal information at the millisecond range (*e.g.* hitting a ball when playing tennis). Our ability to continuously create predictions based on spatial and temporal cues ('spatio-temporal prediction') aids us to make timed, coordinated movements and perceptual judgments in relation to changes in our environment. Using functional magnetic resonance imaging (fMRI), we have shown that co-activation of cerebellum and hippocampus occurred during spatio-temporal prediction when healthy participants were asked to make precisely timed finger movements based on moving visual cues, whereas no co-activation occurred during reactive timing or motor imagery tasks[1]. Interestingly, the participants tended to press buttons slightly prior to the optimal timing of visual cues as learning progressed, indicating anticipation in their responses. Those findings suggest that the cerebellum and hippocampus cooperate to plan ahead and execute precise spatial and temporal motor responses. The exact cerebellar contribution to temporal aspects in this task however, remains uncertain. A previous study has shown that patients with spinocerebellar ataxia (SCA) are impaired at intercepting a moving target by performing a timed button press to launch another moving object for collision, a task also requiring spatio-temporal prediction[2]. Only patients with disorders that affect the cerebellum such as SCA type 6 and 8 and head essential tremor (ET), scored significantly worse on this predictive timing task when compared to those with other neurological disorders, such as Parkinson's disease[3]. During the same task, higher blood oxygenation level-dependent (BOLD) signals in several cerebellar regions as well as thalamus and multiple cortical areas were associated with successful performance. In fact, the activity change during successful trials in several cerebellar regions was found to be higher in controls compared to SCA patients, indicating a role for the cerebellum in spatio-temporal prediction during target interception[4]. In a velocity judgement task that required purely perceptual spatio-temporal prediction, the posterior cerebellar lobule VII crus I was engaged when both temporal and spatial cues, but not when only spatial cues were used.

Psychophysiological interactions (PPI) analysis further revealed that connectivity between the posterior cerebellum and several other upstream areas in the brain increased during spatio-temporal prediction in the perceptual domain[5]. This suggests that the cerebellum is important when integration of temporal information is required to complete the task goal.

Pioneering work to determine cerebellar contribution to timing processes has been done by Ivry and colleagues[6–9]. Their work has received support from multiple studies in which timing elements of tasks were used explicitly or implicitly, depending on whether participants were required to use an overt estimation of time or to use time as a by-product to reach the task goal, respectively[10]. Deficits at both explicit timing tasks (*e.g.* temporal discrimination, temporal reproduction and synchronized repetitive finger-tapping tasks) and implicit timing tasks (*e.g.* spatio-temporal trajectory prediction and serial prediction tasks) have been found in patients with cerebellar disorders[2,3,6,11–16]. These findings complement evidence from neuroimaging studies showing cerebellar activation associated with temporal processing[4,17–19]. Disrupted cerebellar activity would likely be accountable for the observed deficits in these patients. Tasks employing repetitive transcranial magnetic stimulation (rTMS) furthermore show that temporal processing can be disrupted by interfering with cerebellar activity[20,21]. Together, these studies strongly implicate the cerebellum as part of a wider neuronal network involved in timing functions[9].

In the present study, we investigated the role of the cerebellum in spatio-temporal prediction of moving visual stimuli. We tested patients with spinocerebellar ataxia type 6 (SCA6) and healthy age-matched controls on two related motor tasks: a predictive and a reactive motor timing task. This allowed us to study cerebellar contribution to predictive and reactive motor timing functions separately. We further employed an experimental design in which we randomized the sequence order of markers and temporal intervals between them so as to investigate cerebellar involvement in sequence order and temporal interval learning. We hypothesized that cerebellar

patients would show a reduced temporal precision in responses, coinciding with reduced performance on the task requiring spatio-temporal prediction, but not on the reactive timing task. Furthermore, we expected that cerebellar patients would be impaired at both sequence order and temporal interval learning. SCA6 patients form an adequate subject group to test these hypotheses, since the atrophy specifically affects the cerebellum in adults[22,23]. SCA6 is an autosomal dominant genetic disorder caused by a CAG repeat expansion in exon 47 of the CACNA1A gene, which encodes the α1A ($Ca_v2.1$) subunit of neuronal P/Q-type voltage-gated calcium channel. This causes essentially pure cerebellar atrophy with a profound loss of Purkinje cells[24] and manifests with a range of symptoms including imbalance, dysarthria, gait ataxia, upper limb incoordination and tremor[25,26].

Our main finding is that SCA6 patients failed to establish spatio-temporal prediction in timing of their responses, reflecting a deficit in motor anticipation to upcoming events. Whereas healthy participants timed their button presses on average before the optimal timing with better temporal precision, this anticipation was absent in SCA6 patients. Performance of patients was reduced during the predictive timing task, but this deficit was limited to early correct responses that were made during the anticipatory period of the task. On the reactive timing task, randomization of sequence order of stimuli and temporal intervals between them resulted in reduced performance of the healthy controls. In contrast, randomization of temporal intervals did not further reduce performance in SCA6 patients. In summary, our findings suggest that cerebellar dysfunction may impair spatio-temporal prediction and prevent temporal interval learning to occur. These findings lend support to leading views on cerebellar involvement in timing functions.

3.3 Subjects and methods

3.3.1 Participants

We tested 19 patients with spinocerebellar ataxia type 6 (SCA6) (mean age 61.8 ± 7.2, standard deviation (SD), range 49-80) and 14 healthy control participants (mean age 64.5 ± 4.7, SD, range 58-74) for this experiment. We attempted to achieve homogeneity across participants by using several exclusion criteria, including suffering from fatigue, neuropsychological disorders or expertise with musical instruments, since our task requires skills often used in, for example, piano and guitar playing. We excluded 7 patients from our analysis based on the occurrence of severe tremors (unilateral or bilateral) and/or excessive fatigue and 2 control participants based on technical issues of the behavioral task during the experiment. We included the remaining participants: 12 SCA6 patients (3 males; 2 left-handed) and 12 healthy control participants (7 males; 2 left-handed) in our data analysis. The average age of these SCA6 patients was 60.3 ± 6.4, SD (range 49-67) and 64.8 ± 4.8, SD (range 58-74) of control participants [$t_{22} = 1.985$, $P = 0.06$, two-sample *t*-test]. We did not detect significant correlations between age and performance on the predictive timing task ($r = 0.139$, $P = 0.517$, Pearson correlation) or performance on the reactive timing task ($r = -0.213$, $P = 0.318$, Pearson correlation). All participants met the criteria of normal or corrected-to-normal vision, no excessive computer gaming or playing musical instruments for more than five hours a week and no history of other neuropsychological or motor disorders at the time of measurements or in the past. Participants were instructed prior to measurements and a written informed consent was obtained from all participants. A neurological exam was performed by a certified neurologist prior to the experiment to obtain a measurement of severity of cerebellar ataxia, according to the guidelines of the Scale for the Assessment and Rating of Ataxia (SARA)[27]. The average SARA scores in SCA6 patients was 9.5 ± 5.2, SD on a scale of 0-40. This score is the average of scores on eight different subtasks, comprising an assessment of gait, stance, sitting, speech, finger and hand movements, and leg coordination. A score of 0 indicates that no neurological manifestations could be observed, whereas a score of 40 reflects the occurrence of

severe neurological manifestations[27]. This study was approved by the medical ethical committee of Erasmus MC, Rotterdam (MEC-2013-095).

3.3.2 Behavioral task

All participants completed the entire experiment, which included two modified versions of the Serial Interception Sequence Learning task[1,28]: a predictive timing task and a reactive timing task. In both tasks (Figure 1A and B), four empty white circles were placed on top of a gray rectangular background screen. Each of the white circles corresponded to four keys on a standard Qwerty-keyboard, which in turn were associated to a pre-determined finger: the 'e' key corresponded to the left middle finger, the 'f' key to the left index, the 'j' key to the right index and the 'o' key to the right middle. In the predictive timing task, participants were instructed to press the corresponding button on the keyboard at the moment upward moving black circles (moving markers) completely overlapped with the corresponding static white circles (target markers) at the top of the screen (Figure 1A). Only one moving marker could overlap with a target marker at a given moment. The diameter of the moving markers was 20 pixels smaller than that of the target marker to fit completely inside the target markers and not to interfere with the moment of the complete overlap between markers as observed by the participant. Moving markers scrolled from the bottom of the screen to the top at a constant velocity (2.78 milliseconds per pixel). In the reactive timing task, participants were instructed to press the corresponding button on the keyboard as quickly as possible when the white target marker changed (flashed) to red for 200 milliseconds (Figure 1B). Only one target marker could flash at a given moment. Between each trial, a short task instruction appeared on the screen for 3 seconds: *'Press on the corresponding button with your finger as soon as the circles entirely overlap'* and *'Press on the corresponding button with your finger as soon as a circle flashes'* (translated from Dutch), during the predictive and reactive task, respectively. The duration of this task instruction formed the only inter-trial interval time. Between each session, which lasted on average 7.9 ± 0.43 (SD) minutes participants took a short break (1-2 minutes)

to reduce physical and mental fatigue. No feedback to indicate correct responses was given during the task. Both tasks were programmed in MATLAB R2010a (MathWorks, Massachusetts, USA) using Psychtoolbox-3[29,30].

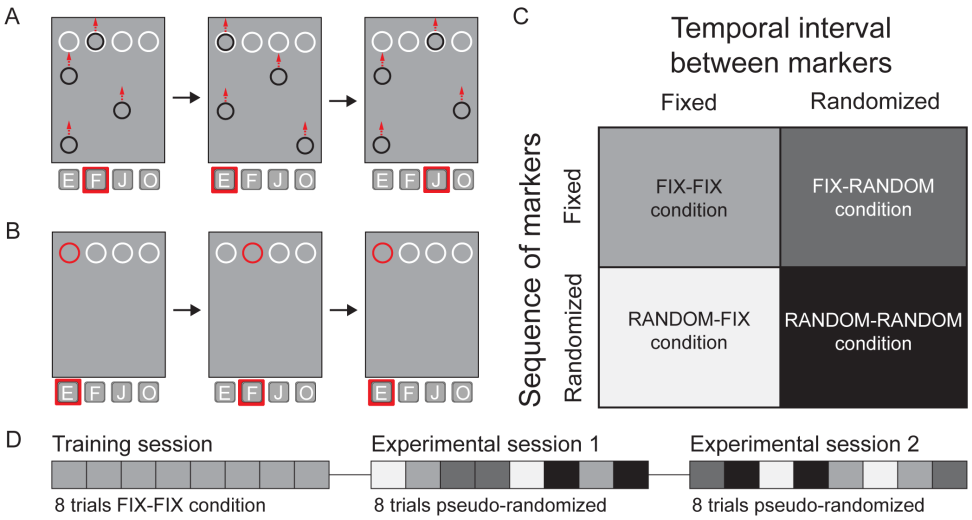

Figure 1. **Behavioral task and experimental conditions.** (A) During the predictive timing task black markers move from the bottom towards the four white target markers at the top of the screen. Participants are instructed to press the corresponding key at the moment that the black moving marker fully overlaps with the target marker (red square highlights the corresponding key). Target markers (from left to right) correspond to the 'e', 'f', 'j' and 'o' keys of a keyboard. (B) In the reactive timing task the white target markers change color to red for 200ms and participants are instructed to press the corresponding key as fast as possible. (C) Trials have one of four possible task conditions based on the sequence of and temporal interval between markers (fixed or randomized). (D) Both in the reactive timing task and predictive timing task, participants first complete a training session containing 8 trials of the FIX-FIX condition (*i.e.* fixed sequence and fixed interval), followed by two experimental sessions in which 2 trials of each condition are presented in a pseudo-randomized order.

3.3.3! Task conditions

We studied the role of the cerebellum in sequence and temporal interval learning by employing in both tasks a 2-by-2 factorial task design with two factors: the sequential order of stimuli and temporal interval between them. The sequences of moving markers (or marker flashes) and the temporal intervals between stimuli were either according to a pre-defined order (FIX) or shuffled based on thepre-defined order (RANDOM)(Figure1C). The combination of these resulted in four task conditions: FIX-FIX (*i.e.* fixed sequence

and fixed intervals), FIX-RANDOM, RANDOM-FIX, and RANDOM-RANDOM. For each condition, a sequence of 12 circles was presented 4 consecutive times, which resulted in 48 moving or flashing markers that were presented during each trial. In FIX-FIX condition of the predictive timing task, the sequence of moving markers followed the same order 4 consecutive times: F_{1386ms}-E_{718ms}-J_{852ms}-E_{852ms}-O_{852ms}-E_{702ms}-J_{969ms}-F_{952ms}-J_{1887ms}-O_{668ms}-F_{1420ms}-O_{668ms} (E: left-most trajectory, F: second trajectory, J: third trajectory, O: right-most trajectory, subscripted rates: temporal differences between moving markers in milliseconds). In FIX-FIX condition of the reactive timing task, the sequence of the marker flashes was E_{707ms}-F_{1345ms}-E_{1078ms}-O_{849ms}-J_{1200ms}-F_{703ms}-O_{1490ms}-E_{844ms}-J_{1824ms}-O_{1180ms}-F_{811ms}-J_{1075ms}. The average temporal interval between appearances was 1001 milliseconds (range 668-1887 milliseconds) in the predictive timing task and 1092 milliseconds (range 703-1824 milliseconds) in the reactive timing task.

3.3.4 Experimental protocol

All experiments were conducted in the participants' homes. A 13 or 15 inch computer screen was used to present the visual stimuli with a resolution of 1280 x 800 pixels (13 inch screen: all SCA6 patients and 4 out of 12 control participants). To rule out that screen size had an effect on performance, we compared performance on both tasks of controls tested using a 13 inch screen (N = 4) versus controls tested using a 15 inch screen (N = 8). We did not find significant differences between these controls on both the predictive timing task [$t_{10} = 0.981$, $P = 0.35$, two-sample *t*-test] and on the reactive timing task [$t_{10} = 0.869$, $P = 0.405$]. Participants were instructed prior to the experiment by an information letter mailed in advance. The tasks were also verbally explained to the participants right before starting the tasks. A summary of the instructions was finally displayed on the screen before the task began. When participants confirmed they fully understood the tasks, we started the experiment. Each task consisted of one training session and two experimental sessions. During the training session, eight trials with the FIX-FIX condition were presented. In each experimental session, each task condition was presented twice in a pseudo-randomized order using randomization algorithms in

MATLAB (Figure 1D). All SCA6 patients and 5 out of 12 control participants started with the predictive timing task, followed by the reactive timing task as part of an experimental sequence. The remaining control participants (N = 7) first started with the reactive timing task, directly followed by the predictive timing task. To rule out that the order of tasks had an effect on performance, we compared performance on both tasks of controls tested first on the predictive task (N = 5) versus controls tested first on the reactive task (N = 7). We did not find significant differences between these controls on both the predictive timing task [t_{10} = 0.157, P = 0.878, two-sample t-test] and on the reactive timing task [t_{10} = 0.727, P = 0.484, two-sample t-test].

3.3.5 Analysis of behavioral data

Classification of correct responses depended on two factors, pressing the corresponding button and pressing the button within a given time window. To maximize the sensitivity of analyzing responses within a set time window, we calculated performance as the area under the curve of the correct ratio (AUCCR). The correct ratio was defined as the number of corresponding (correct) button presses within a time window, divided by the total number of markers within a trial. The minimum temporal interval between markers was 668 milliseconds in the predictive timing task and 703 milliseconds in the reactive timing task. Based on these minimum times, we used a time window between -334ms to +334ms relative to perfect marker overlap in the predictive timing task and 0 to 703ms after marker flash in the reactive timing task throughout our analysis. To assess spatio-temporal prediction in the predictive timing task, we calculated the AUCCR before marker overlap (-334ms to < 0ms) representing early correct responses and after marker overlap (> 0ms to +334ms), representing late correct responses. We ascertained normality of data distributions using the Shapiro-Wilk test. Unless indicated otherwise, we used one-way repeated measures analyses of variance (ANOVA) with trial number (for training sessions) or trial condition (for experimental sessions) as within-subject variable and group as between-subject variable to test AUCCR on both reactive and predictive tasks. We used the Mauchly's test to test the assumption of sphericity and in

case this assumption was violated, we applied the Greenhouse-Geisser correction. Levene's test of equality of error variances was used to test whether the assumption of equal error variances was met. To analyze pooled response and reaction times, we used the non-parametric Wilcoxon rank sum test and Wilcoxon signed rank test with Bonferroni correction for multiple comparisons, since these distributions violated the assumption of normality. We compared variances of these distributions using the Brown-Forsythe test. Comparison of the first principal component (PC1) of the AUCCR of both tasks was done using independent-samples *t*-tests and a correlation analysis was performed using the Pearson correlation. These performance measures were also used in the methods section to test for effects of age, screen size and task order. Statistics were conducted in SPSS version 22 (IBM, New York, USA) and MATLAB R2011b (MathWorks, Massachusetts, USA). Results are reported as mean ± standard error of the mean (SEM), unless indicated otherwise.

3.4 Results

3.4.1 SCA6 patients show lower predictive motor timing perfo-rmance, localized to early correct responses

We used area under the curve of the correct ratio (AUCCR) to analyze performance of responses made within a temporal window around complete marker overlap (-334ms to +334ms; all correct responses). Over the course of the training session, both SCA6 patients and controls learned the sequence and timings of the markers (Figure 2A). Controls showed a significantly higher AUCCR compared to SCA6 patients during the training session, indicating that controls made more correct button presses within the assigned time window [main effect of trials: $F_{7,154} = 7.44$, $P < 0.001$; main effect of group: $F_{1,22} = 10.23$, $P < 0.01$; interaction trials x group: $F_{7,154} = 0.87$, $P = 0.53$]. To assess the effect of spatio-temporal prediction in our task, we segregated the data based on the time of button press. Early and late correct responses are corresponding button responses made before or after the moving marker completely overlapped with the target marker, respectively (Figure 2B and C). When analyzing early correct responses we found that

controls showed a significantly higher AUCCR compared to SCA6 patients, although both groups showed a learning effect [main effect of trials: $F_{7,154} = 10.67$, $P < 0.001$; main effect of group: $F_{1,22} = 15.56$, $P = 0.001$; interaction trials x group: $F_{7,154} = 1.25$, $P = 0.28$]. In contrast, for late correct responses we found no significant differences in AUCCR between groups and no learning effect [main effect of trials: $F_{3.313,\ 72.883} = 0.71$, $P = 0.56$; main effect of group: $F_{1,22} = 0.02$, $P = 0.89$; interaction trials x group: $F_{3.313,\ 72.883} = 2.4$, $P = 0.23$, with Greenhouse-Geisser correction]. A third comparison including all factors revealed a significant interaction between groups and type of correct response (early versus late), confirming that the observed group difference was localized to early correct responses only [$F_{1,\ 22} = 10.09$, $P = 0.004$, with Greenhouse-Geisser correction; two-way repeated measures ANOVA]. In short, our data shows a performance difference between SCA6 patients and healthy controls during training on the predictive timing task, which is localized to (early) correct responses made during the anticipatory period of the paradigm.

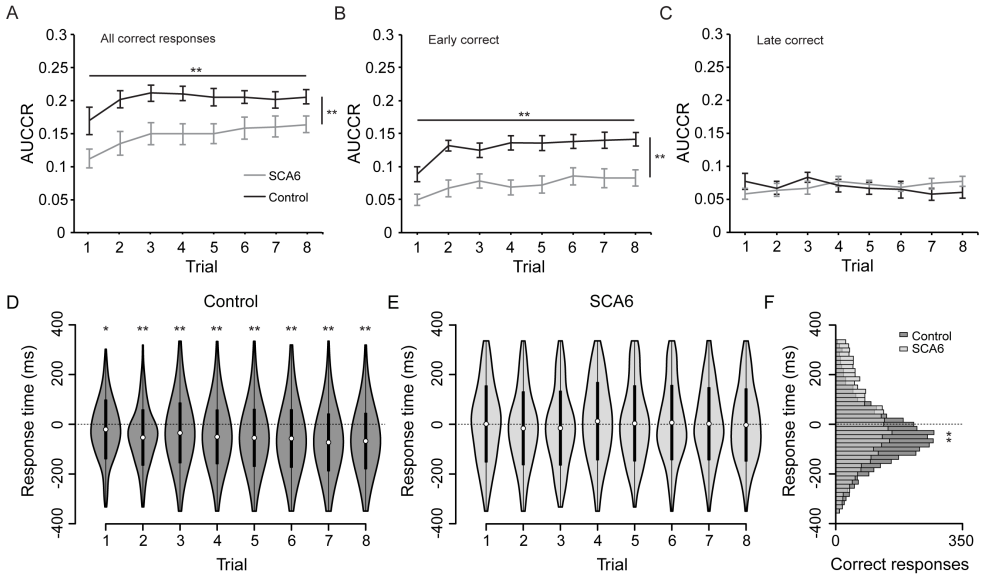

Figure 2. Results training session of predictive timing task. (A) Task performance showing all correct responses, expressed as area under the curve of the correct ratio (AUCCR) for both controls and SCA6 patients, showing a learning effect and a difference between groups. (B) AUCCR of early correct responses only, where the learning effect and group differences are present. (C) AUCCR of late correct responses only, where no learning effect or group differences are present. (D) Response times distributions of correct button presses of controls. Average response times are significantly lower than 0ms on all trials (*asterisks*). (E) Response times distributions of correct button presses of SCA6 patients. Average response times are not significantly different from 0ms on any of the trials. (F) Distribution of pooled response times for all training trials, showing that controls time their button press more precisely as observed by a smaller variance compared to SCA6 patients (*asterisks*). (A, B, C) Error bars represent SEM, ** indicates $P < 0.01$ for main effects of trials (*asterisks* horizontal line) and main effects of group (*asterisks* vertical line). (D, E) White dots represent the mean and black bars represent the SD. (F) Histogram shows 16.7ms bins. * indicates $P < 0.05$, ** indicates $P < 0.01$.

3.4.2 SCA6 patients show impaired anticipation in motor timing

To gain insight in the characteristics of motor timing in the predictive task, we visualized response time distributions of correct button presses of both controls and SCA6 patients (Figure 2D and E). Negative and positive response times correspond to button presses before and after perfect marker overlap, respectively. We pooled response times of correct button presses from all participants per group, since some SCA6 patients had only few correct responses per trial. This resulted in analyses based on a fixed template design. We calculated average response times for each trial of the training session: trial 1

[SCA6: 2.7 ± 154.8ms, control: -20.2 ± 120.3ms; mean ± SD], trial 2 [SCA6: -15.9 ± 148.3ms, control -51.9 ± 113.3ms], trial 3 [SCA6: -14.8 ± 150.3ms, control: -33.9 ± 122.2ms], trial 4 [SCA6: 12.1 ± 157.4ms, control: -49.1 ± 110ms], trial 5 [SCA6: 4.5 ± 152.8ms, control: -53.2 ± 116.6ms], trial 6 [SCA6: 6.9 ± 151.2ms, control: -55.9 ± 117.8ms], trial 7 [SCA6: 1.7 ± 147ms, control: -71.1 ± 116.3ms] and trial 8 [SCA6: -1.4 ± 147ms, control: -65.8 ± 113.5ms]. We found that response times of control participants were significantly lower than those of SCA6 participants on all trials, except on trial 1 and 3 [trial 1: mean difference (MD) = 22.9ms, Z = 2.42, $P = 0.12$; trial 2: MD = 36ms, Z = 4.26, $P < 0.001$; trial 3: MD = 19.1ms, Z = 2.53, $P = 0.09$; trial 4: MD = 61.2ms, Z = 7.0, $P < 0.001$; trial 5: MD = 57.7ms, Z = 6.22, $P < 0.001$; trial 6: MD = 62.8ms, Z = 7.24, $P < 0.001$; trial 7: MD = 72.8ms, Z = 8.37, $P < 0.001$; trial 8: MD = 64.4ms, Z = 7.31, $P < 0.001$; Wilcoxon rank sum test, with Bonferroni correction].

Previous findings have indicated that healthy participants establish spatio-temporal prediction during the training session of this predictive timing task[1], as indicated by average response times lower than 0ms. Indeed, this effect was also present in our control group, since we found that response times were significantly lower than 0ms on all trials of the training session [trial 1: Z = -2.84, $P = 0.04$; trial 2: Z = -9.51, $P < 0.001$; trial 3: Z = -6.5, $P < 0.001$; trial 4: Z = -9.46, $P < 0.001$; trial 5: Z = -9.85, $P < 0.001$; trial 6: Z = -10.16, $P < 0.001$; trial 7: Z = -12.13, $P < 0.001$; trial 8: Z = -11.65, $P < 0.001$; Wilcoxon signed rank test, with Bonferroni correction](Figure 2D). In contrast, we did not find this effect in our SCA6 patient group, given that average response times of SCA6 patients were not different from 0ms on any of the training trials [trial 1: Z = -0.51, $P = 1$; trial 2: Z = -1.87, $P = 1$; trial 3: Z = -1.93, $P = 1$; trial 4: Z = -1.84, $P = 1$; trial 5: Z = -0.27, $P = 1$; trial 6: Z = -0.66, $P = 1$; trial 7: Z = -0.37, $P = 1$; trial 8: Z = -0.24, $P = 1$; Wilcoxon signed rank test, with Bonferroni correction](Figure 2E). These findings indicate that spatio-temporal prediction is established during the training session in control participants, but not in SCA6 patients.

3.4.3 SCA6 patients show reduced temporal precision in predictive motor timing

Since participants were instructed to time their button presses as closely as possible to perfect marker overlap, we investigated whether both groups were able to correctly time their button press. Therefore, we assessed whether there were differences in response time distributions between groups with variance as a measure of precision. A lower variance of response times would indicate a higher precision, whereas a higher variance would suggest a more temporally distributed response pattern, indicating a lower precision. To address this question, we compared the variance of pooled response time distributions of the training session between groups using the Brown-Forsythe test of variances, since this test is relatively robust and insensitive to deviations from normality[31]. We found that SCA6 patients showed a significantly higher variance of response times compared to controls [SCA6: 2.284×10^4 ms^2, control: 1.371×10^4 ms^2, $F_{1,5808.03} = 239.98$, $P < 0.001$] (Figure 2F). To verify that this difference was also present during the experimental sessions, we compared the variance of pooled response times of correct responses during the experimental sessions and we found that also here controls had a significantly higher variance [SCA6: 2.195×10^4 ms^2, control: 1.352×10^4 ms^2, $F_{1, 14580.35} = 239.98$, $P < 0.001$]. These results indicate that correct button presses were more temporally distributed in the SCA6 group, corresponding to a lower temporal precision of responses during both training and experimental sessions. Together, these findings suggest that healthy participants anticipate the upcoming event of a marker overlap with better temporal precision, whereas this anticipation of motor timing from the spatial and temporal cues is impaired in SCA6 patients.

3.4.4 Sequential or temporal order randomization of markers does not affect predictive motor timing performance

We investigated sequential order and temporal interval learning by randomizing the order and temporal intervals of markers, resulting in four conditions that were

presented during experimental sessions (Fig 1C and D). We calculated the AUCCR for both groups during different trial conditions: FIX-FIX condition [SCA6: 0.18 ± 0.01, control: 0.21 ± 0.013], FIX-RANDOM condition [SCA6: 0.178 ± 0.011, control: 0.208 ± 0.012], RANDOM-FIX condition [SCA6: 0.183 ± 0.011, control: 0.208 ± 0.011] and RANDOM-RANDOM condition [SCA6: 0.177 ± 0.01, control: 0.204 ± 0.011]. No significant differences in AUCCR between trial conditions or between groups where found, although the main effect of group approached the significance level and could be considered a trend (Figure 3A). Moreover, there was no interaction effect between conditions and groups [main effect of condition: $F_{3,66} = 0.82$, $P = 0.49$; main effect of group: $F_{1,22} = 3.46$, $P = 0.08$; interaction group x condition: $F_{3,66} = 0.31$, $P = 0.82$]. Therefore, we conclude from these data that randomizing sequences or temporal interval of markers did not lead to differences in performance or overall group differences when considering all correct responses.

Since we had found group differences in predictive motor timing for early correct responses during training (Figure 2B), we hypothesized that specifically these 'anticipatory' responses could be affected by randomization of sequence or temporal interval of markers. Therefore, we analyzed the data based on the timing of button presses and compared performance between conditions and groups (Fig 3B and C). We calculated the AUCCR of early correct responses on the FIX-FIX condition [SCA6: 0.091 ± 0.012, control: 0.139 ± 0.011], FIX-RANDOM condition [SCA6: 0.096 ± 0.012, control: 0.141 ± 0.009], RANDOM-FIX condition [SCA6: 0.099 ± 0.01, control: 0.144 ± 0.009], and RANDOM-RANDOM condition [SCA6: 0.091 ± 0.008, control: 0.137 ± 0.007] and we found that AUCCR differed significantly between groups. However, randomizing the sequence or temporal interval of markers did not lead to performance differences [main effect of condition: $F_{3,66} = 1.94$, $P = 0.132$; main effect of group: $F_{1,22} = 11.95$, $P = 0.002$; interaction group x condition: $F_{3,66} = 0.38$, $P = 0.99$] (Figure 3B). In addition, we investigated whether randomization had an effect on performance for late correct responses (Figure 3C). We calculated the AUCCR during the FIX-FIX condition [SCA6: 0.084 ± 0.007, control: 0.069 ± 0.01], FIX-RANDOM condition [SCA6: 0.079 ± 0.009,

control: 0.064 ± 0.009], RANDOM-FIX condition [SCA6: 0.08 ± 0.007, control: 0.061 ± 0.009], and RANDOM-RANDOM condition [SCA6: 0.082 ± 0.009, control: 0.065 ± 0.008] and performed the same analysis. We found that AUCCR of late correct responses did not differ between groups or between conditions. Also, the data did not reveal an interaction effect [main effect of condition: $F_{3,66} = 1.25$, $P = 0.30$; main effect of group: $F_{1,22} = 2.09$, $P = 0.16$; interaction group x condition: $F_{3,66} = 0.17$, $P = 0.92$]. A third analysis including all factors confirmed that the significant group difference was localized to early correct responses only [interaction group x type of correct response (early versus late): $F_{1,22} = 10.01$, $P = 0.004$; two-way repeated measures ANOVA]. Thus, although there were group differences in early correct responses, randomizing the order and temporal intervals of markers did not influence predictive motor timing performance regardless of the timing of responses.

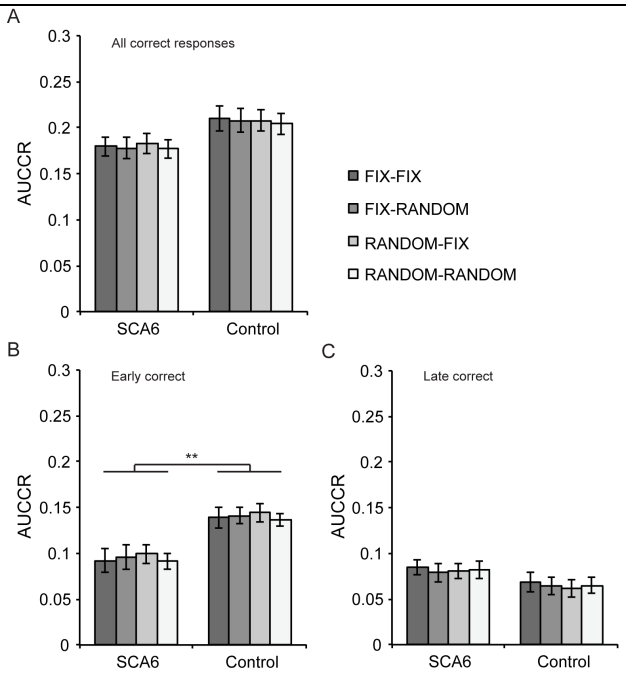

Figure 3. Results experimental sessions of predictive timing task. (A) Task performance on different trial conditions is visualized for both SCA6 patients and controls. No differences between groups or between conditions are observed in all correct responses. (B) AUCCR calculated for early correct responses shows a significant group difference between SCA6 patients and controls, but not between conditions. (C) AUCCR calculated for late correct responses does not show any differences between conditions or between groups. Error bars represent SEM, ** indicates $P < 0.01$.

3.4.5 Lower predictive motor timing performance of SCA6 patients is limited to responses during the anticipatory period

To further compare performance of groups depending on the timing of response, but regardless of the trial condition, we conducted a principal component analysis (PCA) for dimension reduction. AUCCR scores for early correct responses between trial conditions were highly inter-correlated, at least $r = 0.91$ [$P < 0.001$, Pearson correlation]. Kaiser-Meyer-Olkin measure of sampling adequacy was 0.87, Bartlett's test of sphericity was significant [$\chi^2(6) = 142.67$, $P < 0.001$] and all communalities were above 0.94, confirming that this data was suitable for PCA. We found that the first principal component (PC1) explained 95% of the variance and therefore we used this measure to

represent performance of early correct responses. Next, we subjected AUCCR scores for late correct responses to PCA and consistently found a high inter-correlation between performance on different conditions [at least $r = 0.85$, $P < 0.001$, Pearson correlation]. Kaiser-Meyer-Olkin measure of sampling adequacy was 0.87, Bartlett's test of sphericity was significant [$\chi^2(6) = 101.11$, $P < 0.001$] and all communalities were above 0.87. We found that the first principal component (PC1) explained 90.1% of the variance and therefore we used this measure to represent performance of late correct responses. We then used these measures to compare performance between groups, depending on the timing of response, regardless of the trial condition. We found a significant interaction effect between performance (PC1 of early vs late) and group [$F_{1,22} = 9.76$, $P = 0.005$], although the main effect for group in this analysis did not reach the significance level [$F_{1,22} = 3.65$, $P = 0.069$]. *Post-hoc* tests confirmed that the group difference was localized to PC1 of early correct responses, but not to PC1 of late correct responses [early: $t_{22} = 3.34$, $P = 0.006$; late: $t_{22} = -1.44$, $P = 0.328$, two-sample *t*-test with Bonferroni correction]. In summary, although task performance was not influenced by randomization of sequences or temporal intervals, we observed a higher performance of early correct responses in controls only, which is in line with our results from the training session.

3.4.6 SCA6 patients and controls perform comparably during reactive timing task training

To investigate whether SCA6, in addition to predictive motor timing, also affected reactive motor timing functions, we tested all participants on a related reactive motor timing task where no prediction could be made based on visual cues. We calculated AUCCR of corresponding button presses made after marker flash (0-703ms) as performance measure during the training session, in which eight trials of the FIX-FIX condition were presented (Figure 1D). Since this task was purely reactive, we did not make a distinction between early and late responses. Both groups showed learning of the task, evidenced by an increase in AUCCR over the course of the training (Figure 4A). We did not observe a group difference, although P-value approximation to significance

threshold suggested a trend. We also did not observe an interaction effect between groups and trials [main effect of trials: $F_{7,154} = 9.88$, $P < 0.001$; main effect of group: $F_{1,22} = 3.47$, $P = 0.076$; interaction trials x group: $F_{7,154} = 1.41$, $P = 0.21$]. In short, both groups increased their performance during the training, and overall there were no training differences between groups in this respect.

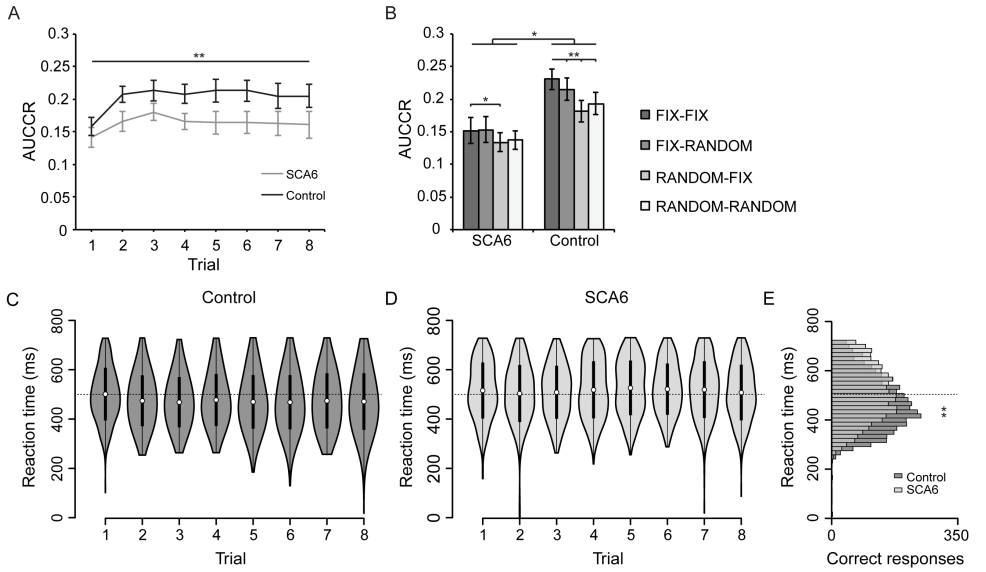

Figure 4. Results of reactive timing task. (A) Task performance expressed as AUCCR of correct responses after marker flash for both controls and SCA6 patients, showing that learning occurs over the course of the trials (*asterisks* horizontal line). (B) AUCCR calculated for different trial conditions during experimental sessions. The data shows group differences, as well as differences between all conditions with the FIX-FIX condition in the control group, but only between the RANDOM-FIX and the FIX-FIX condition in the SCA6 group. (C) Reaction time distributions of correct button presses during training for controls and (D) for SCA6 patients. (F) Distribution of pooled reaction times for all training trials. Variance of the reaction time distribution was smaller in controls (*asterisks*). (A, B) Error bars represent SEM, * indicates $P < 0.05$, ** indicates $P < 0.01$ for main effects of trials (*asterisks* horizontal line panel A) and main effects of condition and group (*asterisks* panel B). (D, E) Dotted line indicates 500ms for visual aid, white dots represent the mean and black bars represent the SD. (F) Histogram shows 16.7ms bins. ** indicates $P < 0.01$.

3.4.7 SCA6 patients and controls show differences in reaction times and precision during reactive timing task training

We visualized reaction time distributions of the reactive timing task, showing development of reaction times of both groups over the training session (Figure 4C and

D). We then calculated average reaction times of pooled correct responses on all trials of the training session: trial 1 [SCA6: 518.9 ± 113.8ms, control: 499.8 ± 107ms; mean ± SD], trial 2 [SCA6: 506.8 ± 115.8ms, control 477.4 ± 103.4ms], trial 3 [SCA6: 510 ± 107.6ms, control: 471.5 ± 102ms], trial 4 [SCA6: 521.6 ± 115.9ms, control: 480.4 ± 105.3ms], trial 5 [SCA6: 529.4 ± 111ms, control: 473.1 ± 108.8ms], trial 6 [SCA6: 524.2 ± 104ms, control: 471.7 ± 110.1ms], trial 7 [SCA6: 522.4 ± 115.5ms, control: 475.2 ± 112.2ms] and trial 8 [SCA6: 510.4 ± 112.9ms, control: 474.3 ± 115ms]. Significantly higher reaction times for SCA6 patients were observed for all trials, except for trial 1 [trial 1: mean difference (MD) = 19.1ms, Z = 2.49, $P = 0.1$; trial 2: MD = 29.4ms, Z = 4.34, $P < 0.001$; trial 3: MD = 38.5ms, Z = 5.64, $P < 0.001$; trial 4: MD = 41.1ms, Z = 5.56, $P < 0.001$; trial 5: MD = 56.3ms, Z = 7.62, $P < 0.001$; trial 6: MD = 52.5ms, Z = 7.3, $P < 0.001$; trial 7: MD = 47.2ms, Z = 6.2, $P < 0.001$; trial 8: MD = 36.1ms, Z = 4.78, $P < 0.001$; Wilcoxon rank sum test, with Bonferroni correction].

Next, we compared variances of pooled reaction times of correct button presses during training between groups and found a small but significant difference in variance, in which the SCA6 patient group showed a higher variance [SCA6: 1.258×10^4 ms^2, control: 1.172×10^4 ms^2, $F_{1,7107.19} = 249.6$, $P < 0.001$, Brown-Forsythe test of variances] (Figure 4E). We did the same analysis for pooled reaction times during the experimental sessions and found a consistent difference in variance between groups [SCA6: 1.342×10^4 ms^2, control: 1.163×10^4 ms^2, $F_{1,13277.38} = 200.21$, $P < 0.001$]. Together, these results indicate that average reaction times were significantly higher for SCA6 patients compared to controls. Furthermore, SCA6 patients also consistently showed a mildly reduced temporal precision, based on the observation that correct responses were more widely temporally distributed within this group.

3.4.8 SCA6 patients show impaired learning of temporal interval order

We hypothesized that SCA6 patients would be impaired at learning of sequences and temporal intervals of stimuli on the reactive timing task. In addition, controls could potentially use this type of learning as strategy to gain increased performance on conditions using fixed sequence or temporal intervals. To test this hypothesis, we visualized the AUCCR during FIX-FIX condition [SCA6: 0.152 ± 0.02, control: 0.231 ± 0.016], FIX-RANDOM condition [SCA6: 0.153 ± 0.02, control: 0.215 ± 0.017], RANDOM-FIX condition [SCA6: 0.134 ± 0.015, control: 0.181 ± 0.014], and RANDOM-RANDOM condition [SCA6: 0.138 ± 0.014, control: 0.193 ± 0.017] (Figure 4B). Using a repeated measures ANOVA we found a main effect of groups, as well as a main effect of condition and an interaction effect [main effect of condition: $F_{1.71, 37.56} = 22.82$, $P < 0.001$; main effect of group: $F_{1,22} = 7.1$, $P = 0.014$; interaction condition x group: $F_{1.71,37.56} = 4.12$, $P = 0.03$, with Greenhouse-Geisser correction]. Closer inspection of only SCA6 performance furthermore showed a main effect of condition [$F_{1.56,\ 17.15} = 4.29$, $P < 0.039$, with Greenhouse-Geisser correction]. Planned contrasts comparing FIX-FIX condition with the other conditions revealed that the difference was located between the FIX-FIX condition and the RANDOM-FIX condition [$F_{1,11} = 6.23$, $P = 0.03$]. Performance of control participants also showed a significant main effect of condition [$F_{3,33} = 23.45$, $P < 0.001$] and contrasts indicated that AUCCR on the FIX-FIX condition was significantly higher compared to all other conditions [versus FIX-RANDOM: $F_{1,11} = 15.49$, $P = 0.002$; versus RANDOM-FIX: $F_{1,11} = 72.05$, $P < 0.001$; versus RANDOM-RANDOM: $F_{1,11} = 21.02$, $P = 0.001$] (Figure 4B). Together, these results show that although overall performance was reduced in the SCA6 patient group, randomizing the sequential order of stimuli resulted in reduced performance in both groups, suggesting that sequential order learning occurred in both groups. In contrast, randomizing the temporal interval order resulted in reduced performance only in the control group, but not in the SCA6 patient group. This suggests that only controls learned the temporal order of stimuli sufficiently, whereas this type of learning was reduced in SCA6 patients.

Complementary to the predictive timing task, we performed a PCA on AUCCR scores of all trial conditions to compare performance on groups independent of trial condition. Scores on all conditions were highly inter-correlated, at least $r = 0.92$ [$P < 0.001$, Pearson correlation]. Kaiser-Meyer-Olkin measure of sampling adequacy was 0.81, Bartlett's test of sphericity was significant [$\chi^2(6) = 173.12$, $P < 0.001$] and all communalities were above 0.93, confirming that this data was suitable for PCA. We found that PC1 explained 96.2% of the variance and therefore we used this measure to represent performance on the experimental sessions of the reactive timing task. Confirming our earlier findings, PC1 differed significantly between groups [$t_{22} = 2.69$, $P = 0.013$, two-sample *t*-test].

3.4.9 Performance on predictive and reactive motor timing tasks does not correlate with SARA scores

We hypothesized that if predictive and reactive motor timing functions are linked to cerebellar function, we could possibly find a relation between SCA6 symptom severity and performance on the tasks. To test this hypothesis, we performed an exploratory correlation analysis between performance on the predictive task and reactive timing task with individual scores on the Scale for the Assessment and Rating of Ataxia (SARA), which we obtained from 11 of the 12 SCA6 participants. Performance of both tasks was represented as the PC1 of scores on each task, as explained earlier. We did not find significant correlations between SARA score and scores on the predictive timing task (PC1 all correct responses) [$r = -0.07$, $P = 0.85$, Pearson correlation], PC1 of early correct responses [$r = -0.509$, $P = 0.11$, Pearson correlation], PC1 of late correct responses [$r = 0.36$, $P = 0.27$, Pearson correlation] and PC1 of reactive timing task [$r = -0.5$, $P = 0.12$, Pearson correlation].

3.5 Discussion

In this study, we subjected cerebellar patients and control subjects to two finger-movement timing paradigms to find out to what extent the cerebellum

contributes to spatio-temporal prediction and whether cerebellar dysfunction leads to changes in motor timing and coordination. We found that SCA6 patients were impaired at establishing spatio-temporal prediction of finger movements based on dynamic visual stimuli. Healthy control participants precisely timed their button-presses before a moving stimulus completely overlapped with a target stimulus, thereby anticipating or even 'over-predicting' their motor timing with approximately 66ms at the end of the training session, a behavioral effect that has also been observed previously[1]. Instead, cerebellar patients failed to establish spatio-temporal prediction and placed their button presses generally more temporally distributed, indicative of reduced temporal precision in responses. Concomitantly, SCA6 patients had significantly lower performance of early correct responses placed in the anticipatory period, but not of late correct responses placed in the period after the moving stimulus overlapped with the target stimulus.

Our results support previous work that has associated the cerebellum with spatio-temporal prediction processes and substantiate recent proposal arguing that the cerebellum is responsible for "monitoring" ongoing timing and adjustment based on temporal predictions[32]. Striking similarities can be found with a study in which cerebellar patients and healthy participants had to precisely time their button press to intercept a moving target with a moving ball[2]. Lower hit-rates were observed in cerebellar patients and errors were equally distributed between (too) early and late responses. Interestingly, both this study and our results show a higher variability in patient response times, although in this study the variability was found to be limited to the late error trials, whereas we did not make such a distinction in our study. Using the same paradigm, cerebellar activation were found to be related to performance and were reduced in SCA patients[4]. Both these and our data indicate a predictive sub-second motor timing deficit in cerebellar patients, which could lead to impaired motor anticipation in daily life situations. For instance, Lang and Bastian (1999) showed that cerebellar patients failed to show anticipatory muscle activity when catching a falling weight, which made them unable to control the impact of the falling weight[33]. In a more general context, a

considerable amount of literature has associated the cerebellum with temporal processing in the sub-second range, which are processes that are also engaged during predictive motor timing. A compelling example of this is that cerebellar patients show increased variation in timing, amplitude and velocity of finger opening in overarm throwing of a ball, which consequently results in reduced precision of throwing[34]. Moreover, cerebellar lesions in humans, as well as in rodents, affect the acquisition and particularly the timing of conditioned responses in Pavlovian eye blink conditioning[35], highlighting that the cerebellar cortex is specifically involved in the time course and amplitude of this learned motor behavior[36,37]. Other studies employing explicit timing tasks, such as rhythmic finger tapping and temporal interval discrimination and reproduction, have provided convincing evidence for cerebellar involvement in sub-second temporal processing. An increased temporal variability during rhythmic tapping with the finger or foot has been found in cerebellar patients[6,11], particularly associated with lesions in the lateral cerebellar regions[12]. Neuroimaging studies have found reliable activation of the cerebellum among several other areas in the cerebello-diencephalic-parietal network during finger-tapping in synchrony or continuation after tones at constant intervals[17–19]. Consistent with this finding, inactivating the ipsilateral cerebellar regions using repetitive transcranial magnetic stimulation (rTMS) introduced variability in the inter-tap interval[20]. Moreover, impaired temporal discrimination in the sub-second range has been found in both cerebellar patients and animal studies[6,13,14,38] (but see also:[39,40]). Gooch et al. (2010) however did not find impairment in temporal discrimination, although they did find impaired temporal estimation, production and reproduction in cerebellar lesion patients[41]. The reproduction of temporal intervals furthermore recruits cerebellar regions[15,16]. This cerebellar activation commonly coincides with activity in other cortical areas, *e.g.* basal ganglia, supplementary motor area (SMA), premotor area and inferior parietal cortex. Inactivating the left and right lateral cerebellum with rTMS impairs performance at a temporal reproduction task on short interval (millisecond range), but not at second range intervals[21,42]. The present view posits that the cerebellum is particularly involved in temporal processing at the sub-second scale, whereas the basal ganglia as part of a

wider cortical network processes information at longer timescales[7,15,16,21,43–46]. This view is however still debated, as some researchers claim that the precise role of the cerebellum in timing processes has not been proven so far[42,47,48].

To assess the relationship between the performance of both tasks and indicators of SCA6 disease progression, we conducted a correlation analysis including the first PC as a measure of task performance in both predictive and reactive timing tasks and scores on the SARA[27]. Against expectations we failed to find a correlation between performance and SARA score. A possible explanation for this is that SARA score is based on multiple sub-scores assessing a wide range of functions, such as walking, stance, sitting and speech, whereas performance on our tasks depends specifically on the ability to precisely coordinate finger movements and to make precisely timed motor executions. A high SARA score does not necessarily translate into reduced fine motor skills, but could be the result of a broad spectrum of symptoms. Not finding a correlation could be explained by the fact that we had a rather small amount of participants for this exploratory correlation analysis, and that the SARA scores of our SCA6 participants were relatively low. Increasing the amount of participants with higher SARA scores could still reveal such an underlying relationship between task performance and SCA6 symptom severity.

In our reactive motor timing paradigm, we found that cerebellar patients overall scored worse than controls, which could indicate a general motor coordination deficit. Nevertheless, randomizing the sequence of stimuli resulted in a lower performance in both groups, indicating that sequence learning did occur in both SCA6 and control participants. Randomizing the temporal interval between markers, however, did not affect the performance of SCA6 patients, suggesting that temporal interval learning is impaired or that a deficit exists in the integration of spatial and temporal information in cerebellar patients. Learning of the sequence and/or temporal interval of stimuli could potentially aid in creating an expectation of which button to press and when to make the motor execution, respectively. This spatial and temporal expectation could be used

within a strategy used during both the predictive and the reactive timing task, although randomization only resulted in performance differences during the reactive timing task. Learning of new motor sequences has been associated with enhanced activity in several brain areas, including the prefrontal cortex (PFC), putamen, intraparietal sulcus region (IPS), precuneus, premotor cortex (PMC), supplementary motor area (SMA) and cerebellum[49–57] (but see:[58]). It has been shown in multiple studies that during the initial stages of motor sequence learning frontal areas in combination with bilateral cerebellar regions show enhanced activation, after which the representation shifts to activation within the cortical-striatal circuit when the sequence has been learned[50,55–57]. Also, a shift in activity from the cerebellar cortex to deep cerebellar nuclei with sequence learning has been shown, suggesting segregation of neural networks involved at different stages of motor sequence learning[50]. Interestingly, the hippocampus has been shown to be active during learning of sequences[59], but also during retrieval of learned sequences[60]. A relationship between neural activity of hippocampal CA1 neurons and nonspatial sequence coding of odors has been found in rats, thus implying a role for the hippocampus in coding for sequential position of nonspatial objects[61]. These hippocampal related findings are interesting in the light of our recent observations of cerebellar-hippocampal interaction during spatio-temporal prediction[1], although the former sequences may not be related to timing at the millisecond level. Within the temporal domain, sustained activity in the lateral cerebellum and several structures within the neocortical-cerebellar network has been associated with temporal sequence learning in the form of intervals and rhythm[49,62,63]. Based on the cerebellar involvement in these forms of sequence learning, it seems likely that the observed deficits in temporal order learning can be attributed to cerebellar Purkinje cell specific degeneration in SCA6. These findings are in agreement with a previous study showing that cerebellar patients are indeed impaired on temporal, but also spatial sequence learning in a serial reaction time task[64]. Still, it should be noted that we were unable to detect sequence learning in cerebellar patients and healthy controls in our paradigm where spatio-temporal cues were available for motor prediction.

There are several limitations to our experimental approach. First, SCA6 covers a wide spectrum of symptoms[25,26], among others poor motor coordination of upper limbs, tremors, physical fatigue and oculomotor deficits. All of these may have affected participants' ability to execute the tasks, since performance on both tasks was not only dependent on motor timing (*i.e.* pressing the button on time or as fast as possible), but also depended on precise finger movement coordination for pressing the right button. The possible influence of reduced motor coordination on predictive timing performance in SCA6 patients, as shown by reactive timing group differences, cannot be fully discounted. We attempted to minimize this influence by designing the paradigm in a way that movement of only one finger at a time was required instead of multiple fingers at the same time, and that the movement-speed of markers was acceptable for both SCA6 and control participants. As such, SCA6 patients showed increasing performance during the training on both tasks, which could indicate that reduced motor coordination has played a relatively limited role in our predictive task. We furthermore excluded SCA6 patients exhibiting unilateral or bilateral tremors or pronounced physical fatigue, thereby attempting to reduce these additional influences. Consequently, this reduced the average SARA score in our patient group. Our findings suggest however that cerebellar patients with relatively mild symptoms (*i.e.* having a low SARA score) already exhibit pronounced deficits in predictive motor timing functions. Attentional deficits may also have played a role in our study. Cerebellar patients have been shown to exhibit deficits in shifting attention between visual stimuli[65,66], although another study argues that response-related preparation processes rather than visuospatial attention shift are affected in cerebellar patients[67]. Both of these are potentially of importance, particularly during motor sequence learning, since differences in brain activation have been found between implicitly and explicitly learned motor sequences, suggesting that a different set of brain structures is activated depending on the degree of attentional resources assigned to the learned motor sequence[52]. Furthermore, cerebellar activity has been shown during a verbal working memory task[68] and a correlation between working memory and performance on temporal estimation, production and reproduction tasks has been found in subjects within cerebellar lesions[41]. although it remains unclear to

what extent SCA6 affects working memory in our patients. The potential influence of oculomotor deficits can also not be fully discounted. Future research using eye-tracking hardware may clarify to what extent eye movement deficits in SCA6 patients affect predictive motor timing. Recently it has been shown that in the mouse inducing the expression of C terminus polypeptides in Purkinje cells, as seen in SCA6 patients, yields both physiological and behavioral consequences, and may provide us with a new mouse model to study disease-related mechanisms of SCA6 in greater depth[23].

To conclude, we hereby provided evidence that SCA6 patients are impaired at establishing spatio-temporal prediction in timing of responses based on dynamic visual stimuli, reflecting a deficit in integration of spatial and temporal information and subsequently motor anticipation to upcoming events, using a task that demanded a prediction of when a stimulus would be at a certain target location. We propose that SCA6 patients are impaired in updating their forward internal model using spatial and temporal cues in the sub-second range, a process that has been postulated to require the cerebellum[69,70].

References

1. Onuki, Y., Van Someren, E. J. W., De Zeeuw, C. I. & Van Der Werf, Y. D. Hippocampal-cerebellar interaction during spatio-temporal prediction. *Cereb. Cortex* **25,** 313–321 (2015).
2. Bares, M. *et al.* Impaired predictive motor timing in patients with cerebellar disorders. *Exp. brain Res.* **180,** 355–65 (2007).
3. Bareš, M., Lungu, O. V., Husárová, I. & Gescheidt, T. Predictive Motor Timing Performance Dissociates Between Early Diseases of the Cerebellum and Parkinson's Disease. *The Cerebellum* **9,** 124–135 (2010).
4. Bares, M. *et al.* The Neural Substrate of Predictive Motor Timing in Spinocerebellar Ataxia. *The Cerebellum* **10,** 233–244 (2011).
5. O'Reilly, J. X., Mesulam, M. M. & Nobre, A. C. The cerebellum predicts the timing of perceptual events. *J. Neurosci.* **28,** 2252–2260 (2008).
6. Ivry, R. B. & Keele, S. W. Timing functions of the cerebellum. *J. Cogn. Neurosci.* **1,** 136–152 (1989).
7. Ivry, R. B. The representation of temporal information in perception and motor control. *Curr. Opin. Neurobiol.* **6,** 851–857 (1996).
8. Ivry, R. B., Spencer, R. M. C., Zelaznik, H. N. & Diedrichsen, J. The cerebellum and event timing. *Ann. N. Y. Acad. Sci.* **978,** 302–317 (2002).
9. Spencer, R. M. C. & Ivry, R. B. in *Handbook of the Cerebellum and Cerebellar Disorders* (eds. Manto, M., Schmahmann, J. D., Rossi, F., Gruol, D. L. & Koibuchi, N.) 1201–1219 (Springer Netherlands, 2013).
10. Coull, J. T. & Nobre, A. C. Dissociating explicit timing from temporal expectation with fMRI. *Curr. Opin. Neurobiol.* **18,** 137–144 (2008).
11. Matsuda, S. *et al.* The 3-Second Rule in Hereditary Pure Cerebellar Ataxia: A Synchronized Tapping Study. *PLoS One* **10,** e0118592 (2015).
12. Ivry, R. B., Keele, S. W. & Diener, H. C. Dissociation of the lateral and medial cerebellum in movement timing and movement execution. *Exp. brain Res.* **73,** 167–180 (1988).
13. Grube, M., Cooper, F. E., Chinnery, P. F. & Griffiths, T. D. Dissociation of duration-based and beat-based auditory timing in cerebellar degeneration. *Proc. Natl. Acad. Sci. U. S. A.* **107,** 11597–11601 (2010).
14. Casini, L. & Ivry, R. B. Effects of divided attention on temporal processing in patients with lesions of the cerebellum or frontal lobe. *Neuropsychology* **13,** 10 (1999).
15. Bueti, D., Walsh, V., Frith, C. & Rees, G. Different brain circuits underlie motor and perceptual representations of temporal intervals. *J. Cogn. Neurosci.* **20,** 204–214 (2008).
16. Jahanshahi, M., Jones, C. R. G., Dirnberger, G. & Frith, C. D. The substantia nigra pars compacta and temporal processing. *J Neurosci* **26,** 12266–12273 (2006).
17. Rao, S. M. *et al.* Distributed neural systems underlying the timing of movements. *J. Neurosci.* **17,** 5528–35 (1997).
18. Jänke, L., Loose, R., Lutz, K., Specht, K. & Shah, N. J. Cortical activations during paced finger-tapping applying visual and auditory pacing stimuli. *Cogn. Brain Res.* **10,** 51–66 (2000).
19. Pollok, B., Gross, J., Kamp, D. & Schnitzler, A. Evidence for anticipatory motor control within a cerebello-diencephalic-parietal network. *J. Cogn. Neurosci.* **20,** 828–840 (2008).
20. Del Olmo, M. F., Cheeran, B., Koch, G. & Rothwell, J. C. Role of the cerebellum in externally paced rhythmic finger movements. *J. Neurophysiol.* **98,** 145–52 (2007).
21. Koch, G. *et al.* Repetitive TMS of cerebellum interferes with millisecond time processing. *Exp. Brain Res.* **179,** 291–299 (2007).
22. Zhuchenko, O. *et al.* Autosomal dominant cerebellar ataxia (SCA6) associated with small polyglutamine expansions in the alpha1A-voltage-dependent calcium channel. *Nat. Genet.* **15,** 62–69 (1997).
23. Mark, M. D. *et al.* Spinocerebellar Ataxia Type 6 Protein Aggregates Cause Deficits in Motor Learning and Cerebellar Plasticity. *J. Neurosci.* **35,** 8882–8895 (2015).
24. Koeppen, A. The pathogenesis of spinocerebellar ataxia. *The Cerebellum* **4,** 62–73 (2005).
25. Solodkin, A. & Gomez, C. M. Spinocerebellar ataxia type 6. *Ataxic Disord.* **103,** 461–473 (2011).
26. Gomez, C. M. *et al.* Spinocerebellar ataxia type 6: gaze-evoked and vertical nystagmus, Purkinje cell degeneration, and variable age of onset. *Ann. Neurol.* **42,** 933–950 (1997).

27. Schmitz-Hübsch, T. *et al.* Scale for the assessment and rating of ataxia Development of a new clinical scale. *Neurology* **66,** 1717–1720 (2006).
28. Gobel, E. W., Parrish, T. B. & Reber, P. J. Neural correlates of skill acquisition: Decreased cortical activity during a serial interception sequence learning task. *Neuroimage* **58,** 1150–1157 (2011).
29. Brainard, D. H. The Psychophysics Toolbox. *Spat. Vis.* **10,** 433–436 (1997).
30. Pelli, D. G. The VideoToolbox software for visual psychophysics: transforming numbers into movies. *Spat. Vis.* **10,** 437–442 (1997).
31. Brown, M. B. & Forsythe, A. B. Robust Tests for the Equality of Variances. *J. Am. Stat. Assoc.* **69,** 364 (1974).
32. Petter, E. A., Lusk, N. A., Hesslow, G. & Meck, W. H. Interactive roles of the cerebellum and striatum in sub-second and supra-second timing: Support for an initiation, continuation, adjustment, and termination (ICAT) model of temporal processing. *Neuroscience and Biobehavioral Reviews* **71,** 739–755 (2016).
33. Lang, C. E. & Bastian, A. J. Cerebellar subjects show impaired adaptation of anticipatory EMG during catching. *J. Neurophysiol.* **82,** 2108–2119 (1999).
34. Timmann, D., Watts, S. & Hore, J. Failure of cerebellar patients to time finger opening precisely causes ball high-low inaccuracy in overarm throws. *J. Neurophysiol.* **82,** 103–114 (1999).
35. Topka, H., Valls-Solé, J., Massaquoi, S. G. & Hallett, M. Deficit in classical conditioning in patients with cerebellar degeneration. *Brain* **116,** 961–969 (1993).
36. McCormick, D. A. & Thompson, R. F. Neuronal responses of the rabbit cerebellum during acquisition and performance of a classically conditioned nictitating membrane-eyelid response. *J. Neurosci.* **4,** 2811–2822 (1984).
37. Perrett, S. P., Ruiz, B. P. & Mauk, M. D. Cerebellar cortex lesions disrupt learning-dependent timing of conditioned eyelid responses. *J. Neurosci.* **13,** 1708–1718 (1993).
38. Breukelaar, J. W. C. & Dalrymple-Alford, J. C. Effects of lesions to the cerebellar vermis and hemispheres on timing and counting in rats. *Behav. Neurosci.* **113,** 78–90 (1999).
39. Nichelli, P., Alway, D. & Grafman, J. Perceptual timing in cerebellar degeneration. *Neuropsychologia* **34,** 863–871 (1996).
40. Mangels, J. A., Ivry, R. B. & Shimizu, N. Dissociable contributions of the prefrontal and neocerebellar cortex to time perception. *Cogn. Brain Res.* **7,** 15–39 (1998).
41. Gooch, C. M., Wiener, M., Wencil, E. B. & Coslett, H. B. Interval timing disruptions in subjects with cerebellar lesions. *Neuropsychologia* **48,** 1022–1031 (2010).
42. Harrington, D. L. Does the representation of time depend on the cerebellum?: Effect of cerebellar stroke. *Brain* **127,** 561–574 (2004).
43. Meck, W. H., Penney, T. B. & Pouthas, V. Cortico-striatal representation of time in animals and humans. *Curr. Opin. Neurobiol.* **18,** 145–152 (2008).
44. Lee, K.-H. *et al.* The role of the cerebellum in subsecond time perception: evidence from repetitive transcranial magnetic stimulation. *J. Cogn. Neurosci.* **19,** 147–157 (2007).
45. Aso, K., Hanakawa, T., Aso, T. & Fukuyama, H. Cerebro-cerebellar interactions underlying temporal information processing. *J. Cogn. Neurosci.* **22,** 2913–2925 (2010).
46. Fierro, B. *et al.* Role of the cerebellum in time perception: A TMS study in normal subjects. *J. Neurol. Sci.* **263,** 107–112 (2007).
47. Harrington, D. L. Reply to: Evaluating the role of the cerebellum in temporal processing: beware of the null hypothesis. *Brain* **127,** E14–E14 (2004).
48. Ivry, R. B. & Spencer, R. M. C. Evaluating the role of the cerebellum in temporal processing: beware of the null hypothesis. *Brain* **127,** E13; author reply E14 (2004).
49. Sakai, K., Ramnani, N. & Passingham, R. E. Learning of sequences of finger movements and timing: frontal lobe and action-oriented representation. *J. Neurophysiol.* **88,** 2035–46 (2002).
50. Doyon, J. *et al.* Experience-dependent changes in cerebellar contributions to motor sequence learning. *Proc. Natl. Acad. Sci. U. S. A.* **99,** 1017–22 (2002).
51. Grafton, S. T., Hazeltine, E. & Ivry, R. Functional mapping of sequence learning in normal humans. *J. Cogn. Neurosci.* **7,** 497–510 (1995).
52. Hazeltine, E., Grafton, S. T. & Ivry, R. Attention and stimulus characteristics determine the locus of motor-sequence encoding. A PET study. *Brain* **120,** 123–140 (1997).
53. Honda, M. *et al.* Dynamic cortical involvement in implicit and explicit motor sequence learning. A PET study. *Brain* **121,** 2159–2173 (1998).

54. Jenkins, I. H., Brooks, D. J., Nixon, P. D., Frackowiak, R. S. & Passingham, R. E. Motor sequence learning: a study with positron emission tomography. *J. Neurosci.* **14,** 3775–3790 (1994).
55. Jueptner, M. *et al.* Anatomy of motor learning. I. Frontal cortex and attention to action. *J. Neurophysiol.* **77,** 1313–1324 (1997).
56. Sakai, K. *et al.* Transition of brain activation from frontal to parietal areas in visuomotor sequence learning. *J. Neurosci.* **18,** 1827–1840 (1998).
57. Toni, I., Krams, M., Turner, R. & Passingham, R. E. The time course of changes during motor sequence learning: a whole-brain fMRI study. *Neuroimage* **8,** 50–61 (1998).
58. Seidler, R. D. *et al.* Cerebellum activation associated with performance change but not motor learning. *Science* **296,** 2043–6 (2002).
59. Schendan, H. E., Searl, M. M., Melrose, R. J. & Stern, C. E. An FMRI study of the role of the medial temporal lobe in implicit and explicit sequence learning. *Neuron* **37,** 1013–1025 (2003).
60. Ross, R. S., Brown, T. I. & Stern, C. E. The retrieval of learned sequences engages the hippocampus: Evidence from fMRI. *Hippocampus* **19,** 790–799 (2009).
61. Allen, T. A., Salz, D. M., McKenzie, S. & Fortin, N. J. Nonspatial Sequence Coding in CA1 Neurons. *J. Neurosci.* **36,** 1547–1563 (2016).
62. Schubotz, R. I. & von Cramon, D. Y. Interval and ordinal properties of sequences are associated with distinct premotor areas. *Cereb. Cortex* **11,** 210–222 (2001).
63. Ramnani, N. & Passingham, R. E. Changes in the human brain during rhythm learning. *J. Cogn. Neurosci.* **13,** 952–966 (2001).
64. Shin, J. & Ivry, R. B. Spatial and temporal sequence learning in patients with Parkinson's disease or cerebellar lesions. *Cogn. Neurosci. J.* **15,** 1232–1243 (2003).
65. Akshoomoff, N. A. & Courchesne, E. ERP evidence for a shifting attention deficit in patients with damage to the cerebellum. *Cogn. Neurosci. J.* **6,** 388–399 (1994).
66. Courchesne, E. *et al.* Impairment in shifting attention in autistic and cerebellar patients. *Behav. Neurosci.* **108,** 848–865 (1994).
67. Yamaguchi, S., Tsuchiya, H. & Kobayashi, S. Visuospatial attention shift and motor responses in cerebellar disorders. *J. Cogn. Neurosci.* **10,** 95–107 (1998).
68. Desmond, J. E., Gabrieli, J. DE, Wagner, A. D., Ginier, B. L. & Glover, G. H. Lobular patterns of cerebellar activation in verbal working-memory and finger-tapping tasks as revealed by functional MRI. *J. Neurosci.* **17,** 9675–9685 (1997).
69. Wolpert, D. M., Miall, R. C. & Kawato, M. Internal models in the cerebellum. *Trends Cogn. Sci.* **2,** 338–347 (1998).
70. Miall, R. C. & Wolpert, D. M. Forward models for physiological motor control. *Neural Networks* **9,** 1265–1279 (1996).

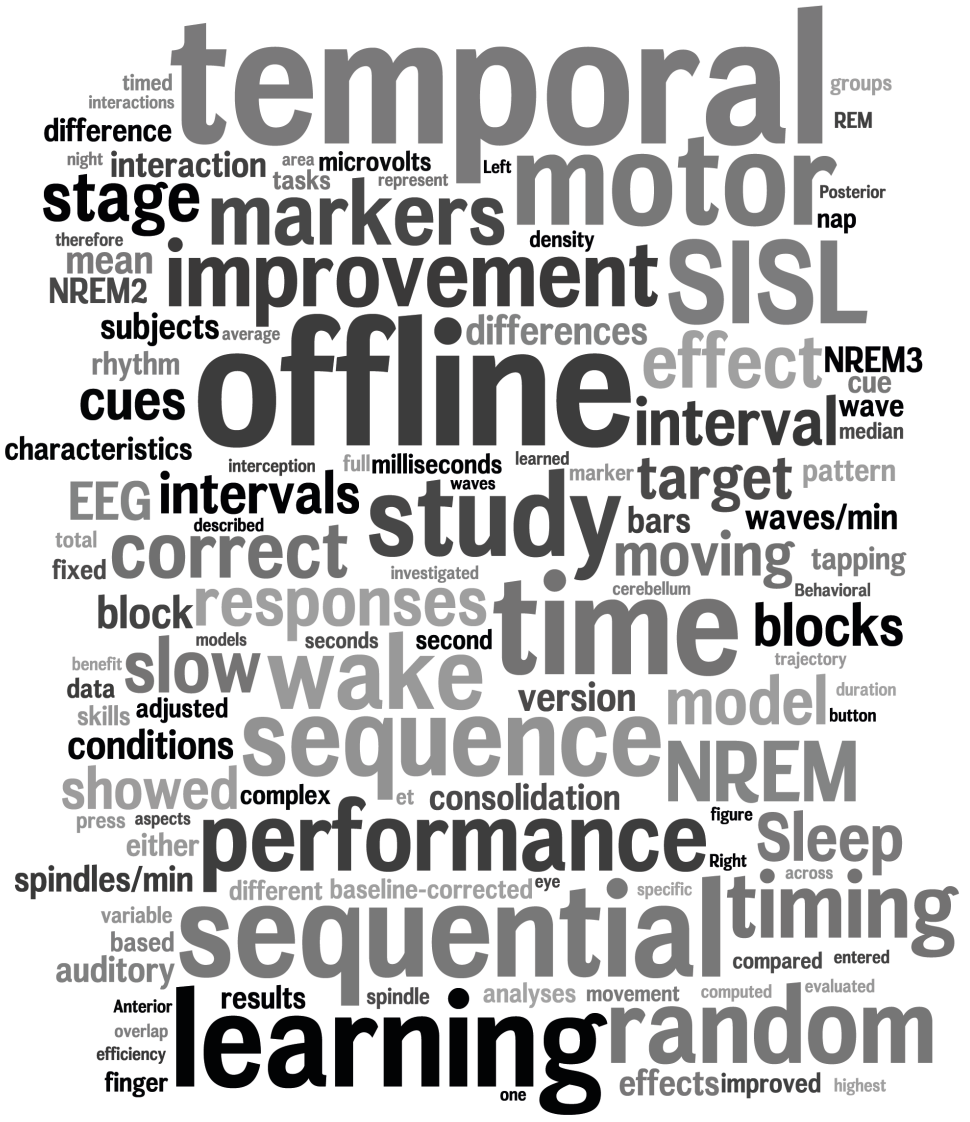
temporal
timed
interactions
groups
REM
difference
night
interaction
area
microvolts
tasks
represent
Left
motor
stage
markers
Posterior
nap
therefore
density
mean
NREM2
improvement
SISL
subjects
average
differences
offline
effect
NREM3
cue
rhythm
cues
wave
median
interval
characteristics
interception
full
milliseconds
learned
waves
marker
target
pattern
EEG
intervals
study
bars
waves/min
described
total
correct
moving
tapping
fixed
investigated
cerebellum
Behavioral
block
responses
time
blocks
models
seconds
second
trajectory
benefit
slow
wake
data
version
model
duration
skills
adjusted
button
conditions
sequence
NREM
showed
complex
et
consolidation
press
aspects
figure
performance
Sleep
either
Right
spindles/min
different
baseline-corrected
eye
specific
across
sequential
timing
variable
based
auditory
compared
entered
Anterior
results
spindle
analyses
movement
computed
evaluated
overlap
learning
random
efficiency
finger
one
effects
improved
highest

Chapter 4. Sleep to the beat: A nap favours consolidation of timing

Ilse M. Verweij*, Yoshiyuki Onuki*, Eus J.W. Van Someren,
and Ysbrand D. Van der Werf

* These authors contributed equally.

Published in:
Behavioral Neuroscience, 2016
DOI: 10.1037/bne0000146

4.1 Abstract

Growing evidence suggests that sleep is important for procedural learning, but few studies have investigated the effect of sleep on the temporal aspects of motor skill learning. We assessed the effect of a 90-minute day-time nap on learning a motor timing task, using two adaptations of a serial interception sequence learning (SISL) task. Forty-two right-handed participants performed the task before and after a 90-minute period of sleep or wake. Electroencephalography (EEG) was recorded throughout. The motor task consisted of a sequential spatial pattern and was performed according to two different timing conditions, i.e. either following a sequential or a random temporal pattern. The increase in accuracy was compared between groups using a mixed linear regression model. Within the sleep group, performance improvement was modeled based on sleep characteristics, including spindle- and slow-wave density. The sleep group, but not the wake group, showed improvement in the random temporal, but especially and significantly more strongly in the sequential temporal condition. None of the sleep characteristics predicted improvement on either general of the timing conditions. In conclusion, a daytime nap improves performance on a timing task. We show that performance on the task with a sequential timing sequence benefits more from sleep than motor timing. More important, the temporal sequence did not benefit initial learning, because differences arose only after an offline period and specifically when this period contained sleep. Sleep thus appears to aid in the extraction of regularities for optimal subsequent performance.

4.2 Introduction

Sleep plays an important role in offline consolidation of motor skills[1,2] although it remains insufficiently understood which aspects of motor performance benefit from sleep. Especially the role of sleep in consolidation of the temporal aspects of motor skills has not received much attention in the literature to date. The timing of complex motor actions is a critical factor to perform quick and precise skills, involved in many everyday activities such as crossing the road, and playing musical instruments. Timed performance can be learnt in various ways, e.g. through estimating a period of time and comparing it to a memorized standard[3]. This is often the case in studies where auditory inputs are used for motor timing and rhythm learning, such as in the study of Lewis, Couch, and Walker (2011)[4]. This study has shown that motor skills, i.e. tapping a finger in time with a learned sequence, improve after a night of sleep, compared with after a period of wake. Performance on a perceptual task, where subjects had to monitor a learned auditory sequence for deviants by pressing a button also improved after subjects had slept. These results imply that explicit learning of an auditory sequence in a finger tapping task is facilitated by sleep. A second route for learning to perform timed actions is engaged during tasks with non-temporal goals, when temporally structured sensorimotor information can be used to predict future events[3]. Genzel et al. (2012) investigated complex motor skill learning involving motor timing prediction using a dancing game where participants were taught to dance a set choreography by reacting to cues moving on a screen towards target markers[5]. Whenever the cue reached a target marker, participants had to step on a corresponding marker on a dance mat. Participants were retested on accuracy after an offline period of either wake (group A) or sleep (group B) and then retested again after another offline period of wake (group B) or sleep (group A). Sleep significantly improved performance of the group B that slept immediately after the task. Even though this study showed that sleep benefits specific sequence learning of a complex motor task, the study design did not allow for distinguishing the effect of sleep on the performance of a sequence with a sequential vs. random temporal pattern. Here, we aim to elucidate the role of sleep in motor timing

with a sequential or random temporal sequence through a sequential complex motor task, using an adaptation of the serial interception sequence learning (SISL) task[6,7]. The SISL task requires a precisely timed response, tapping multiple fingers at a time and adjusting the timing to upcoming visual cues, in contrast to other motor tasks, where a fast and voluntary response is required[6]. Two versions of this task were created. One version had random time intervals between moving markers, while the other version had a sequential temporal pattern of time intervals between the moving markers. This allowed us to distinguish the effect of sleep on motor timing (i.e. an accurate prediction of a motor response by the upcoming cues in the absence of a learned timing sequence) from the temporal sequence learning component (i.e. prediction of the timed motor pattern).

4.3 Subjects and methods

4.3.1 Participants

Fifty-seven right-handed individuals were recruited for the study. Participants had no prior history of drug or alcohol abuse, neurological, or psychiatric disorders. All participants were screened for sleep disorders using the Pittsburgh Sleep Quality Index[8] (mean = 2.5, SD = 1.3). Because restricted night-time sleep can have an unfavourable effect on performance[9], we instructed participants to keep a regular sleep/wake rhythm and sleep at least six hours during the night before participating in the study. This was verified with a sleep diary, and actigraphy (GENEActiv, Cambridge UK). Based on their actiwatch data and sleep diary, eight subjects were excluded from analysis. Participants playing musical instruments or rhythmic games on a regular basis, were excluded from participating in the study because the SISL task involved similar visuo-motor skills. All participants were requested to refrain from drinking alcohol or caffeine 24 hours before participating in the study.

Three subjects had incomplete task data or did not show a learning curve and four subjects did not reach stage 2 sleep during the nap, and were therefore excluded from

analysis. The final sample for data analysis included 42 participants (mean age=22.3, SD=3.0, 17 males). The average of their sleep duration, as judged from the actigraphy, was 7h30min (standard deviation: 59 mins) in the night preceding the experiment. All participants gave their informed consent prior to taking part in the study. The study was approved by the ethics committee of the Department of Psychology, the University of Amsterdam, The Netherlands. Participants received financial compensation for their participation.

4.3.2 Procedure

The study was carried out in the sleep laboratory at the Department of Sleep and Cognition at the Netherlands Institute of Neuroscience (NIN) and in the sleep laboratory of the Department of Integrative Neurophysiology, Center for Neurogenomics and Cognitive Research (CNCR) at the Vrije Universiteit (VU) Amsterdam. Participants arrived at 11.00 am at the sleep laboratory and were familiarized with the sleep room and the procedure of the study. At noon, lunch was served. Participants were randomly assigned to either the sleep (n=21) or wake (n=21) group. Both groups participated in the SISL task (described below) before and 30 minutes after an offline period (wake or sleep). The offline period started at 01.00 pm and lasted 90 minutes. During the offline period, the wake group was allowed to engage in activities with low physical effort such as reading a book and the sleep group was asked to take a nap. EEG was acquired during the SISL task and the offline period with an Electrical Geodesics Inc. (Electrical Geodesics Inc., EGI, Eugene, OR) EEG system (sampling rate: 500Hz, high and low-pass filter 0.01 Hz and 200 Hz, respectively). A 257 channel EGI EEG cap (including EOG channels) referenced to the Cz electrode was used. A general outline of the study protocol is shown in Figure 1.

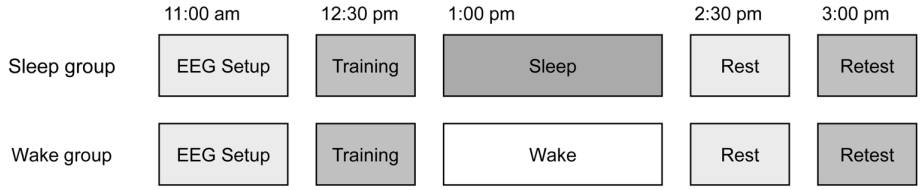

Figure 1. Study design. Subjects were trained on two versions of the serial interception sequence learning (SISL) task before the offline period (wake or sleep) and retested after the offline period after a period of rest. Electroencephalography (EEG) was measured throughout the experiment.

4.3.3 Task

A modified version of the Serial Interception Sequence Learning (SISL) task[6,7] was used. Participants were required to press a computer keyboard key with the non-dominant hand at the moment that the upward moving black circles (referred to as cue markers) overlapped with the corresponding fixed white circles in the top row (referred to as target markers). From left to right, the targets were assigned to four horizontal keys of a computer keyboard and subjects needed to press with their little (A), ring (S), middle (D) and index (F) fingers respectively using their left, non-dominant, hand when the moving cues overlapped with the target markers. The moving cue markers appeared in a fixed spatial sequence and moved at a constant velocity (2.8 milliseconds per pixel). The diameter of the target markers was 20% of the middle third of the display width while the diameter of moving markers was 20 pixels smaller than that of the target marker to fit completely inside the target markers and not to interfere with the moments of the complete overlap between markers observed by participants. In the original SISL task, cues appear one by one in the target zone, whereas in the modified SISL task up to two cues can intercept simultaneously with the specific target zone. As a consequence, the participants are required to use one finger or variable combinations of two fingers at the same time to press the key corresponding with the perceptual cues (Figure 2).

Unbeknownst to the participants, the SISL task used in present study consisted of two conditions. The sequential temporal interval condition was similar to the original SISL

task with a specific pattern of inter-trial timing: D_{360ms}-F_{293ms}-AS_{400ms}-DF_{400ms}-SD_{373ms}-A_{293ms}-SF_{373ms}-AF_{400ms}-S_{347ms}-AD_{360ms}. (A: left-most trajectory, S: second trajectory, D: third trajectory, F: right-most trajectory, subscripted rates: temporal differences between black markers in milliseconds). The average temporal interval between appearances was 359 milliseconds (range 293-400 milliseconds). A trial was defined as the passage of a moving cue through its target. The fixed spatial sequence of moving cues consisted of the 10 trials mentioned above and appeared five times every block. In the condition with random temporal sequence, the time between the cues was based on the shuffled time intervals used in the condition with sequential temporal intervals. The sequence of the moving cue markers remained fixed in both the random temporal and the sequential temporal interval condition. The sequential temporal interval condition was implemented to investigate consolidation of only specifically timed sequences of motor actions, whereas the random temporal interval condition would mostly reflect general visuo-motor skill learning of sequences without a particular temporal sequence. The SISL task contained 20 blocks (duration per block 21.5 seconds), i.e. 10 blocks with sequential temporal intervals and 10 random temporal interval blocks. The SISL task administered before was identical to the task after the offline period. All blocks, alternating between the sequential and random temporal condition, were preceded by text-based cues, which appeared on the screen with a duration of 2 seconds and were followed by a block of rest (30 seconds) to minimize the fatigue of the hand and body posture. Participants did not receive information about the different conditions (sequential vs. random temporal intervals) and were simply told that the task contained 20 consecutive blocks and that the instruction for all those blocks was the same, i.e. to indicate as accurately as possible the moment of perfect overlap between the moving and target markers using button presses. During the block of rest, participants were instructed to focus on a fixation cross in the centre of the screen. The total duration of the task was ~20 minutes. The order of the alternating sequential and random temporal interval blocks was counter-balanced across the participants. The SISL task was programmed in MATLAB version 7.10 (Mathworks, Natrick, MA) using Psychophysics toolbox version 3[10–12].

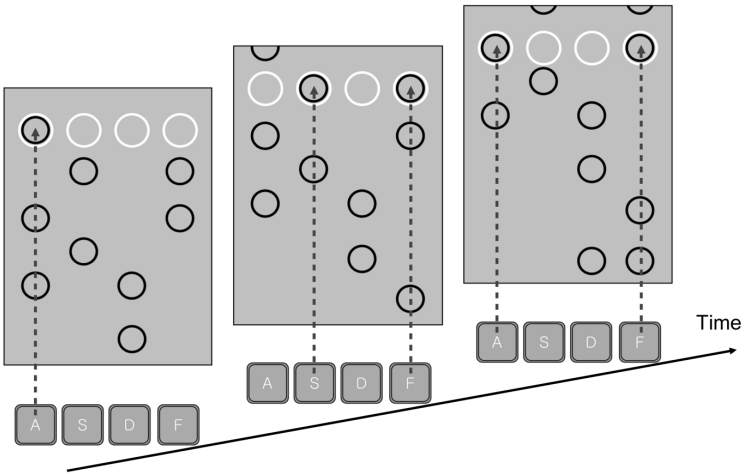

Figure 2. The serial interception sequence learning task. Subjects have to press corresponding (A-S-D-F) keys when the continuously moving cue markers overlap the target markers.

4.3.4 Behavioral analysis

Behavioural performance of the SISL task was assessed by the number of correct trials for each block. The average percentage of correctly timed responses (correct responses) was calculated for each trial for each block. A motor response was regarded correct if it was made within an interval of -120 to 120 milliseconds of the time of perfect overlap of the target marker and moving marker; 120 milliseconds is the time needed for the center of the moving markers to move from the edge to the center of the target markers.

4.3.5 EEG analysis

Sleep scoring. Sleep EEG recordings were re-referenced to the mastoids for sleep scoring. Sleep was scored by two independent raters until the inter-rater agreement was > 85 %, using a modified version of the FASST toolbox[13] on 30 second epochs according to the standard criteria of the AASM[14]. Sleep EEG signals were rated visually, epoch by epoch, as either NREM stages 1-3, rapid eye movement (REM) sleep, wake or movement time.

Total sleep time was computed as the time spent from sleep onset until waking up from the nap. Sleep efficiency was calculated as the time spent asleep divided by the total sleep time. The percentage of time in every sleep stage relative to total sleep time was also computed and used for statistical analysis.

Pre-processing. For slow wave and spindle count, 192 electrodes covering the scalp were selected for analysis, discarding electrodes on the cheek and neck. EEG data were detrended, resampled to 250 Hz, and high- and low pass filtered (0.3 Hz and 45 Hz respectively). Bad electrodes were automatically removed based on their mean absolute deviation (MAD) from the median of the signal (in microvolts). The minimal MAD was set to MAD -10 microvolts and the maximum MAD was set to MAD +8 microvolts, electrodes outside that range were discarded. Bad epochs were selected based on a one-second 50% overlapping sliding window. Epochs were selected for rejection when they had had a median > median of all signals in the data +30*MAD or a median < median of all data – 15*MAD. Finally, bad channels were interpolated using the average of the four nearest channels.

Slow wave detection. For slow wave and spindle detection, sleep EEG recordings were re-referenced to the mastoids. Slow waves were automatically detected using methods described previously[15–17] with in-house code written in MATLAB version 7.13 (Mathworks, Natrick, MA). The EEG signal was averaged in four non-overlapping areas (frontal, posterior and lateral areas as described in the previous study[15], and subsequently band-pass filtered between 0.2 and 4 Hz. To identify slow waves, the following criteria were used: a minimal negative peak of -60 microvolts, a distance between the negative and subsequent positive zero crossing of 0.2-1 seconds, a peak-to-peak difference between the negative and positive zero crossing of >75 microvolts (based on[15]). For each subject and aforementioned areas on the scalp, slow wave density was calculated by dividing the number of slow waves in NREM stage 2 and NREM stage 3 by the time (minutes) spent in each sleep stage.

Spindle detection. Spindles were automatically detected using previously described methods[17–19]. In brief, EEG signals were averaged for each abovementioned area on the scalp, band pass filtered between 11 and 16 Hz and subsequently transformed into the envelope of the Hilbert transform. Spindles were identified when the signal envelope exceeded 3 microvolts for 0.5- 4 seconds. For each participant and scalp area, spindle density was computed by dividing the number of spindles during NREM stage 2 and NREM stage 3 by the amount of time (minutes) spent in each sleep stage.

4.3.6 Statistical analysis

In order to determine whether sleep facilitates offline consolidation of the random and sequential temporal interval conditions, linear mixed models were fitted using R[20]. Optimization of all models was done using a likelihood ratio test (LRT).

The first model (model 1) evaluated whether sleep and/or wake improves performance on the task. The percentage of correct responses was entered in the model as the dependent variable, condition (random/sequential), time (before/after the offline period) and group (sleep/wake), and their interactions were entered in the model as fixed variables and participant was entered in the model as a random variable. We repeated the full model (time by group by condition) analyses with the first three trials after the offline period.

A second model (model 2) evaluated if there was a difference between the sleep and wake group in terms of improvement over time and whether there was an interaction with condition. The highest performance before the offline period was subtracted from all blocks after the offline period (i.e. the baseline-corrected correct responses) and this difference was entered in the model as the dependent variable. We repeated the full model (group by condition) analyses with the first three trials after the offline period.

Additional analyses were done only within the sleep group, testing whether the density of spindles and slow waves and their interaction with condition (four separate models

for the four different brain regions) accounted for variation in performance improvement (baseline-corrected correct responses). Performance improvement was also modelled based on total sleep time, sleep efficiency, %NREM stage 1 sleep, % NREM stage 2 sleep and % NREM stage 3 sleep (six linear mixed models).

4.4 Results

4.4.1 Behavioral results

Average learning curves are shown in Figure 3. Regression analyses showed a strong and significant improvement across the 10 blocks before the offline period, regardless of group and condition ($t=10.7$, $p=2\times10^{-16}$). We therefore computed the mean of the three blocks with the highest % correct responses before sleep and wake (highest performance before the offline period) separately for both the random and sequential temporal interval conditions as an indication of maximum performance. The regression analyses showed no change across blocks after the offline period regardless of group and condition ($t=1.7$, $p=0.1$), indicating that after the offline period participants had reached a stable performance level. For this reason we included all trials after sleep and wake, for the random and sequential temporal interval conditions; the difference values from before to after the offline period thus serve as a robust measure of improvement. Model 1, exploring the effect of time (before to after) on performance and the interaction with condition and group, showed that participants improved (t-value=2.09, p=0.04). Also, an interaction effect was found between time and group (t-value 2.31, p=0.02). A post-hoc comparison showed that the sleep group significantly improved (z-value=5.4, adjusted $p<0.001$) while the wake group did not (z-value=2.1, adjusted p=0.11). There were no differences between groups in correct responses before the offline period (z-value=-0.09, p=1) or after the offline period (z-value=0.46, p=0.96) (see Figure 4). Repeating the full model (time by group by condition) analysis with the first three trials after the offline period showed a non-significant improvement over time (t-value=1.045, p=0.297), of group by time (t-value=0.772, p=0.440) and of group by time by condition (t-value=1.164, p=0.245). Although the changes were in the same

direction as seen in the main analysis, effects measured using the first three trials after the offline period did therefore not attain significance.

Model 2, which included the baseline-corrected correct responses as a dependent variable showed that there was an interaction effect between group and condition (t-value=2.23, p=0.03). There was no effect of condition (t-value=-0.33, p=0.74) or group (t-value=0.95, p=0.35). There was no effect of block on baseline-corrected correct responses (t-value=1.64, p=0.10) or an interaction effect between block and group (t-value=0.29, p=0.77). Post hoc analysis of the interaction effect between group and condition showed that the sleep group improved more on the sequential temporal interval blocks compared to the random blocks (z-value 2.83, adjusted p=0.02) but that the wake group did not (z-value=-0.32, adjusted p=0.98). There were no differences in baseline-corrected correct responses between groups for the random (z-value=0.94, p=0.73) or the sequential temporal interval condition (z-value= 1.96, p=0.16) (see Figure 5).

Repeating the full model (group by condition) analysis with the first three trials after the offline period showed a non-significant effect of group (t-value=0.61, p=0.54) of condition (t-value=-0.98, p=0.33) and of group by condition (t-value=1.57, p=0.12). Again, although the changes were in the same direction as seen in the main analysis, effects measured using the first three trials after the offline period did therefore not attain significance.

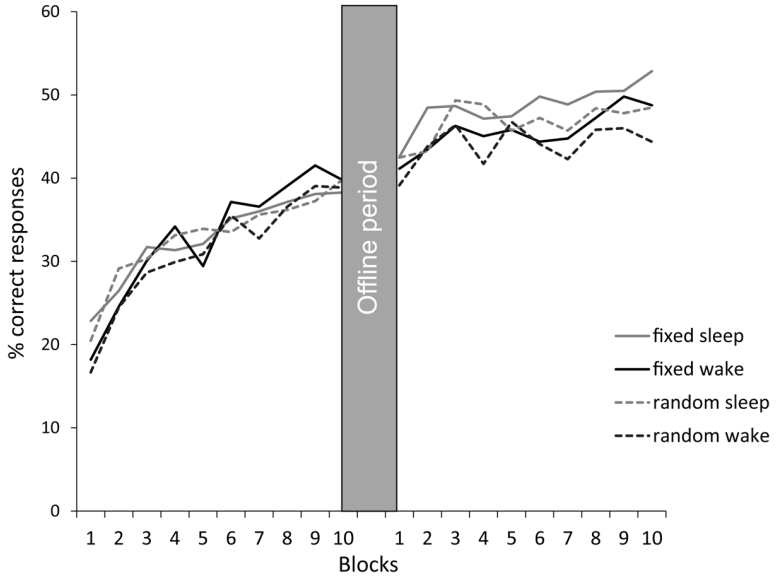

Figure 3. Behavioral results for the sleep and wake group on a block- by-block basis, with random and sequential temporal intervals timing between the cue markers. Points in the graph represent the mean of percent correct responses for each block and condition in both groups. The gray bar indicates the offline period.

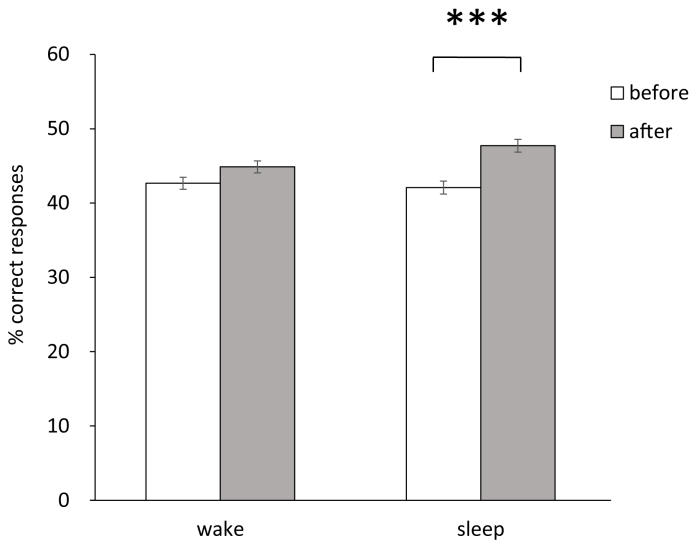

Figure 4. Percentage of correct responses before (white bars) and after (gray bars) the offline period. The bars representing the correct responses before the offline period, represent the mean over the highest three trials, while the bars representing the correct responses after the offline period represent the mean over all trials after the offline period. Error bars indicate the within-subject SEM[21]. The sleep group had significantly more correct responses after the offline period compared with before the offline period (adjusted $p < 0.001$), while the wake group did not show an improvement.

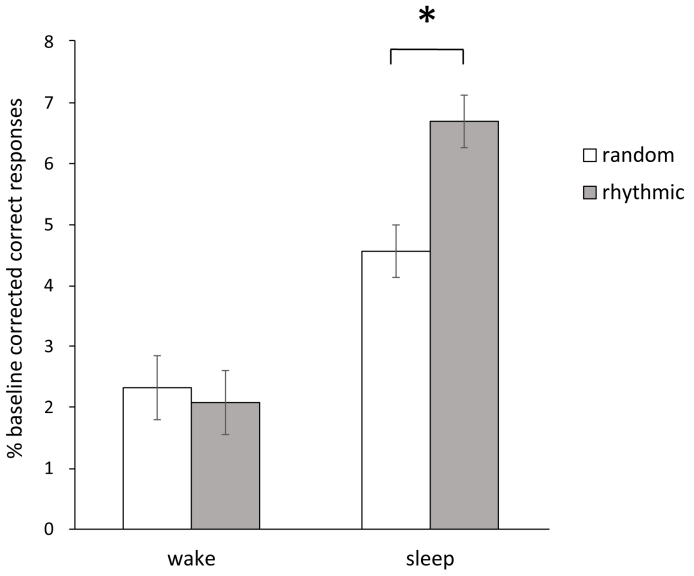

Figure 5. Percentage of baseline-corrected correct responses for the sleep and wake group, in the random (white bars) and sequential temporal intervals (gray bars) condition. Error bars represent SEM[21]. The sleep group improved more on the sequential temporal intervals condition than on the random condition (adjusted $p < 0.05$), while there was no difference in improvement between the random and sequential temporal intervals condition for the wake group.

4.4.2 Sleep characteristics

There was a large variation in sleep characteristics (see Table 1) in the sleep group. Therefore, we explored whether sleep characteristics were related to improvement on the task within the sleep group. Two subjects did not reach NREM 3 sleep and only six subjects showed rapid eye movement (REM) sleep.

The first model evaluated the effects of total sleep time, sleep efficiency, % NREM stage 1, % NREM stage 2, % NREM stage 3 and the interactions of these effects with condition. No significant effects were found for any of the mentioned effects, or their interactions (all $p>0.05$). The second model evaluated the effects of condition and spindle- and slow wave density and their interaction with condition and stage (NREM 2 / NREM 3) on performance improvement. No significant effects were found for any of the fixed factors or their interactions (all $p>0.44$).

After the experiment, participants were queried about the task; although the repeating sequence of markers was readily observed, none of the participants remarked on the presence of timing differences between conditions, or that the markers had sequential temporal intervals.

Table 1 Sleep characteristics of participants in the sleep group

Sleep characteristics	Mean	SD
Total sleep time	83.57	17.32
Sleep efficiency	82.73	16.43
% NREM 1	36.74	17.6
% NREM 2	38.77	14.45
% NREM 3 (19 participants)	22.63	15.13
% REM (6 participants)	14.06	10.82
Anterior spindles/min NREM2	11.64	3.4
Anterior spindles/min NREM3	12.34	5.02
Left spindles/min NREM2	9.35	3.32
Left spindles/min NREM3	8.45	5.25
Right spindles/min NREM2	9.42	3.7
Right spindles/min NREM3	7.33	4.64
Posterior spindles/min NREM2	8.84	3.33
Posterior spindles/min NREM3	8.16	4.5
Anterior slow waves/min NREM2	3.54	0.91
Anterior slow waves/min NREM3	12.44	6.66
Left slow waves/min NREM2	2.49	0.7
Left slow waves/min NREM3	5.67	3.45
Right slow waves/min NREM2	2.67	0.53
Right slow waves/min NREM3	5.77	2.88
Posterior slow waves/min NREM2	2.27	0.84
Posterior slow waves/min NREM3	4.62	2.3

Note. Shown are the mean and SD for each sleep characteristic. NREM = nonrapind eye movement sleep; REM = rapid eye movement sleep.

4.5 Discussion

The current study investigated the effect of sleep on the consolidation of a complex motor task, using two adaptations of the Serial Interception Sequence Learning (SISL) task[6]. This task allowed us to study whether sleep facilitates the learning of motor timing, with or without sequential temporal intervals.

Our results show that sleep facilitated improvement on the SISL task, regardless of version. In contrast, there was no improvement found for either task across wake. When applying a baseline correction on the performance after the offline period, participants that had slept showed a higher improvement above and beyond their maximal pre-interval performance for the sequential temporal interval condition than the random condition. Thus, this study shows that the effect of sleep is not only limited to the timing of motor sequence recitation but shows an even stronger effect for the abstract representation of a temporal sequence. This difference is not caused by a different baseline learning level, as the learning curves for the two tasks did not differ from each other. As the two tasks show no difference in learning curves before the offline period and as the wake group shows no differential improvement between the two tasks, it would follow that sleep is needed to benefit from the temporal pattern in the task. Repeating the analyses using only the first three trials after the offline period showed non-significant differences in improvement for the sleep group in either condition, although the numerical differences were in the same direction. This may be a consequence of variability of the first three trials after the offline period, or it may mean that sleep augments learning during the second administration of the task, i.e. results in a higher capacity for learning. Of note, the outcome measure of our task, i.e. 'correct responding' requires both accuracy (pressing the appropriate button) and synchrony (timing the button press to the visual input) and it is as yet unclear whether these aspects would show differential learning rates between the sequential and random temporal interval conditions or whether sleep affects them separately. The results of this study show similarities to motor sequence learning studies, where consolidation takes place during a nap[22] as well as during a full night of sleep[4,23,24]. In the study of Antony et al (2012), auditory cues, tightly associated with the SISL task, were played during slow wave sleep, leading to performance improvement on the SISL task[25]. Based on this study, we expected to find an effect of slow wave sleep on performance on our version of the SISL task. However, we were not able to attribute the found improvement on the SISL task to a specific sleep characteristic. It is possible that small task differences, such as the use of auditory cues, could have caused discrepancies between our study and the study

of Antony et al (2012)[25]. Other motor sequence learning studies emphasize the contribution of NREM stage 2 sleep spindles to overnight improvement on a finger tapping task[26,27]. There is also evidence that REM sleep[23,28,29] is crucial for consolidation of motor sequence learning tasks. Clearly, the mechanism behind the benefit of sleep for complex motor skills needs to be further investigated. A study of Lewis et al (2011), has shown that auditory rhythm learning (tapping a finger in time with an auditory rhythm) is facilitated by sleep[4]. Moreover, activation of the cerebellum, striatum and supplementary motor area (SMA) was increased for the learned rhythm during the finger tapping task after sleep compared to after wake. These results imply that the striatum and cerebellum serve a memory function in rhythm learning. Based on this study, one would expect to also find differences in cerebellum, striatum and supplementary motor area activity after sleep for the SISL task. However, the study of Lewis et al (2011) is different from our study in the sense that explicit timing is used[4]. Furthermore, the mechanism behind auditory rhythm tapping may be different than the learning of sequential temporal intervals in the SISL task, where only visual cues are used. Interestingly, previous research in our group[7] has shown that performance on the SISL task specifically relies on the interplay between the hippocampus and the cerebellum. Whether sleep introduces changes in co-activation of these regions after performing the SISL task, would be of interest for future research.

References

1. Walker, M. P. & Stickgold, R. Sleep-dependent learning and memory consolidation. *Neuron* **44,** 121–133 (2004).
2. Diekelmann, S. & Born, J. The memory function of sleep. *Nat. Rev. Neurosci.* **11,** 114–26 (2010).
3. Coull, J. T. & Nobre, A. C. Dissociating explicit timing from temporal expectation with fMRI. *Curr. Opin. Neurobiol.* **18,** 137–144 (2008).
4. Lewis, P. A., Couch, T. J. & Walker, M. P. Keeping time in your sleep: Overnight consolidation of temporal rhythm. *Neuropsychologia* **49,** 115–123 (2011).
5. Genzel, L. *et al.* Complex motor sequence skills profit from sleep. *Neuropsychobiology* **66,** 237–243 (2012).
6. Gobel, E. W., Parrish, T. B. & Reber, P. J. Neural correlates of skill acquisition: Decreased cortical activity during a serial interception sequence learning task. *Neuroimage* **58,** 1150–1157 (2011).
7. Onuki, Y., Van Someren, E. J. W., De Zeeuw, C. I. & Van Der Werf, Y. D. Hippocampal-cerebellar interaction during spatio-temporal prediction. *Cereb. Cortex* **25,** 313–321 (2015).
8. Buysse, D. J., Reynolds, C. F., Monk, T. H., Berman, S. R. & Kupfer, D. J. The Pittsburgh sleep quality index: A new instrument for psychiatric practice and research. *Psychiatry Res.* **28,** 193–213 (1989).
9. Van Dongen, H. P. A., Maislin, G., Mullington, J. M. & Dinges, D. F. The cumulative cost of additional wakefulness: dose-response effects on neurobehavioral functions and sleep physiology from chronic sleep restriction and total sleep deprivation. *Sleep* **26,** 117-26 (2003).
10. Brainard, D. H. The Psychophysics Toolbox. *Spat. Vis.* **10,** 433–436 (1997).
11. Pelli, D. G. The VideoToolbox software for visual psychophysics: transforming numbers into movies. *Spat. Vis.* **10,** 437–442 (1997).
12. Kleiner, M. *et al.* What's new in Psychtoolbox-3? *Perception* **36,** S14 (2007).
13. Phillips, C., Leclercq, Y., Schrouff, J., Noirhomme, Q. & Maquet, P. FMRI artefact rejection and sleep scoring toolbox. *Comput. Intell. Neurosci.* **2011,** (2011).
14. Iber, C., Ancoli-Israel, S., Chesson, A. L. & Quan, S. F. *The AASM manual for the scoring of sleep and associated events: rules,terminology,and technical specifications American Academy of Sleep Medicine, Westchester, IL,1st edition*. (2007).
15. Massimini, M., Huber, R., Ferrarelli, F., Hill, S. & Tononi, G. The sleep slow oscillation as a traveling wave. *J. Neurosci.* **24,** 6862–70 (2004).
16. Dang-vu, T. T. *et al.* Spontaneous neural activity during human. *Proc.Natl.Acad.Sci.U.S.A* **105,** 15160–15165 (2008).
17. Piantoni, G. *et al.* Disrupted directed connectivity along the cingulate cortex determines vigilance after sleep deprivation. *Neuroimage* **79,** 213–222 (2013).
18. Mölle, M., Marshall, L., Gais, S. & Born, J. Grouping of spindle activity during slow oscillations in human non-rapid eye movement sleep. *J. Neurosci.* **22,** 10941–10947 (2002).
19. Ferrarelli, F. *et al.* Reduced sleep spindle activity in schizophrenia patients. *Am. J. Psychiatry* **164,** 483–492 (2007).
20. Team, R. C. *R: A language and environment for statistical computing. R Foundation for Statistical Computing*. (2012).
21. Cousineau, D. Confidence intervals in within-subject designs: A simpler solution to Loftus and Masson's method. *Tutor. Quant. Methods Psychol.* **1,** 42–45 (2005).
22. Korman, M. *et al.* Daytime sleep condenses the time course of motor memory consolidation. *Nat. Neurosci.* **10,** 1206–1213 (2007).
23. Fischer, S., Hallschmid, M., Elsner, A. L. & Born, J. Sleep forms memory for finger skills. *Proc. Natl. Acad. Sci. U. S. A.* **99,** 11987–91 (2002).
24. Walker, M. P. *et al.* Sleep and the Time Course of Motor Skill Learning. *Learn. Mem.* **10,** 275–284 (2003).
25. Antony, J. W., Gobel, E. W., O'Hare, J. K., Reber, P. J. & Paller, K. A. Cued memory reactivation during sleep influences skill learning. *Nat. Neurosci.* **15,** 1114–1116 (2012).
26. Barakat, M. *et al.* Fast and slow spindle involvement in the consolidation of a new motor sequence. *Behav. Brain Res.* **217,** 117–21 (2011).
27. Fogel, S. M. *et al.* fMRI and sleep correlates of the age-related impairment in motor memory consolidation. *Hum. Brain Mapp.* **35,** 3625–3645 (2014).

28. Smith, C. T., Aubrey, J. B. & Peters, K. R. Different Roles for REM and Stage 2 Sleep In Motor Learning: A Proposed Model. *Psychol. Belg.* **44,** 81–104 (2004).
29. Plihal, W. & Born, J. Effects of Early and Late Nocturnal Sleep on Declarative and Procedural Memory. *J. Cogn. Neurosci.* **9,** 534–547 (1995)

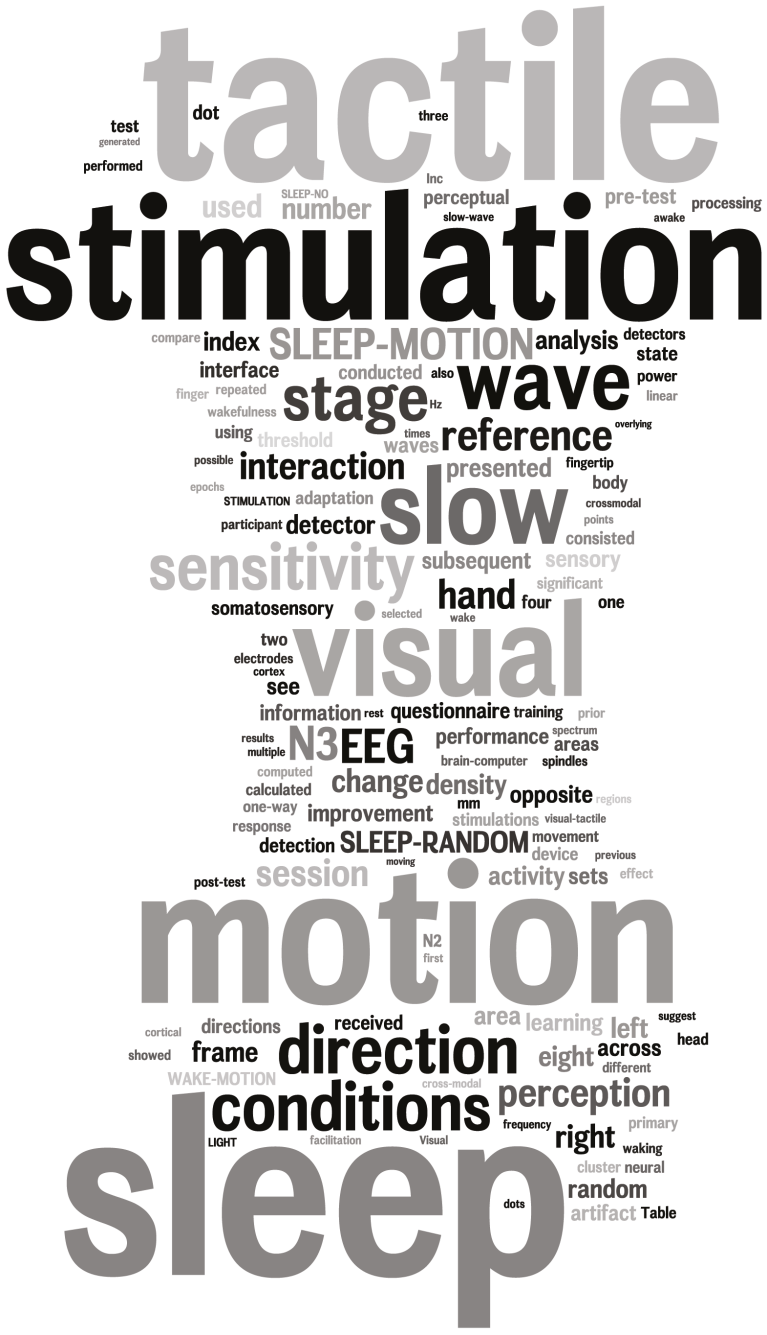
tactile
stimulation
motion
sleep
visual
slow
wave
stage
sensitivity
interaction
reference
direction
conditions
perception
SLEEP-MOTION
SLEEP-RANDOM
WAKE-MOTION
EEG
N3
test
generated
performed
dot
three
used
number
SLEEP-NO
perceptual
slow-wave
pre-test
processing
awake
compare
index
analysis
detectors
state
interface
conducted
also
power
finger
repeated
Hz
linear
wakefulness
overlying
using
threshold
times
waves
possible
fingertip
presented
body
epochs
STIMULATION
adaptation
crossmodal
participant
detector
points
consisted
subsequent
sensory
significant
somatosensory
selected
four
one
wake
two
electrodes
cortex
see
information
rest
questionnaire
training
prior
results
multiple
spectrum
areas
performance
brain-computer
spindles
computed
calculated
change
density
opposite
regions
one-way
improvement
mm
stimulations
visual-tactile
response
detection
movement
device
previous
moving
post-test
session
activity
sets
effect
N2
first
area
learning
left
suggest
head
cortical
directions
received
showed
frame
eight
across
different
cross-modal
frequency
primary
LIGHT
facilitation
Visual
right
waking
cluster
neural
random
dots
artifact
Table

Chapter 5. Tactile sensation during sleep biased the enhancement of visual learning

Yoshiyuki Onuki, Oti Lakbila-Kamal, Bo Scheffer, Eus J.W. Van Someren, and Ysbrand D. Van der Werf

In Submission

5.1 Abstract

Our visual perception can be biased by physical sensations in an awake state. However, it is still unknown whether novel sensory information even during sleep can bias our visual perception. We found that tactile motion stimulation on a finger tip during sleep selectively enhanced visual motion perception in subsequent wake and that the improvement was positively associated with slow wave activity over the somatosensory cortical area. In addition, such cross-modal interaction during sleep was processed based on the hand reference frame, the primary source of the tactile sensation in our body reference scheme of tactile perception. Our finding of a crossmodal interaction during sleep suggests that neuronal ensembles across different sensory circuits maintain functional interplay during sleep.

5.2 Introduction

In daily life our brain integrates tactile information such as texture and hardness with visual information, which resulted in even biasing our visual perception. However, it is still unknown such a system for our tactile perception is active even during sleep so that it can shape post-sleep visual perception. Furthermore, our tactile perception is a consequence through a competition of multiple sensory references such as hand and head.

Two experiments show that tactile motion stimulation on a finger tip during sleep selectively enhanced subsequent waking visual motion perception and that the improvement was positively associated with slow wave activity over the somatosensory cortical area. In addition, the cross-modal interaction during sleep was processed based on the hand reference frame, the primary source of the tactile sensation. Our finding of a crossmodal interaction during sleep suggests that neuronal ensembles across different sensory circuits maintain functional interplay during sleep.

In daily life our brain processes tactile information such as texture and hardness that can influence our visual perception. Our tactile perception is a consequence through a competition of multiple sensory references such as hand and head. However, it is still unknown such a system for our tactile perception is active even during sleep so that it can shape post-sleep visual perception.

Visual perceptual learning, i.e. the facilitation of sensitivity by repeated visual training, can be strengthened through sleep-dependent consolidation[1]. Individual differences in cross-sleep visual perceptual improvements correlate with the extent to which specifically the trained visual cortical region shows increased activation[2] and with slow-wave initiation[3] during sleep.

Visual motion perception can also be strengthened in the direction of the tactile sensory inputs when the two modalities are presented synchronously; conversely, visual inputs affect tactile perception[4,5]. When visual and tactile stimuli are presented with a delay, however, repeated exposure to tactile motion stimulation produces a counterphase motion aftereffect in the visual modality afterward[6]. The effect of temporal context of the sensory inputs reflects processes of both facilitation and adaptation in the crossmodal interaction between the visual and tactile domains.

The presumed neural mechanism for the interaction between visual and tactile information relies on processing in partially overlapping neural circuits. The primary visual cortex and human middle temporal/V5 complex (hMT/V5), for example, show activation during tactile orientation and motion processing[7,8]. In addition, the primary somatosensory cortex (S1) shows directionally selective neural responses to both visual and tactile motion stimulation[9,10].

To date, reports of visual and tactile cross-modal interaction concern processing during the awake state, while such an interaction in sleep has not yet been addressed. The described role of sleep in the facilitation of visual perceptual learning and the interaction between the visual and tactile modalities suggest that tactile motion stimulation during slow wave sleep could facilitate subsequent visual motion sensitivity in a direction-selective manner: either in the direction of the presented tactile stimulation, or in the direction opposite to the tactile motion due to adaptation.

It has not previously been explored whether the correspondence of somatotopic representations of the body from visual and tactile perspectives during wakefulness still persist during sleep. In the awake state, the intrinsic coordination of the tactile motion perception depends on the context of the task demand and one of multiple spatial references such as skin (hand)-, arm-, head-, and visual-based references[11,12] can be a dominant reference over the rest of references. However, it has not previously been explored which reference contributes on the visual-tactile interaction during sleep.

Therefore, the present study addressed two questions; the visual-tactile crossmodal interaction during sleep and the dominant reference frame for the multisensory interaction.

5.3 Methods

5.3.1 Participants

In experiment 1, 83 right-handed healthy participants who passed the online questionnaire (see under 'Online questionnaire prior to the recruitment' below) were recruited for the sleep experiment. The protocol of the experiment was approved by the ethics committee of the Department of Psychology, the University of Amsterdam, The Netherlands. All participants signed a consent form prior to the experiment.

27 participants were excluded from the analysis for the following reasons: awareness of the direction of the tactile motion stimulation during sleep (n = 1), an insufficient number (≦ 10 times) of tactile stimulations presented in sleep stage N3 (stage 3 non-rapid eye movement sleep) (n = 10), accidental detachment of index fingers from the tactile stimulation device owing to spontaneous body movements in sleep (n = 4), technical failure of the brain-computer interface (n = 8), or excessive response bias (≧ 100 times) towards one or more of the eight response options during the visual motion task (n = 4).

Accordingly, the remaining 56 participants were included in the analysis (18 males, 38 females, 23.0 ± 0.47 (mean ± SEM) years old). None of the participants had a history of excessive intake of alcohol and/or drugs, neurological, psychological, sleep or sensory disorders, or medication that may affect cognitive function. The participants were instructed to refrain from any intake of caffeine and medicine for 24 hours before the sleep experiment.

In experiment 2, 50 right-handed participants passed the online questionnaire and 38 participants were recruited for the experiment. 14 participants [14 female, 22 ± 0.99 (mean ± SEM) years old] were included for the analysis. The 24 participants were measured but excluded for the analysis due to the shallow sleep (n = 13), awareness of the direction of the tactile motion stimulation during sleep (n = 2), excessive response bias (n = 3), an insufficient number (≦ 10 times) of tactile stimulations presented in sleep stage N3 (n = 2), technical failure of the brain-computer interface (n = 1), accidentally detachment of index finger from the tactile device (n = 1), and changed arm position due to body movements during sleep (n = 2). All participants passed the online questionnaire and followed the same instruction used in the experiment 1.

5.3.2 Online questionnaire prior to the recruitment

All participants were examined by the online questionnaire before their recruitment as participants. The online questionnaire consisted of questions regarding medication and current or prior diagnoses of neurological or psychiatric disorders, the Athens Insomnia Scale (AIS)[13], Pittsburgh Sleep Quality Index (PSQI)[14], and Ford Insomnia Response to Stress Test (FIRST)[15] to check the daily sleep quality, daily habits, medication, fatigue, absence of sleep disorders, and resilience against possible sleep disturbances in response to stress and fatigue during the visual motion task and preparation of polysomnography. All selected participants scored below cut-off for insomnia or other sleep disorders (PSQI < 5, AIS < 6) and stress responsivity (FIRST < 19).

5.3.3 Sleep quality check prior to the experiment

To verify regular sleep cycles three days prior to the experiment, wrist movements were recorded by the actigraph (GENEActiv, Activeinsights Ltd, UK). During the actigraphy, participants were instructed to keep a sleep diary[16]. All participants slept > 7 hours daily and maintained their regular bedtimes in the days preceding the experiment.

5.3.4 Experimental procedure

In the experiment 1, participants were randomly assigned to one of three conditions (Figure 1a). In the first condition (SLEEP-MOTION), participants received the tactile motion stimulation during stage N3 sleep (stage 3 non-rapid eye movement sleep). In the second condition (WAKE-MOTION), participants also received the same tactile motion stimulation but remained awake. In the third condition (SLEEP-RANDOM), participants received the tactile random stimulation during stage N3 sleep. In the two sleep conditions, the participants who only entered light sleep (stage N1–N2) without receiving tactile stimulation were re-categorized as the LIGHT SLEEP-NO STIMULATION condition. Each condition consisted of 14 participants.

The experiment was conducted in a soundproof bedroom of the sleep laboratory at the Department of Sleep and Cognition, the Netherlands Institute for Neuroscience. The behavior of each participant during the experiment was monitored by an infrared video camera (IPELA, Sony. Inc, Japan). The experiment was held from 10:30 am to 3:30 pm to keep the same experimental schedule across participants thereby avoiding the effects of circadian rhythm on cognitive performance (time-of-day effects)[17].

The pre-test session of the visual motion task subsequent to the assessment sessions was conducted from 10:30 am to 11:30 am, to determine the motion coherence threshold for the task after which the pre-test was administered.

Following the 30-minute lunch intermission and 60-minute preparation of the polysomnography including electroencephalography (EEG), electrooculography (EOG), and chin electromyography (EMG) for the sleep conditions, the sleep session in all sleep conditions or rest session in the wake condition took place from 1:00 pm to 2:30 pm. In the sleep session, participants lay down on the bed and received the tactile stimulation from the tactile device on the bed. In the rest session for the wake condition, participants sat upright behind a desk and received the tactile motion stimulation from

the device on the tabletop, following previous investigations of visual-tactile motion perception[6].

After the 30-minute intermission to recover from sleep inertia for the sleep conditions[18], the post-test session of the visual motion task was conducted with the same threshold used in the pre-test session. Subsequently, participants filled out the post-experiment questionnaire and the surface areas of their right index fingertips were measured (see under "Post-experiment questionnaire" and "Measurement of fingertip areas", below).

In the experiment 2, participants received the upward linear tactile stimulation used in the SLEEP-MOTION condition. All procedure was conducted in the same manner as the experiment 1 except the body posture of the participants. When they receive the tactile stimulation during sleep, their right arms were tilted 90 degree vertically against their bodies (Figure 4a, b).

5.3.5 Visual random dot motion task

To quantify the visual motion sensitivity in different directions, participants performed the random dot motion task[19] in the pre-test and post-test sessions (Figure 1b). The stimulus consisted of a subset of dots moving coherently toward one of eight particular directions (0°, 45°, 90°, 135°, 180°, 225°, 270°, and 315° in polar coordinates) within the noise of randomly moving dots. The moving dots were presented for 500 ms after displaying each trial number for 1 second. The dot speed was 8° per sec. The dot density was 0.935 dots per deg^2. The diameter of the stimulation area was 14.6°. The task was programmed in Psychtoolbox 3[20,21] installed in MATLAB (R2011b, Mathworks. Inc, U.S.). The stimulation was displayed on a gamma-corrected CRT monitor (Dell Trinitron P1130, DELL. Inc, U.S.) under dark conditions. The distance between the computer screen and the eyes of participants was 43 cm. To keep the same distance across trials and to minimize fatigue during the task, the participant's head was supported by a chinrest (HeadSpot, UHCO Technical Services, US).

Preceding the pre-test session, assessment sessions were held for 15 minutes to measure the individual threshold of visible motion coherence level (50% performance level in a two-alternative forced choice task) using a staircase method[22]. A one-way ANOVA was conducted to compare the threshold of the visible motion coherence level between conditions (Supplementary Table 2).

After the assessment sessions, participants performed the pre-test session of the random dot motion task with eight possible response options (an eight-alternative forced choice task) for approximately 30 to 40 minutes. The task consisted of 240 trials with a 1-minute intermission after every 48 trials to minimize fatigue during the task. No time restriction was applied for giving the response. The task was repeated in the post-test session with the same threshold of the pre-test session, following the 30-minute intermission subsequent to the sleep or rest session.

5.3.6 Tactile stimulation

Tactile stimulation was presented to a right index fingertip on the custom-made MR-compatible tactile stimulator (950 mm height × 1920 mm width × 280 mm depth) in the sleep or rest session. The tactile stimulator consisted of eight piezoelectric actuators (Braille cell B11, Metec AG, Germany) to form the 8 × 8 active plastic pin area (21 mm height × 21 mm width) with 64 stimulation spaces (2.45 mm height × 2.45 mm width). Each pin is pushed up 0.7 mm by the actuator and can be operated independently by MATLAB (R2011b, Mathworks, Inc, U.S.).

For both SLEEP- and WAKE-MOTION conditions, adjacent linear stimulation of eight pins was presented eight times at 25 ms each to achieve the 200-ms motion sensation of one of four directions (up, down, left, right) (Supplementary Figure 1a). For the SLEEP-RANDOM condition, eight consecutive stimulations that consisted of eight pins chosen randomly from the 8 × 8 pin area was presented with the same parameters as the linear motion stimulation. It ensured that each pin would provide stimulation only

once every cycle of 200 ms and the total surface area covered in each stimulation cycles was identical between all stimulation types (Supplementary Figure 1b). The distal and proximal interphalangeal joints of the index finger were taped on the tactile device to maintain the same position on the active area of the instrument during the sleep experiment. A gel mousepad was placed under the palm and wrist of the right hand for supporting the hand.

In all sleep conditions, the final position of the hand joint was tilted slightly upward to maintain a hand posture that would produce the perception of a movement towards the fingertip as an upward movement, consistent with a head-hand reference frame as if the participant was looking down at the back of his/her hand, while at the same time maintaining comfort not to disturb sleep. The tactile device was placed under a thick blanket to avoid any sounds from the stimulation device potentially disturbing the participants' sleep. In wake condition, the hand posture was the same as the sleep conditions, but the hand was placed on the desk in front of the participant such that visual and tactile coordinates were retinally congruent.

For the delivery of the tactile motion stimulation in sleep or rest session of SLEEP- and WAKE-MOTION conditions, one of four possible directions (up, down, left, right) was selected by the criteria based on the score of the random dot motion task in pre-test session; the selected direction should be visually perceived at more than chance level (12.5% in an eight-alternative forced choice task) and could not be the most frequently selected direction across the eight directions to avoid the incidental facilitation of participants' response preferences instead of the facilitation of motion sensitivity. The number of each motion direction assigned to participants in the SLEEP-MOTION condition were four up, one down, four left, and five right, whereas that of the WAKE-MOTION condition was four up, three down, four left, and three right.

To equalize the inter-stimulus intervals of the tactile stimulation in the WAKE-MOTION condition with those of the SLEEP-MOTION and SLEEP-RANDOM conditions, we

generated the data set of inter-stimulus intervals from the kernel probability distribution that was fitted to data within 95th percentiles of the distributions of inter-stimulation intervals in both sleep conditions. The data generation was performed by the MATLAB function called "fitdist" in the Statistics toolbox (Mathworks, Inc, U.S.). A one-way ANOVA was conducted to compare the difference of the number of tactile stimulations and mean inter-stimulus intervals between conditions (Supplementary Table 2).

5.3.7 Post-experiment questionnaire

The questionnaires were provided to participants after the post-test session to assess participants' awareness of the tactile stimulation and the stimulation direction, to record the contents of participants' sleep mentation, and to check the hand preference. One participant indicated the correct direction of the tactile motion stimulation and was excluded from the analysis (see above under 'Participants'). Sleep mentation reports were collected to check the task- or stimulation-related dream experiences that may induce the improvement of post-sleep performance[23] (Supplementary Table 3). The hand preferences of participants were evaluated by the modified version of the Edinburgh handedness test[24] to confirm that all participants were right-handed. A one-way ANOVA was conducted to compare the scores of Edinburgh handedness inventory (Supplementary Table 2).

5.3.8 Measurement of fingertip areas

The anterior areas of the participants' right index fingertip were measured after the post-experiment questionnaire since it has been shown that the tactile acuity of the fingertip is reflected by its surface area[25]. Right index fingers were scanned at 1200 dpi as images of Tagged Image File Format (TIFF) by a digital scanner (HP Scanjet G4010, Hewlett-Packard Development Company, U.S.). The regions from the tip to the first joint in the image were defined and segmented manually. The segmented images were converted into binary images by the global image threshold[26]. Subsequently, the areas

of the index fingertips from the images were calculated as the number of pixels[27], and the scale was converted from pixels to mm^2. All calculations were performed using MATLAB Image Processing Toolbox (Mathworks, Inc, U.S.). A one-way ANOVA was conducted to compare differences in the surface area between the four conditions (Supplementary Table 2).

5.3.9 Brain-computer interface for automatic slow-wave detection and tactile stimulation

To present tactile stimulation to participants during slow wave sleep, we created a brain-computer interface to detect slow wave activities and to present tactile stimulation in real time. This interface consisted of the streaming of EEG data, preprocessing, slow-wave detection, and tactile stimulation (Figure1c).

The 256-ch EEG data was acquired at 500 Hz sampling frequency using a Geodesic EEG system and Amp server pro SDK (Electrical Geodesics, U.S.) implemented in Mac Pro (Apple. Inc, U.S.). The acquired data was streamed in chunks of 1024 data points to the EEG processing computer. In the processing computer, the streamed data was imported by BCI2000 [28] and the 3ch-EEG data of the frontal electrode (Fz), left and right mastoids were used for the further analysis. The streamed EEG data (Fz) were re-referenced by using the average EEG data of the left and right mastoids, detrended, band-pass filtered from 0.5 to 50 Hz, multiplied by a Hanning window, and converted to a frequency spectrum by the absolute values of Fast-Fourier Transform (FFT).

The epochs of preprocessed data were analyzed by the artifact detector and slow-wave detector. The artifact detector assessed the preprocessed EEG data first and subsequently the slow wave detector examined it when the data was passed by the artifact detector because body and respiration movements caused similar high-amplitude EEG characteristics as slow wave activity, which cause a false detection by the slow wave detector.

The tactile stimulation was delivered on the right index fingertip from the custom-made tactile device. The stimulation was initiated when the slow wave detector classified EEG epochs as the slow wave activity more than 15 times in the preceding 60 seconds.

5.3.10 Construction of artifact and slow wave detectors

To construct the detectors of movement artifact and slow wave activity, we used a machine-learning algorithm, the Support Vector Machine (SVM), implemented in the LIBSVM toolbox[29]. To optimize the classifier, we used the grid parameter search in LIBSVM toolbox to adjust the radial-basis-function (RBF) kernel parameter γ and the penalty parameter *C*.

All data sets for training and testing the classifiers were generated from 90-minute sleep EEG data of 15 participants of other sleep experiments conducted in the sleep laboratory of the Department of Sleep and Cognition, the Netherlands Institute for Neuroscience. The sleep data were recorded using the same 256-channel high-density electroencephalography at 500 Hz sampling frequency. None of the participants or sleep scorers of the data sets utilized for the classifiers was involved in this experiment to keep independence of training data sets for the classifiers and the test data sets for the real-time classifications in the brain-computer interface. All data sets were preprocessed in the same manner as the real-time preprocessing (see under "Brain-computer interface for automatic slow-wave detection and tactile stimulation" above).

For the construction of the artifact detector, 12 participants' data sets (9 participants' data used for training slow wave detector and 3 additional participants' data) were used to get sufficient training data sets of breathing and movement artifacts. A total of 38 epochs of 1024 data points was generated from each participant's data. The training data sets for the artifact detection consisted of the artifact data and the concatenated data of stage W ("Wake"), sleep N1, N2, and N3.

For the construction of the slow wave detector, data sets of 12 participants were used. The total 1008 epochs of 1024 data points were generated from each participant data. The training data sets for the slow-wave detection consisted of the concatenated data of the stage W and light sleep (stage N1, and N2), and the data of stage N3.

5.3.11 Offline tests of slow wave and artifact detectors

The prediction accuracies of each detector were evaluated by a leave-one-subject-out cross-validation. The 12 cross-validation data sets were generated; the 11 participant data sets were used for training the detectors and the remaining one was used for testing the detectors. This procedure was repeated 12 times by changing data to validate the accuracies of each detector. To evaluate the accuracies of the detectors in the cross-validation, we drew the receiver operating characteristic (ROC) curve by shifting the detection threshold of the output probability estimates from the support vector machine and calculated area under the curve (AUC).

5.3.12 Offline sleep scoring

For qualifying the sleep state, the 90-minute polysomnographic data recorded in the sleep sessions was scored every 30 seconds by two well-trained sleep scorers, following the standardized sleep score manual[30]. The two sleep scorers were not involved in scoring the sleep EEG data used for the construction of the artifact and slow wave detectors. To compare durations of each sleep stage, two-sample *t* test between two conditions (SLEEP-MOTION and SLEEP-RANDOM) and one-way ANOVA between three conditions (the previous conditions and LIGHT SLEEP-NO STIMULATION condition) were performed, respectively.

5.3.13 Power spectrum analysis during the tactile stimulation

To compare the spectral contents between the different tactile stimulation in slow wave sleep, the power spectra during the tactile stimulation were computed in both the SLEEP-MOTION and SLEEP-RANDOM conditions. The total number of EEG epochs in stage N3 was 2822 in SLEEP-MOTION condition and 3744 in SLEEP-RANDOM condition.

The 256-channel EEG data were re-referenced by the average EEG data of the left and right mastoids, and band-pass filtered (0.5 to 40 Hz) after DC offset removal. EEG data were chunked as 1024-milisecond post-stimulus periods of the tactile stimulation (512 data points). EEG data with poor signal quality were excluded by visual inspection of the data. The average values of the log-transformed power spectrum of the post-stimulus period were computed (window length of 512 points, fast Fourier transform length of 512 points, non-overlap), using the spectopo function from EEGLAB toolbox[31]. The average power spectrum was computed on each electrode of the post-stimulus power spectrum in each frequency band (Delta: 0.5–4Hz, Theta: 4–8Hz, Alpha: 8–12Hz, Beta: 12–24Hz, Sigma: 8–13Hz, and Gamma: 24–40Hz). The difference of the power spectrum between conditions was computed in each frequency band and all frequency bands (0.5–40Hz). Electrodes exceeding the threshold of the t-statistic ($P < 0.05$ for two-tailed *t* test) were subsequently used by a cluster-based permutation test (cluster size correction $P < 0.05$) with 10^4 iterations[32–35].

5.3.14 Quantification of the behavioral measurements

The sensitivity (d') of visual motion discrimination was calculated in each pre-test and post-test session. The sensitivity changes served as the effect of primary interest and were calculated by subtracting the performance of the pre-test session from the performance of the post-test session for all eight directions.

All statistical analyses were computed with IBM SPSS Statistics (SPSS version 22, Chicago, IL). To compare behavioral performances between SLEEP-MOTION and WAKE-MOTION conditions, a two-way repeated measures ANOVA was performed. Holm-Bonferroni post

hoc tests were applied afterward when significant differences in the omnibus test were found.

We also used two separate permutation tests for the SLEEP-RANDOM and LIGHT SLEEP-NO STIMULATION conditions using 10^5 iterations, to test whether values of the sensitivity change in each condition exceeded the sensitivity change in the opposite direction to the tactile motion stimulation in the SLEEP-MOTION condition. In the permutation test, the sensitivity change data of eight directions in each SLEEP-RANDOM and LIGHT SLEEP-NO STIMULATION condition was shuffled in random order within each participant. Subsequently, we calculated the p-value, comparing the sensitivity change in the SLEEP-MOTION condition against the distribution of the sensitivity change from the randomized data.

5.3.15 Quantification of the number and density of spindles and slow waves

The numbers and densities of spindles and slow waves in each sleep stage N2 and N3 were computed by using previously described methods for offline spindle and slow wave detection[36–40].

After applying a 0.2–4 Hz bandpass filter to the EEG potentials on each electrode, slow waves were identified when the EEG activity met three criteria that conformed to the sleep scoring manual[30]: 0.2–1 second duration of a signal between a zero-down crossing and zero-up crossing, less than -60 μV amplitude of the negative peak, and at least 75 μV peak-to-peak amplitude. The slow wave density in stage N2 and N3 was calculated as the number of slow waves per minute (Supplementary Figure 2a).

For the spindle detection, all EEG potentials were processed by 11–16 Hz bandpass filtering and subsequently the signal envelopes were computed by the Hilbert transform. Spindles were detected when the envelope was above a 3 μV threshold. Spindle density

in stage N2 and N3 was calculated as the number of spindles per minute (Supplementary Figure 2b).

5.3.16 Multivariate regression analysis and correlation analysis to assess the relationship between the behavioral performance and other variables

A stepwise multiple linear regression analysis in SPSS (SPSS version 22, Chicago, IL) was performed to examine the influence of multiple variables on the individual cross-sleep sensitivity change in the direction opposite to the tactile motion stimulation in the SLEEP-MOTION condition. Age, index finger areas, numbers of tactile stimulation, numbers and densities of slow waves and sleep spindles in stages N2 and N3 from non-overlapping regions (anterior, posterior, left, right) were selected as candidate factors to explain the sensitivity change. Electrodes of four non-overlapping regions were selected based on a previous study[37]. Following the results of the regression analysis, Pearson's correlation coefficient was calculated to assess associations between the slow wave density of stage N3 across all electrodes and the sensitivity change of the opposite direction to the tactile motion stimulation in the SLEEP-MOTION condition. Significant clusters were determined by a cluster-based permutation test[32–35].

5.4 Results

We examined the changes in visual motion sensitivity across periods of sleep and wakefulness with tactile motion or random pattern stimulation to the index finger using a custom-made 64-pin braille-type tactile device (Figure 1b and Supplementary Figure 1).

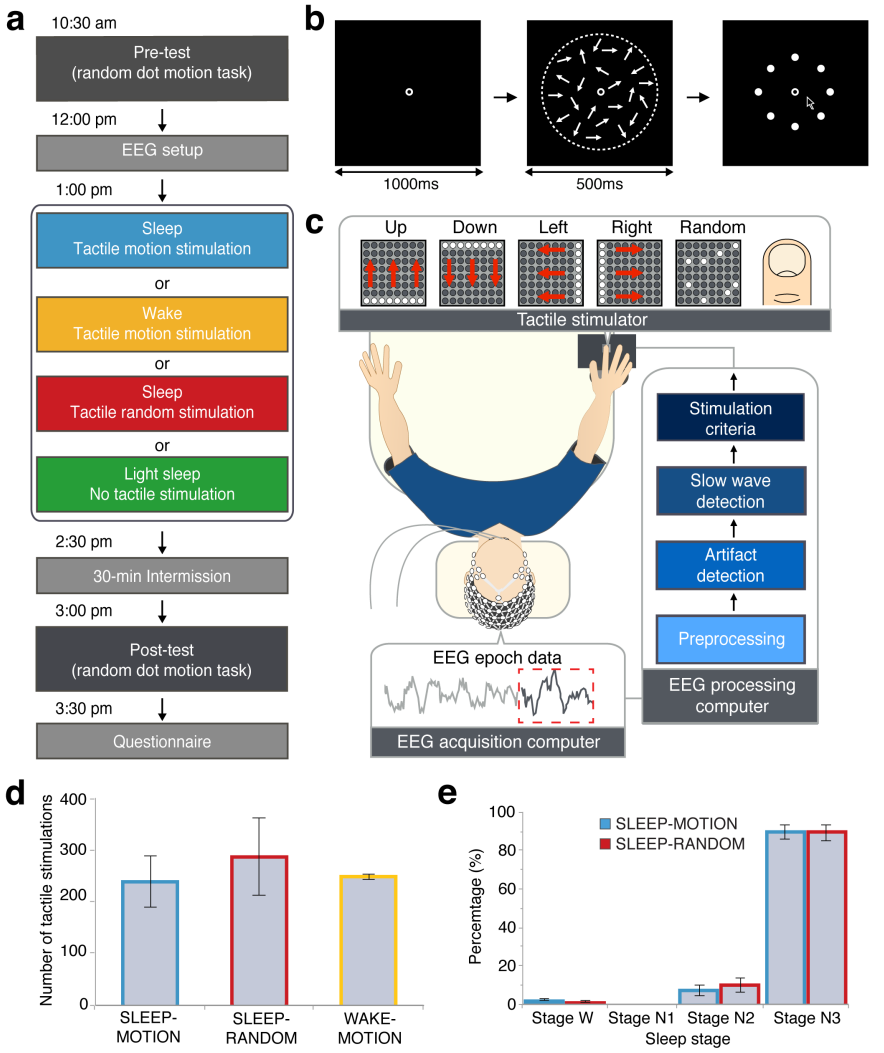

Figure 1. Experimental procedure and the visual motion task, the setup of the brain-computer interface for the sleep experiment, and offline analyses of tactile stimulation in the different conditions and across sleep stages. (a) Experimental procedure and timeline. (b) In one trial of the random dot motion task, a fixation screen was followed by an array of moving dots. Subsequently, the subject chose the perceived direction from eight response options (white filled circles) by a mouse click. (c) The brain-computer interface presented tactile stimulation upon the assessments of the artifact and slow wave detectors (support vector machine) and the stimulation criteria (a minimum of 15 slow waves in the preceding minute). (d) The number of tactile stimulations in three different conditions. (e) The percentages of tactile stimulations across sleep stages verified that the slow wave detector succeeded in detecting slow wave activities and allowed for selective timing of tactile stimulation during stage N3 sleep. The stimulations in stage N2 were presented in the transition period between stage N2 and N3 while the incidental stimulation during stage W followed sudden waking epochs immediately after stage N3.

In the SLEEP conditions participants received tactile motion stimulation (SLEEP-MOTION) or random pattern stimulation (SLEEP-RANDOM) timed to sleep slow waves in sleep stage N3 (stage 3 non-rapid eye movement sleep) (see Supplementary Figure 1). In the WAKE condition participants received tactile motion stimulation during wakefulness (WAKE-MOTION). Participants originally assigned to the sleep conditions who remained in lighter sleep (stage N1–N2) without receiving the tactile stimulation were re-categorized as the LIGHT SLEEP-NO STIMULATION condition.

While participants in the WAKE-MOTION condition maintained quiet wakefulness in between the two performance assessments, those assigned to the SLEEP conditions had the opportunity to sleep for up to 90 minutes. Polysomnography was recorded including 256-channel high-density electroencephalography (EEG) and stored for offline scoring of sleep stages and for counting slow waves and sleep spindles (Supplementary Figure 2). The durations and percentage distributions of sleep stages did not differ between the SLEEP-MOTION and SLEEP-RANDOM conditions (Supplementary Table 1).

For the delivery of tactile stimulation during sleep, we created a brain-computer interface for automatically presenting tactile stimulation upon real-time detection of slow wave activity from a midline frontal (Fz) EEG electrode (Figure 1c). The interface accommodated two subsequent classifiers detecting motion or respiratory artifacts and slow wave activity, respectively (Supplementary Figure 3). The classifiers successfully detected slow waves in real time (Supplementary Figure 4a) and slow wave-triggered tactile stimulations were continuously presented in both the SLEEP-MOTION and SLEEP-RANDOM conditions (Supplementary Figure 4b). Posthoc analysis showed that conditions did not differ with respect to the number of stimulations ($F_{2,39} = 0.91$, $P = 0.41$, one-way ANOVA) or the mean inter-stimulus intervals ($F_{2,39} = 2.18$, $P = 0.127$, one-way ANOVA) (Figure 1d and Supplementary Table 2**)**. In both conditions, 90% of the stimulation was presented in sleep stage N3 (Figure 1e**)**. None of the included participants reported awareness of the direction of tactile motion stimulation and task-related sleep mentation (Supplementary Table 3).

To assess changes in visual motion sensitivity, we measured performance on the visual random dot motion task to detect eight possible motion directions from moving dots displayed on a computer screen with pre-defined threshold levels of motion coherence between dots[19] in the morning (pre-test) and in the afternoon (post-test). The performance was evaluated by the sensitivity value d'. Its change from the morning to the afternoon was used as the effect of primary interest. Thresholds of dot motion coherence for the task did not differ between conditions ($F_{3,52}$ = 1.57, P = 0.21, one-way ANOVA; Supplementary table 2).

The assessment of visual motion sensitivity change of participants that received tactile motion stimulation across sleep and wake showed a significant interaction effect between condition (2 levels: SLEEP-MOTION and WAKE-MOTION conditions) and direction (8 levels) (Interaction effect: $F_{7,182}$ = 3.499, P = 0.002, η^2 = 0.12; main effect of condition: $F_{1,26}$ = 0.39, P = 0.54, η^2 = 0.015; main effect of direction: $F_{7,182}$ = 0.44, P = 0.88, η^2 = 0.014). As shown in Figure 2, a significant improvement for the visual motion sensitivity across sleep occurred only in the direction opposite to the tactile motion stimulation during slow wave sleep (t_{26} = 3.98, P < 0.005, Hedges' g = 1.46, Holm-Bonferroni correction). No improvement in any direction occurred when participants received the tactile stimulation during waking. This indicates that slow wave sleep represents a more optimal state to facilitate cross-modal interaction than wakefulness [41]. Furthermore, participants in the SLEEP-RANDOM and LIGHT SLEEP-NO STIMULATION conditions showed no improvement of motion sensitivity in any direction (Supplementary Figure 5, 6), suggesting that both tactile motion information and slow wave sleep are required to induce a direction-selective facilitation of the visual motion perceptual learning.

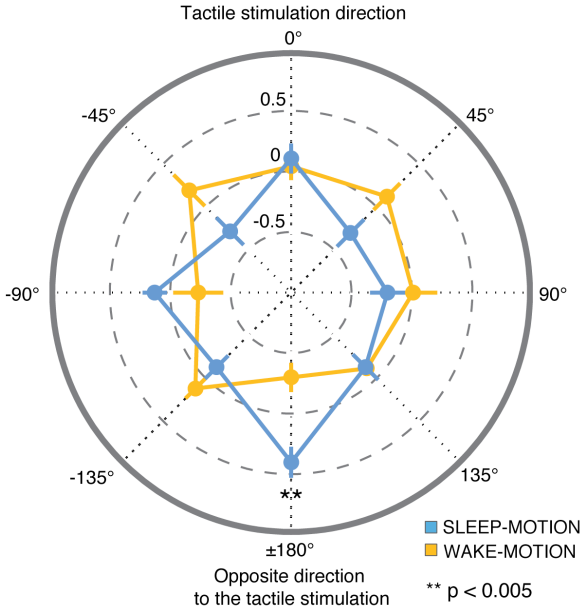

Figure 2. Visual motion sensitivity change. The sensitivity change (d') from the morning to the afternoon as assessed by the random dot motion task after tactile motion stimulation during slow wave sleep or wake. Visual motion sensitivity improved in the direction opposite to the tactile stimulation direction (+/- 180°) only in the sleep condition. The degrees denote the angle of the visual coherent motion relative to the tactile motion direction. Error bar denotes SEM. ** $P < 0.005$ (Holm-Bonferroni correction).

To investigate factors involved in individual differences in the cross-sleep motion sensitivity improvement, we used multiple linear regression analysis including the following regressors: age, index finger areas, number of tactile stimulation, number and density (the average number of slow waves or spindles per minute) of slow waves and spindles in stage N2 and N3 in four non-overlapping scalp regions (anterior, posterior, left, right). The improvement was explained only by stage N3 slow wave density over the left scalp region ($F_{1,12} = 10.52$, $P < 0.007$, $r = 0.68$, Figure 3a and see methods for more details). Furthermore, a cluster of scalp electrodes overlying the left somatosensory cortical area showed a significant association of stage N3 slow wave density with the visual motion sensitivity enhancement exclusively in the direction opposite to tactile motion stimulation (Figure 3b, c, and see methods for more details).

To assess whether the tactile motion stimulation activates the sleeping brain's visual regions in agreement with previous reports during the waking state[7,8], we compared the EEG power spectral density during the post-stimulus periods of every tactile motion stimulation versus tactile random stimulation in sleep stage N3 (see methods for more details). The results showed that the SLEEP-MOTION condition had a higher EEG broadband power (0.5–40Hz) than the SLEEP-RANDOM condition in a cluster of electrodes overlying the visual cortex (Supplementary Figure 7). Since the motion and random stimulation conditions were matched for spatial-temporal features of the stimulation except the motion aspect (Supplementary Figure 1), this suggests visual cortical processing of tactile motion information during sleep. Conversely, a cluster of electrodes overlying the left somatosensory area showed lower spectral power during the SLEEP-MOTION condition as compared with the SLEEP-RANDOM condition. The lower responsiveness of somatosensory motion-sensitive neurons in SLEEP-MOTION condition than SLEEP-RANDOM condition likely reflects adaptation to the tactile motion stimulation. This region also corresponds to the areas showing a significant positive relation between stage N3 slow wave density and the cross-sleep visual motion detection enhancement (Figure 3b). Together, the findings suggest that the ongoing slow wave activity over the somatosensory area provides a certain state for neural adaptation by the repeated tactile stimulation, to influence the visual cortical regions involved in both motion processing[7] and sleep-dependent consolidation of visual perceptual learning[2,3].

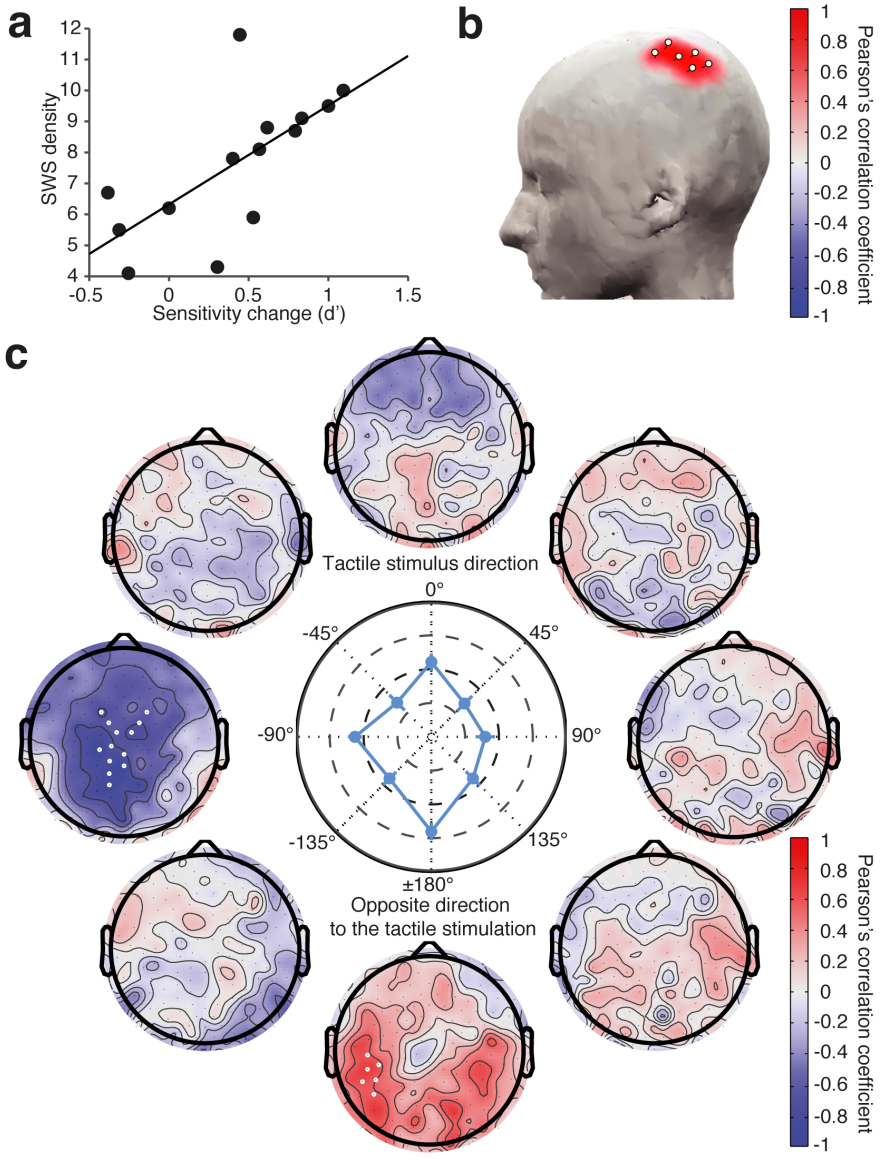

Figure 3. The correlation relationship between the visual sensitivity change and slow wave density in the SLEEP-MOTION condition. (a) The significant sensitivity changes in the direction opposite to the tactile stimulation in the SLEEP-MOTION condition correlated with stage N3 slow wave density from electrodes over the left hemispheric region ($r = 0.68$, $P = 0.007$). (b) 3D head model of the topographic map shows a significant correlation for the electrode cluster overlying the left somatosensory region ($P < 0.05$, cluster size corrected). (c) Topographic maps of the relation between the stage N3 slow wave density and the sensitivity change of eight directions in SLEEP-MOTION condition. Significant clusters were found only for the -90 degree and +/-180 degree directions of the tactile motion stimulation. White locations demarcate electrodes in a significant cluster after 10^4 iterations of a cluster-based permutation test ($P < 0.05$, cluster size corrected).

Our results in the first experiment suggest the tactile information during sleep biased the visual perceptual learning, but the contribution and mechanism of such a bodily reference frame to the visual improvement needs to be borne out. To examine the body reference frame to dominate the tactile perception during sleep, we conducted the second experiment that dissociates the head and hand reference frames. The experimental setup and stimulus parameters were the same as the first experiment. We induced the tactile linear motion from the bottom row to the top row on the index fingers of the new participants whose right arms were stretched out at 90 degree to the side (Figure 4a, b). The linear motion can be recognized either as "UP" direction from the hand reference frame or "RIGHT" direction from the head reference frame. In the behavioral performance, the visual motion sensitivity change showed an improvement only on the orientation of the hand reference frame, especially down direction (t_{13} = 4.2633, P = 0.007 < 0.01, Holm-Bonferroni correction. Figure 4c).

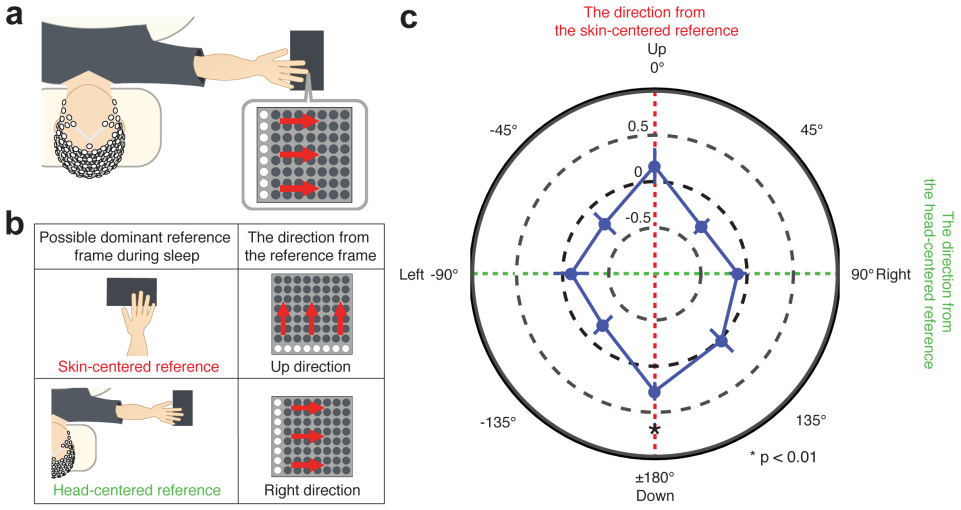

Figure 4. The experimental setup, the schematic diagram for the hand and head reference frame, and visual motion sensitivity change. (a) The diagram of the experimental setup. (b) The schematic diagram of the expected outcomes from the possible dominant reference frames: skin-centered reference frame and head-centered reference frame. (c) Visual motion sensitivity improved in the direction opposite to the tactile stimulation direction (+/- 180°), which was observed in Experiment 1. The improvement anchored only to the direction from the skin-centered reference frame. The degrees denote the angle of the visual coherent motion relative to the tactile motion direction. Error bar denotes SEM. * P < 0.01 (Holm-Bonferroni correction).

5.5 Discussion

We here report that the automatic delivery of tactile motion stimulation triggered by slow wave activity during sleep significantly improved subsequent visual motion sensitivity exclusively in the direction opposite to the tactile motion stimulation. The findings suggest that i) tactile information can be processed during sleep through the thalamocortical system, without inducing waking[42], ii) neuronal ensembles across different sensory circuits maintain functional interaction during sleep and iii) repeated tactile motion stimulation during sleep causes an adaptation process.

Our findings are in agreement with the report that repetitive sound stimulation induced a stimulus-specific adaptation during both non-rapid and rapid eye movement sleep[43] and commensurate with previous work showing an opposite visual motion aftereffect after directional tactile stimulation during wakefulness[6]. The neural mechanism of this aftereffect is thought to involve a selective neural adaptation resulting in an imbalance between the activities of subpopulations of direction-selective neurons in visual motion-processing areas such as hMT/V5[44]. Our results agree with the notion that repetitive tactile motion information during sleep leads to a direction-selective imbalance in visual motion processing, biasing the ongoing consolidation process of visual perceptual learning[45].

Individual differences in cross-sleep visual motion sensitivity improvement were positively associated with slow wave density in electrodes overlying the somatosensory cortex. Recurrent neuronal interactions between the primary somatosensory cortex (S1) and secondary motor cortex (M2) underlie tactile perception from passive tactile inputs[46]. Slow wave activity can be modulated by external sensory stimuli to enhance memory consolidation[47] and reflects processes of experience-dependent plasticity[48] that support perceptual learning[3]. The association that we observed here therefore suggests that the tactile stimulation triggered by the ongoing slow wave activity spurred processing in the neural circuit between S1 and M2, providing an optimal state for

visual-tactile cross-modal interaction to improve subsequent waking performance of visual motion perception.

Previous studies coupled multimodal sensory stimuli prior to sleep for subsequent targeted memory reactivation during sleep to induce selective memory enhancement[49–51]. We here show that it is also possible to facilitate the subsequent waking performance by inducing a cross-modal interaction of novel tactile information provided during sleep with the consolidation of recent visual learning.

In addition to the finding of the experiment 1, our results (Figure 4) in the experiment 2 suggest for the first time that the maintenance of a bodily spatial reference during sleep that fosters a contribution to subsequent visual learning, anchoring to the hand reference frame, the primary sensory resource. In the awake state, the visual illusion and perceptual learning were not only restricted to retinal location but also can be established at the body reference such as the hand- and head-centered reference[52,53]. However, all studies were reported in the awake state, and the further exploration is required to understand the underlying mechanisms of the body reference for the tactile perception during the sleep.

We here report that the automatic delivery of tactile motion stimulation triggered by slow wave activity during sleep significantly improved subsequent visual motion sensitivity exclusively in the direction opposite to the tactile motion stimulation.

Our findings are in agreement with the report that repetitive sound stimulation induces a stimulus-specific adaptation during sleep[43] and commensurate with previous work of a visual-tactile motion aftereffect[6]. The mechanism of the motion aftereffect likely represents a neural adaptation resulting in an imbalance between the activities of direction-selective neurons in visual motion-processing areas such as human middle temporal/V5 complex (hMT/V5)[44] that are also activated during visual-tactile crossmodal interaction[7]. Our results suggest that slow wave sleep represents a more optimal state

than wakefulness[41] for biasing the ongoing sleep-dependent consolidation process of perceptual learning through crossmodal interaction.

References

1. Mednick, S., Nakayama, K. & Stickgold, R. Sleep-dependent learning: a nap is as good as a night. *Nat. Neurosci.* **6,** 697–698 (2003).
2. Yotsumoto, Y. *et al*. Location-Specific Cortical Activation Changes during Sleep after Training for Perceptual Learning. *Curr. Biol.* **19,** 1278–1282 (2009).
3. Mascetti, L. *et al.* The Impact of Visual Perceptual Learning on Sleep and Local Slow-Wave Initiation. *J. Neurosci.* **33,** 3323–3331 (2013).
4. Pei, Y. C. *et al.* Cross-modal sensory integration of visual-tactile motion information: instrument design and human psychophysics. *Sensors (Basel).* **13,** 7212–7223 (2013).
5. Bensmaïa, S. J., Killebrew, J. H. & Craig, J. C. Influence of visual motion on tactile motion perception. *J. Neurophysiol.* **96,** 1625–37 (2006).
6. Konkle, T., Wang, Q., Hayward, V. & Moore, C. I. Motion Aftereffects Transfer between Touch and Vision. *Curr. Biol.* **19,** 745–750 (2009).
7. Hagen, M. C. *et al.* Tactile motion activates the human middle temporal/V5 (MT/V5) complex. *Eur. J. Neurosci.* **16,** 957–964 (2002).
8. Zangaladze, A, Epstein, C. M., Grafton, S. T. & Sathian, K. Involvement of visual cortex in tactile discrimination of orientation. *Nature* **401,** 587–590 (1999).
9. Pei, Y. C., Hsiao, S. S., Craig, J. C. & Bensmaia, S. J. Shape invariant coding of motion direction in somatosensory cortex. *PLoS Biol.* **8,** (2010).
10. Pei, Y. C. & Bensmaia, S. J. The neural basis of tactile motion perception. *J. Neurophysiol.* **112,** 3023–3032 (2014).
11. Heed, T., Buchholz, V. N., Engel, A. K. & Röder, B. Tactile remapping: From coordinate transformation to integration in sensorimotor processing. *Trends Cogn. Sci.* **19,** 251–258 (2015).
12. Pei, Y.-C. & Bensmaïa, S. J. The neural basis of tactile motion perception. *J. Neurophysiol.* **60637,** jn.00391.2014 (2014).
13. Soldatos, C. R., Dikeos, D. G. & Paparrigopoulos, T. J. Athens Insomnia Scale: validation of an instrument based on ICD-10 criteria. *J. Psychosom. Res.* **48,** 555–560 (2000).
14. Buysse, D. J., Reynolds, C. F., Monk, T. H., Berman, S. R. & Kupfer, D. J. The Pittsburgh sleep quality index: A new instrument for psychiatric practice and research. *Psychiatry Res.* **28,** 193–213 (1989).
15. Chang, P. P., Ford, D. E., Mead, L. A., Cooper-Patrick, L. & Klag, M. J. Insomnia in young men and subsequent depression. The Johns Hopkins Precursors Study. *Am. J. Epidemiol.* **146,** 105–114 (1997).
16. Carney, C. E. *et al.* The consensus sleep diary: standardizing prospective sleep self-monitoring. *Sleep* **35,** 287–302 (2012).
17. Barrett, T. R. & Ekstrand, B. R. Effect of sleep on memory: III. Controlling for time-of-day effects. *J. Exp. Psychol.* **96,** 321–327 (1972).
18. Tassi, P. & Muzet, A. Sleep inertia. *Sleep Med. Rev.* **4,** 341–353 (2000).
19. Shadlen, M. N. & Newsome, W. T. Motion perception: seeing and deciding. *Proc. Natl. Acad. Sci. U. S. A.* **93,** 628–633 (1996).
20. Brainard, D. H. The Psychophysics Toolbox. *Spat. Vis.* **10,** 433–436 (1997).
21. Pelli, D. G. The VideoToolbox software for visual psychophysics: transforming numbers into movies. *Spat. Vis.* **10,** 437–442 (1997).
22. García-Pérez, M. A. Forced-choice staircases with fixed step sizes: asymptotic and small-sample properties. *Vision Res.* **38,** 1861–1881 (1998).
23. Wamsley, E. J., Tucker, M., Payne, J. D., Benavides, J. A. & Stickgold, R. Dreaming of a Learning Task Is Associated with Enhanced Sleep-Dependent Memory Consolidation. *Curr. Biol.* **20,** 850–855 (2010).
24. Oldfield, R. C. The assessment and analysis of handedness: The Edinburgh inventory. *Neuropsychologia* **9,** 97–113 (1971).
25. Peters, R. M., Hackeman, E. & Goldreich, D. Diminutive Digits Discern Delicate Details: Fingertip Size and the Sex Difference in Tactile Spatial Acuity. *J. Neurosci.* **29,** 15756–15761 (2009).
26. Otsu, N. A Threshold Selection Method from Gray-Level Histograms. *Syst. Man Cybern. IEEE Trans.* **9,** 62–66 (1979).
27. van der Bilt, A., Speksnijder, C. M., de Liz Pocztaruk, R. & Abbink, J. H. Digital image processing versus visual assessment of chewed two-colour wax in mixing ability tests. *J. Oral Rehabil.* **39,** 11–17 (2012).

28. Schalk, G., McFarland, D. J., Hinterberger, T., Birbaumer, N. & Wolpaw, J. R. BCI2000: A general-purpose brain-computer interface (BCI) system. *IEEE Trans. Biomed. Eng.* **51,** 1034–1043 (2004).
29. Chang, C. C. & Lin, C. J. LIBSVM: A library for support vector machines. *ACM Trans. Intell. Syst. Technol.* **2,** 1–27 (2011).
30. Iber, C., Ancoli-Israel, S., Chesson, A. & Quan, S. *The AASM Manual for the Scoring of Sleep and Associates Events: Rules, Terminology and Technical Specifications*. *American Academy of Sleep Medicine* (American Academy of Sleep Medicine, 2007). doi:10.1002/ejoc.201200111
31. Delorme, A. & Makeig, S. EEGLAB: An open source toolbox for analysis of single-trial EEG dynamics including independent component analysis. *J. Neurosci. Methods* **134,** 9–21 (2004).
32. Bullmore, E. T. *et al.* Global, voxel, and cluster tests, by theory and permutation, for a difference between two groups of structural MR images of the brain. *IEEE Trans. Med. Imaging* **18,** 32–42 (1999).
33. Maris, E. & Oostenveld, R. Nonparametric statistical testing of EEG- and MEG-data. *J. Neurosci. Methods* **164,** 177–190 (2007).
34. Groppe, D. M., Urbach, T. P. & Kutas, M. Mass univariate analysis of event-related brain potentials/fields I: A critical tutorial review. *Psychophysiology* **48,** 1711–1725 (2011).
35. Manly, B. F. *Randomization, bootstrap and Monte Carlo methods in biology, third edition*. (Chapman & Hall/CRC, 2007).
36. Piantoni, G. *et al.* Individual differences in white matter diffusion affect sleep oscillations. *J. Neurosci.* **33,** 227–233 (2013).
37. Massimini, M., Huber, R., Ferrarelli, F., Hill, S. & Tononi, G. The sleep slow oscillation as a traveling wave. *J. Neurosci.* **24,** 6862–70 (2004).
38. Dang-Vu, T. T. *et al.* Spontaneous neural activity during human slow wave sleep. *Proc. Natl. Acad. Sci.* **105,** 15160–15165 (2008).
39. Mölle, M., Marshall, L., Gais, S. & Born, J. Grouping of spindle activity during slow oscillations in human non-rapid eye movement sleep. *J. Neurosci.* **22,** 10941–10947 (2002).
40. Ferrarelli, F. *et al.* Reduced sleep spindle activity in schizophrenia patients. *Am. J. Psychiatry* **164,** 483–492 (2007).
41. Diekelmann, S., Büchel, C., Born, J. & Rasch, B. Labile or stable: opposing consequences for memory when reactivated during waking and sleep. *Nat. Neurosci.* **14,** 381–6 (2011).
42. McCormick, D. A. & Bal, T. Sensory gating mechanisms of the thalamus. *Curr. Opin. Neurobiol.* **4,** 550–556 (1994).
43. Nir, Y., Vyazovskiy, V. V., Cirelli, C., Banks, M. I. & Tononi, G. Auditory responses and stimulus-specific adaptation in rat auditory cortex are preserved across NREM and REM sleep. *Cereb. Cortex* **25,** 1362–1378 (2015).
44. Mather, G., Pavan, A., Campana, G. & Casco, C. The motion aftereffect reloaded. *Trends Cogn. Sci.* **12,** 481–487 (2008).
45. Sasaki, Y., Nanez, J. E. & Watanabe, T. Advances in visual perceptual learning and plasticity. *Nat. Rev. Neurosci.* **11,** 53–60 (2009).
46. Manita, S. *et al.* A Top-Down Cortical Circuit for Accurate Sensory Perception. *Neuron* **86,** 1304–1316 (2015).
47. Ngo, H. V. V, Martinetz, T., Born, J. & Mölle, M. Auditory closed-loop stimulation of the sleep slow oscillation enhances memory. *Neuron* **78,** 545–553 (2013).
48. Wilhelm, I. *et al.* Sleep Slow-Wave Activity Reveals Developmental Changes in Experience-Dependent Plasticity. *J. Neurosci.* **34,** 12568--12575 (2014).
49. Rudoy, J. D., Voss, J. L., Westerberg, C. E. & Paller, K. A. Strengthening individual memories by reactivating them during sleep. *Science* **326,** 1079 (2009).
50. Rasch, B., Büchel, C., Gais, S. & Born, J. Odor cues during slow-wave sleep prompt declarative memory consolidation. *Science* **315,** 1426–1429 (2007).
51. van Dongen, E. V. *et al.* Memory stabilization with targeted reactivation during human slow-wave sleep. *Proc. Natl. Acad. Sci. U. S. A.* **109,** 10575–10580 (2012).
52. Zhang, E. & Li, W. Perceptual learning beyond retinotopic reference frame. *Proc. Natl. Acad. Sci.* **107,** 15969–15974 (2010).
53. Matsumiya, K. & Shioiri, S. Moving one's own body part induces a motion aftereffect anchored to the body part. *Curr. Biol.* **24,** 165–169 (2014).

Supplementary figures and tables

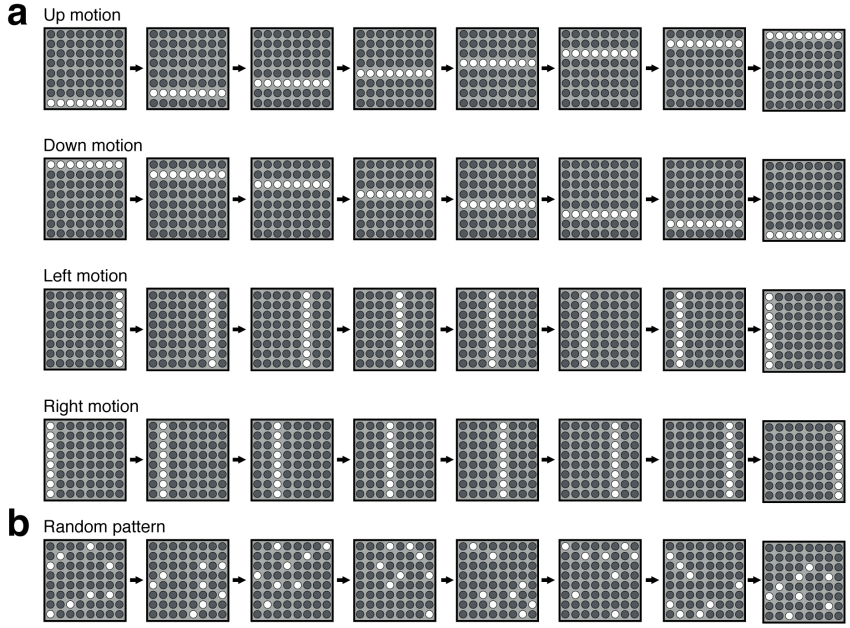

Supplementary Figure 1. Examples of the time course of the tactile stimulation. (a) In the tactile motion stimulation conditions, 8 adjacent white plastic pins forming a line popped up simultaneously for 25 ms and moved in one of four directions (up, down, left, right) to establish the sensation of a linear movement. (b) In the tactile random stimulation, every plastic pin popped up once per stimulation, thus stimulating the entire index fingertip and maintaining the same spatial-temporal features between both stimulation types except the motion feature. In both types of stimulation, one stimulation lasted 200 ms and stimulations were repeated for a given number of times depending on the duration of the continued detection of slow waves.

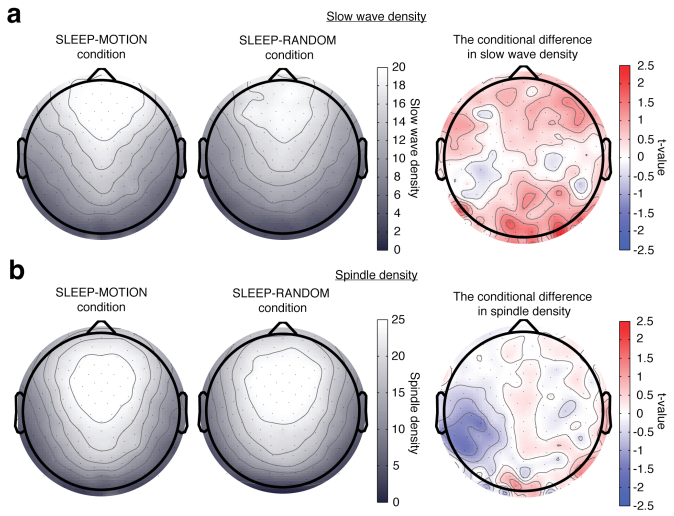

Supplementary Figure 2. Spatial distribution of slow wave density and spindle density during sleep stage N3 in the SLEEP-MOTION condition (left side) and SLEEP-RANDOM condition (middle side), and the difference between conditions (right side). Both slow waves (a) and spindles (b) were detected with a preference for the frontal region. Although no significant clusters were found to show differences between conditions after 10^4 iterations during a cluster-based permutation test ($P < 0.05$, cluster size corrected), the area overlying the left somatosensory region showed a tendency for lower slow wave density and spindle density in the SLEEP-MOTION condition than in the SLEEP-RANDOM condition. The found region overlapped with the region that showed the significant correlation between the stage N3 slow wave density and the cross-sleep sensitivity improvement in the opposite tactile stimulation direction (**Figure 3c**) and the region that showed the relative decrease in the differences of the absolute power spectrum between tactile motion and random stimulation (**Supplementary Figure 7**).

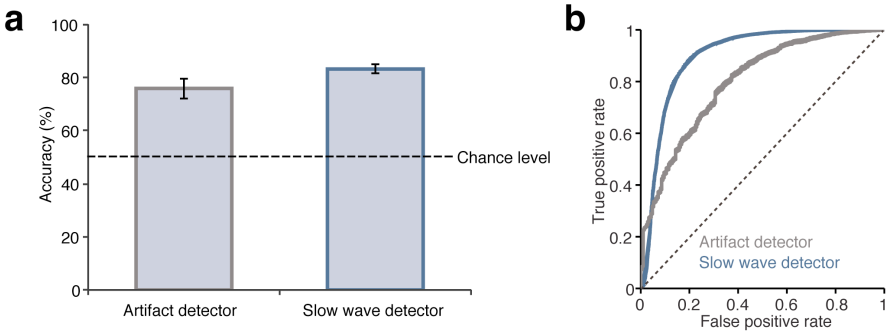

Supplementary Figure 3. Performance of the artifact and slow wave detectors. (a) The leave-one-subject-out cross-validation confirmed that the artifact detector successfully classified EEG epochs as artifact and normal EEG above chance level ($t_{11} = 6.80$, $P < 10^{-4}$, one-sample t test), and the slow wave detector classified EEG epochs as slow wave activity (SWA) or no slow wave activity (No-SWA) above chance level ($t_{11} = 20.66$, $P < 10^{-9}$, one-sample t test). Chance level is 50%. Error bars denote SEM. (b) The area under the curve (AUC) calculated by the receiver operating characteristic (ROC) curve with the cross-validation of each detector confirmed that both detectors had sufficient accuracies (AUC of the artifact detector = 0.82 ± 0.0059 (mean ± SEM), AUC of the slow wave detector = 0.90 ± 0.0011). The dotted line denotes the baseline.

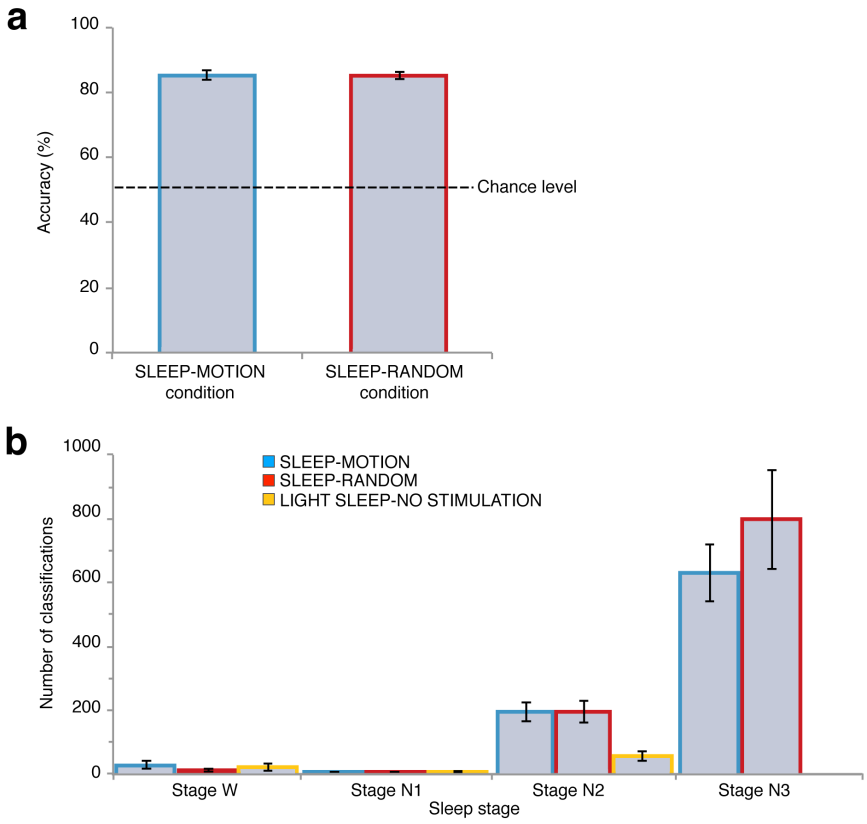

Supplementary Figure 4. Offline analyses of the slow wave detector in the different conditions and across sleep stages. (a) The performance of the slow wave detector confirmed that the detector successfully classified EEG epochs as SWA or No-SWA above chance level (SLEEP-MOTION: $t_{13} = 23.70$, $P < 10^{-11}$; SLEEP-RANDOM: $t_{13} = 34.48$, $P < 10^{-13}$, one-sample t test). Chance level is 50%. Error bars denote SEM. (b) Number of EEG epochs classified as slow wave activity by the slow wave detector in the SLEEP-MOTION condition, SLEEP-RANDOM condition, and LIGHT SLEEP-NO STIMULATION condition. The result verified that the slow wave detector succeeded in detecting slow wave activities and allowed for selective timing of tactile stimulation during stage N3 sleep. Post-hoc verification indicated that the classification results in stage N2 were derived from the transition period between stage N2 and N3, while the results in stage W were derived from the sudden waking epochs immediately after stage N3.

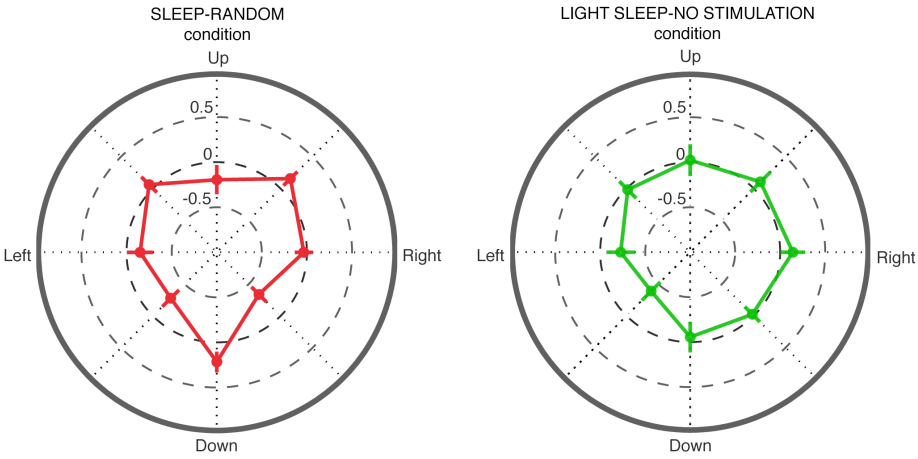

Supplementary Figure 5. Sensitivity changes in SLEEP-RANDOM and LIGHT SLEEP-NO STIMULATION conditions. No significant differences in the sensitivity change were found in any of the eight directions of either condition (all $t_{13} < 1.77$, $P > 0.05$, one-sample t test, Holm-Bonferroni correction for multiple comparisons). The radial axis plots sensitivity change as the change in d'. The red dashed circle denotes zero improvement in sensitivity change. Error bar denotes SEM.

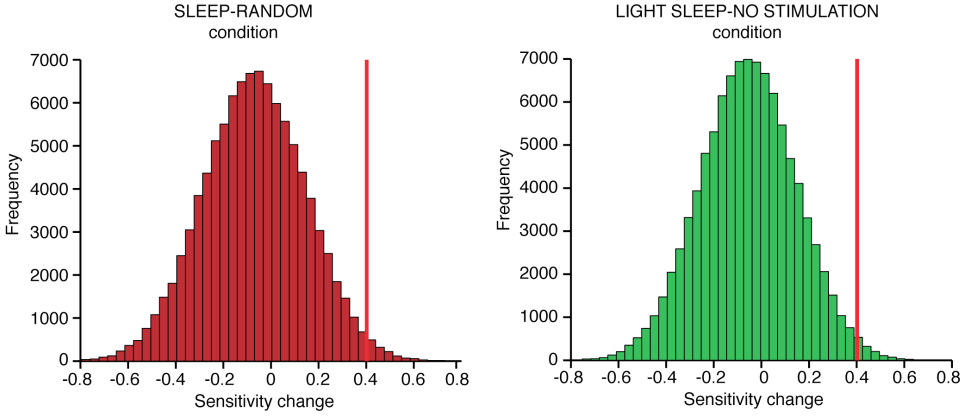

Supplementary Figure 6. Results of the permutation analysis in SLEEP-RANDOM and LIGHT SLEEP-NO STIMULATION conditions. The results showed that approximately 99% of the randomized data in both conditions fell below the sensitivity change (indicated by the red vertical line) of the opposite direction to the tactile motion stimulation seen in the SLEEP-MOTION condition (SLEEP-RANDOM condition: $P = 0.99$, LIGHT SLEEP-NO STIMULATION condition: $P = 0.99$).

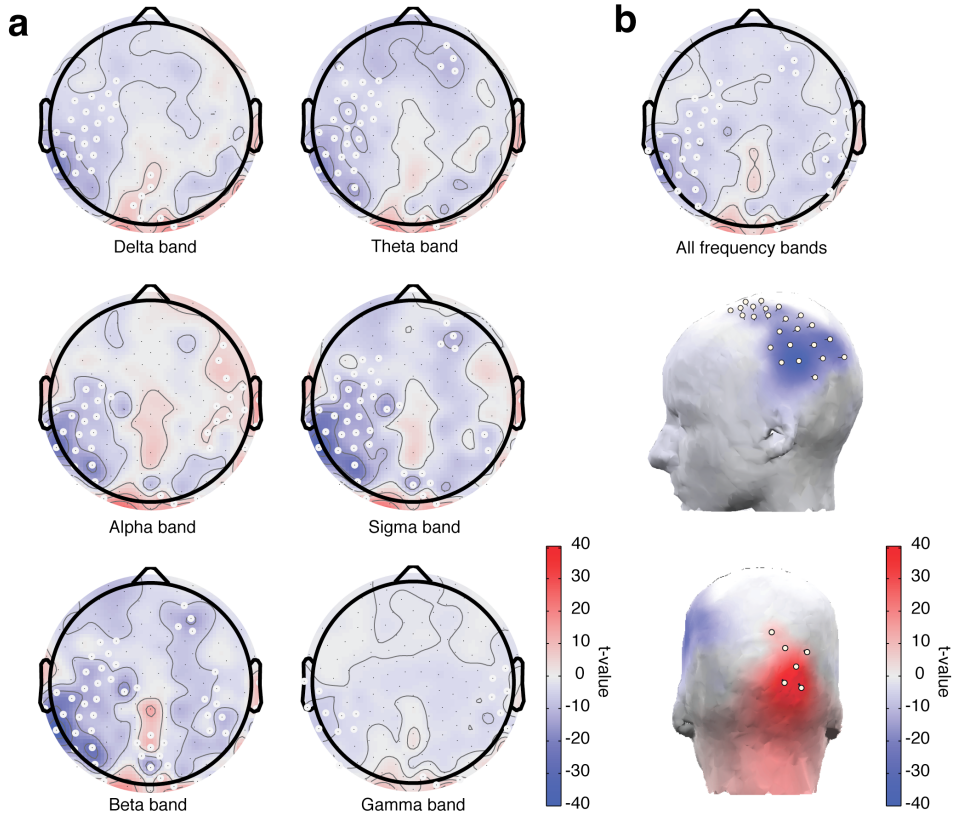

Supplementary Figure 7. Topographic maps of the difference in absolute power between the tactile motion and random stimulation conditions in sleep stage N3. (a) The topographic maps of the absolute power difference between conditions in six frequency bands (Delta: 0.5–4Hz, Theta: 4–8Hz, Alpha: 8–12Hz, Beta: 12–24Hz, Sigma: 8–13Hz, and Gamma: 24–40Hz). (b) The topographic map and 3D head plot in the broad-spectrum (0.5–40Hz) showed that the activations during the tactile motion stimulation were significantly lower in an area overlying the left somatosensory area and higher in an area overlying the visual area, respectively, compared with the tactile random stimulation. White locations demarcate electrodes in a significant cluster after 10^4 iterations of a cluster-based permutation test ($P < 0.05$, cluster size corrected).

Supplementary Table 1. The results of sleep architectures (mean ± SEM).

Experiment 1						
	Stage W (min)	Stage N1 (min)	Stage N2 (min)	Stage N3 (min)	Stage R (min)	Sleep efficiency (%)
1. SLEEP-MOTION	16.9 ± 4.0	8.7 ± 1.5	39.6 ± 2.6	24.0 ± 2.9	0 ± 0	81.3 ± 4.2
2. SLEEP-RANDOM	13.3 ± 3.0	8.0 ± 2.6	36.8 ± 3.8	32.0 ± 4.2	0 ± 0	85.3 ± 3.4
3. LIGHT SLEEP-NO STIMULATION	43.7 ± 7.0	14.8 ± 2.9	30.5 ± 6.9	0 ± 0	0 ± 0	51.0 ± 7.7
P-value (Condition 1 vs 2)	0.4877	0.8155	0.5916	0.1101	N.A.	0.4816
Experiment 2						
	Stage W (min)	Stage N1 (min)	Stage N2 (min)	Stage N3 (min)	Stage R (min)	Sleep efficiency (%)
ALTERED POSTURE	14.1 ± 2.8	6.6 ± 1.5	37.5 ± 3.1	28.4 ± 2.9	0 ± 0	83.6 ± 3.1

Supplementary Table 2. The number of tactile stimulation, and mean inter-stimulus intervals of the tactile stimulations, the motion coherence threshold in the random dot motion task, the surface area of the index fingertip, and the scores of Edinburgh handedness inventory (mean ± SEM).

Experiment 1					
	Number of tactile stimulation	Mean inter-stimulus intervals	Motion coherence threshold (%)	Surface area (mm2)	Hand score (points)
1. SLEEP-MOTION	238.4 ± 49.7	9.4 ± 2.1	7.8 ± 1.6	272.9 ± 11.9	91.0 ± 4.1
2. SLEEP-RANDOM	286.3 ± 73.7	9.8 ± 1.7	4.8 ± 0.6	266.9 ± 12.8	89.8 ± 3.6
3. LIGHT SLEEP-NO STIMULATION	N.A.	N.A.	5.0 ± 0.9	278.1 ± 12.3	86.4 ± 4.9
4. WAKE-MOTION	248.4 ± 3.1	6.2 ± 1.7	5.9 ± 0.9	281.1 ± 12.7	86.6 ± 4.3
P-value (Condition 1 vs 2)	0.41	0.127	0.21	0.86	0.89
Experiment 2					
	Number of tactile stimulation	Mean inter-stimulus intervals	Motion coherence threshold (%)	Surface area (mm2)	Hand score (points)
ALTERED POSTURE	131.2 ± 36.7	8.7 ± 1.9	10.4 ± 1.6	264.1 ± 5.1	83.8 ± 6.3

Supplementary Table 3. The reports of sleep mentation.

Experiment 1		
	ID	Summary of sleep mentation
SLEEP-MOTION	58	I was looking inside an empty paper box while two Asian people were looking at me. I was thinking why I was looking at an empty paper box and who these people were.
	99	I was in the sleep laboratory and I had some secrets to keep from other participants.
	139	I was thinking about the ticket to the Netherland for my grandmother's future birthday present.
	144	I was driving a car.
	181	I had two weird dreams; I was with younger brother and a sheep drawn in a painting bit me, and an experimenter removed my EEG cap easily.
	392	I saw several dreams about holidays, friends, and my school.
	* Eight participants did not see nor remember any dream contents.	
SLEEP-RANDOM	157	I was a holiday in a country where there were only girls in a mountainous region. We had do some sort of competition of rolling down a hill.
	216	I dreamed about going back to my home country.
	250	I saw flashes of different scenes.
	280	I had some conversations about several topics of yesterday's work with my girlfriend.
	289	I was thinking about how to make myself fall asleep in my dream.
	342	I dreamed about my work though I didn't remember the detail.
	* Eight participants did not see nor remember any dream contents.	
LIGHT SLEEP-NO STIMULATION	230	I dreamed that I struggled with sleep and then a scientist came to the room and said to start the experiment again. I wanted but failed to run away.
	303	I stayed with other people in a similar room of the sleep laboratory.
	365	A girl friend and I took a picture at the hospital. We were also watching the children who got cancer and danced with songs.
	366	I saw that giant spiders were coming out of peaches.
	* Ten participants did not see nor remember any dream contents.	
Experiment 2		
	ID	Summary of sleep mentation
ALTERED POSTURE	523	I was in a free market and two Spanish men sell a extremely expensive thing that was actually cheap.
	582	Wake up after too early and left the department.
	565	Dream about going back to Lesotho, African county, talking with friends.
	576	In the dream, someone was fighting and the subject observed and joined in it.
	577	Walking somewhere and lost in the way, and need to find Chinese person.
	* Nine participants did not see nor remember any dream contents.	

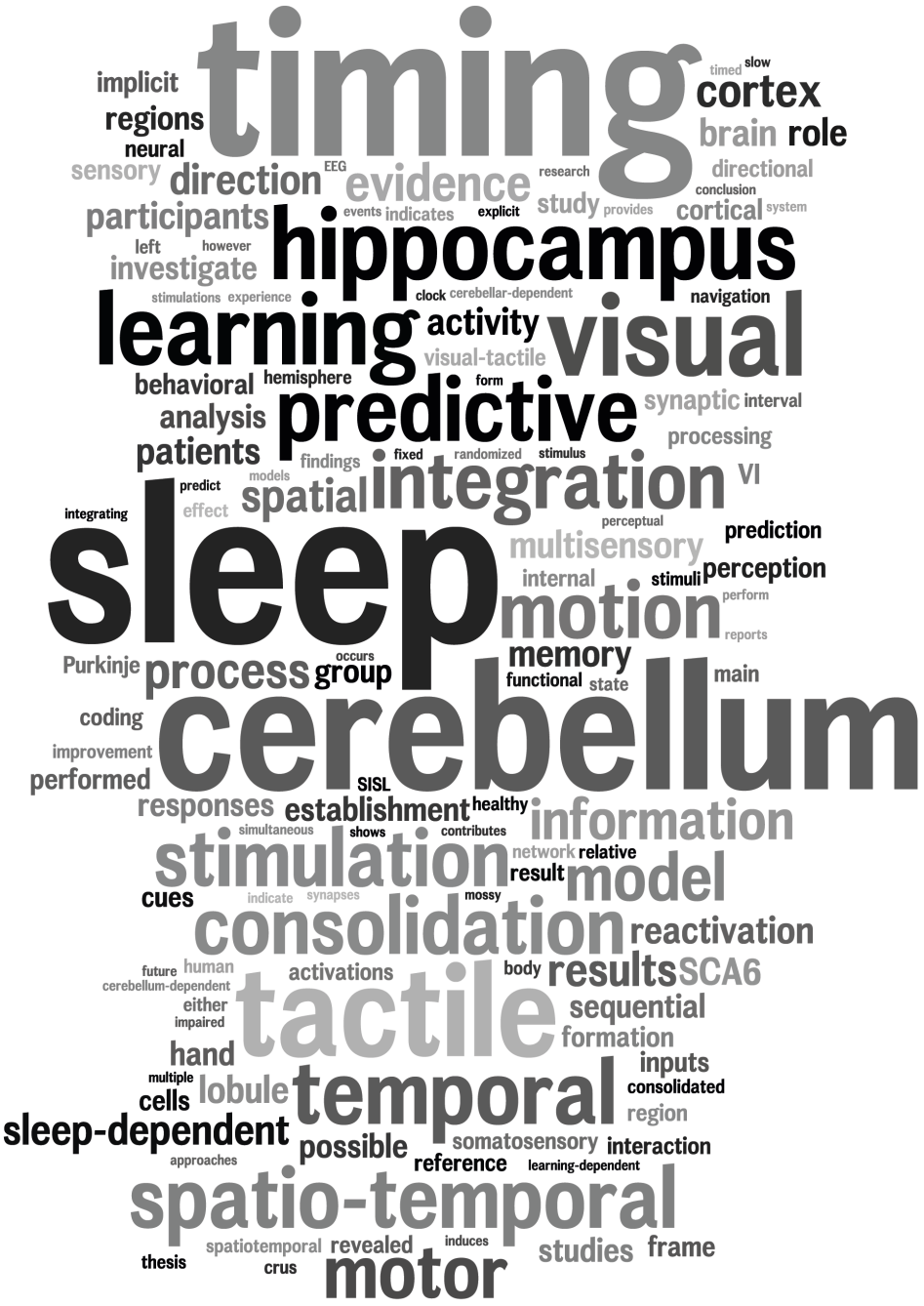
timing
implicit
regions
neural
sensory
direction
EEG
evidence
research
timed
slow
cortex
brain
role
directional
conclusion
participants
events
indicates
explicit
study
provides
cortical
system
left
however
investigate
hippocampus
stimulations
experience
clock
cerebellar-dependent
navigation
learning
activity
visual
visual-tactile
behavioral
hemisphere
form
predictive
synaptic
interval
analysis
processing
patients
findings
fixed
randomized
stimulus
models
predict
integration
VI
integrating
effect
spatial
perceptual
prediction
sleep
multisensory
perception
internal
stimuli
motion
perform
reports
Purkinje
process
occurs
group
memory
functional
state
main
coding
cerebellum
improvement
performed
SISL
responses
establishment
healthy
information
simultaneous
shows
contributes
network
relative
stimulation
result
model
cues
indicate
synapses
mossy
consolidation
reactivation
future
human
activations
body
results
SCA6
cerebellum-dependent
tactile
either
impaired
sequential
formation
hand
inputs
multiple
lobule
temporal
consolidated
cells
region
sleep-dependent
possible
somatosensory
interaction
approaches
reference
learning-dependent
spatio-temporal
spatiotemporal
revealed
induces
studies
frame
thesis
crus
motor

Chapter 6. General discussion

6.1 Overview of the thesis

The central aim of this thesis was to investigate the sleep contribution to the consolidation process of spatial-temporal and multisensory integration, in relation to the human cerebellum. Multiple experimental approaches were used to answer research questions addressed in the various chapters.

6.2 Summary of the main fidnings

Chapter 2: The cerebellum interacts with the hippocampus during the establishment of spatio-temporal predictive timing

In **Chapter 2**, we investigate the neural representation of the establishment of spatio-temporal prediction. Sixteen right-handed subjects who did not have rhythmic exercise experience such as music and games performed the task inside the MRI scanner. To elucidate the brain activity related to space-time estimation, motor coordination, and mental rehearsal, the various forms of the SISL task that require timed motor responses following the visual motion cues were employed. Performance on the task demonstrated that all participants developed responses that were approximate 50-millisecond early to, i.e. predictive of, the stimuli on the screen in the course of the task. This indicates the establishment of learning-dependent predictive timing. Furthermore, the main effect analysis of fMRI data to examine brain activations that reflected the spatiotemporal prediction, motor coordination, and mental rehearsal showed that both left hippocampus and cerebellar lobule VI activated specifically during spatiotemporal estimation. Furthermore, to investigate whether the activities of the left hippocampus and cerebellar activity are synchronized, the functional connectivity between the cerebellum and hippocampus was calculated by using psychophysiological interaction (PPI) analysis with the activity of the left hippocampus as a seed region. This revealed hipocampal co-activations of bilateral lobule VI, the right hemisphere of the lobule VIIa crus I, and the left hemisphere of lobule VIIIb. Of note, the

cerebellum lobule VI is the region that overlapped in both the main effect analysis and the functional connectivity analysis. In brief, our study revealed that the spatio-temporal predictive timing of motor executions based on visual motion cues induces synchronized activations of the cerebellum and hippocampus.

Chapter 3: The cerebellar impairment induces the failure in the establishment of the spatio-temporal predictive timing

In **Chapter 3**, we investigated the causal role of the cerebellum on the formation of the spatio-temporal predictive timing by assessing SCA6 patients with a version of the same task. A total of 12 SCA6 patients and 12 healthy volunteers performed four types of the modified SISL task. In the experiment, participants performed the task that consisted of either fixed or randomized stimulus sequences with two different temporal interval between stimuli each, for a 2-by-2 factorial design. Behavioral analysis on the predictive timing showed that SCA 6 patients had significantly impaired predictive timing responses, i.e. the early responses, during the spatio-temporal predictive timing task. From this result, it was concluded that the capabilty for spatio-temporal prediction is severely compromised due to the SCA6 syndrome. Performance on the Reactive timing task revealed that both SCA6 patients and healthy controls showed the capacity to perform the required motor coordination for the button presses, ruling out a trivial motor-related explanation for the deficits on the predictive timing task. Rather, the results indicate that SCA6 patients failed to learn and predict the sequential timing of responses with the aid of visual cues. Together, these results suggest that the impaired cerebellar architecture induces the failure of the establishment of the temporal processing, which supports the hypothesis that the cerebellum plays a causal role in the estalibhsment of spatio-temporal predictive timing.

Chapter 4: Enhancement of spatio-temporal processing by sleep

In order to investigate the role of sleep on the consolidation of spatio-temporal integration, we conducted a sleep experiment. A total of 42 participants was assigned to either the sleep condition or the awake condition. Participants performed the SISL task with conditions of either a fixed or random temporal order of stimuli before and after taking 90-minute nap or staying awake. As a result, a significant behavioral improvement was seen only in the sleep group, especially in the sequential temporal interval condition. It indicates that sequential temporal learning is consolidated during sleep. No EEG features of sleep such as spindle and slow wave density in NREM stage 2 and 3, however, showed a correlation with the degree of the behavioral improvement in the sleep group. This results indicate that sleep facilitates the learning of sequential timed motor responses. These results suggest that the learning of a cerebellar-dependent timing process shows sleep-dependent consolidation.

Chapter 5: New formation of the cross-modal integration during sleep

Sleep-dependent consolidation has been successfully shown for associative learning, i.e. events paired during pre-sleep learning. In addition, our brain is capable of cross-modal perception by integrating multiple types of sensory information without learning. It is not known whether such integration can actually take place during sleep and impinge on sleep-dependent consolidation. In this study, we employed visual and tactile stimulations, modialities to which the cerebellum is sensitive. In total, 42 participates were assigned into four conditions: one group perceived a directional tactile stimulation during sleep, the second group perceived a randomized tactile stimulation during sleep, the third group did not receive any tactile stimulation during sleep, and the fourth group underwent directional tactile stimulation during the wake state. All groups performed a visual psychophysical task to investigate the sensitivity to visual motion before and after sleep. Improvement of visual motion perception in the direction

opposite to the tactile stimulus direction was confirmed only in the sleep group that had received tactile motion stimulation. This result suggests that tactile stimulation is integrated with the visual motion learning consolidation process during sleep, possibly in the form of a visual-tactile motion after-effect[1].

In tactile information, it was known that multiple references frame such as the position of the hand, head, and body including a surroding environment determine the direction of tactile motion sensation. As an additional experiment to the previous experiment that assessed the body reference frame driving this phenomenon, we recruited 14 additional participants and let them stretch their arm sideways during sleep. During sleep, we presented tactile stimulation along the length of the fingertip, i.e. upward direction relative to the hand reference frame but rightward relative to the head reference frame. The results show that the sensitivity to vertical visual motion sensation was improved after the sleep. In summary, visual-tactile integration occurs during sleep anchored to the hand reference frame.

The role of the cerebellum in the formation of the spatial-temporal timing

This thesis aimed to examine possible sleep-dependent consolidation in the cerebellar-depedent spatial-temporal integration. At first, we attempted to validate a cerebellar-involvement in the spatio-temporal predictive timing. **Chapter 2** provides the behavioral evidence that participants integrated spatial and temporal information to establish predictive timing, i.e., a tendency to press the button 50-milliseconds prior to the timing of visual cues, in parallel to learning of the sequential motor responses. The fMRI main effect analysis during the spatio-temporal predictive timing condition revealed bilateral activations within the cerebellum lobule VI during learning of predictive timing. The activated regions partially match the cerebellar regions found in the previous studies in the sensory-motor timing and temporal perceptual judgement tasks[2–5], with the differences presumably deriving from the type of the timing, being

either explicit or implicit. Explicit timing tasks demand participants to use temporal information as a primary source for the generation and judgement of temporal intervals, a procedure called "explicit timing"[6]. In our task, however, the timing information is a secondary product derived from visual motion cues, which is called implicit timing, demanding the integration of spatial and temporal information.

Using the same motor timing task of **Chapter 2**, detailed behavioral analysis in **Chapter 3** confirmed that SCA6 patients display impaired learning of both predictive and reactive timing, compared with healthy controls. SCA6 is characterized by cerebellar cortex degeneration and atrophy of the dentate nucleus[7]. The Purkinje cells are selectively degenerated and the width of the molecular layer is decreased due to the disappearance of the Purkinje cell dendrites in the cerebellar cortex of SCA6 patients. Pathological evidence fits with earlier findings that LTD of the Purkinje cells in the cerebellar hemisphere is essential for the formation of the learning-dependent timing[8].

Chapter 2 also provides evidence that the cerebellar hemispheres of lobule VI, VII crus I, and VIIIb synchronize its activity with the hippocampus, during the establishment of the spatiotemporal estimation. In recent years, it is becoming evident that the cerebellum performs both temporal and spatial processing, cooperating functionally with hippocampus whose memory formation properties highly depend on sleep. For temporal coding, several studies support a cerebellar-hippocampal cooperation in controlling temporal aspects of learning-dependent motor output such as trace conditioning[8–12] and cued fear conditioning[13,14]. Examples of spatial coding include spatial navigation and adaptation of goal-oriented behavior[15,16]. Interestingly, the inhibition of the protein kinase C-dependent plasticity at the Purkinje cell impairs spatial coding of place cells only in the condition demanding self-centered navigation (spatiotemporal memory). Furthermore, lateralized regions within hippocampus and cerebellum interact during sequential route-based navigation and map-based navigation in humans[17].

Several theoretical models propose a possible functional role of the cerebellum and hippocampus for the establishment of predictive motor timing. For example, one theoretical model proposes that the cerebellum works as a timer to represent a temporal interval in a sub-second range, and the cortical and subcortical regions such as the basal ganglia and frontal lobe keep track of the supra-second time by adding up the cerebellar sub-second outputs[18]. Another example is that neural circuits of the hippocampus may modulate attention to cues, while the timing circuit (internal clock) of the olivocerebellar system may control timing of motor planning and execution[19,20]. The hippocampal clock may thus cooperate with the cerebellar clock and its forward modeling[21], i.e., the internal model of motor timing, to learn the interval between the moving markers and the timing of motor execution and to predict the upcoming perceptual events. The latter model fits to the recent research observation; the patient with the cerebellar degenerative disease and focal lesion failed to recalibrate their prediction from the consequences of perceptual events, which indicates that the cerebellum functions to optimize the internal model of spatio-temporal prediction[22].

In the cerebellar network, the motor and sensory inputs from the cerebral cortex and subcortical regions project onto the granule cells of the cerebellar cortex through the mossy fibers. The signals of the mossy fibers are transmitted to the cerebellar nucleus via the Purkinje cells. The cerebellar nuclei in turn synthesize and transfer inputs to the cerebral cortex. From existing experimental evidence, theoretical considerations and our results in **Chapter 2** and **3**, a possible conceptual model can be built, stating that the hippocampus contributes to establishing spatio-temporal prediction by integrating complex motor execution and specific timing onsets in a network of several brain regions responsible for appropriate and timed output. It does so with the aid of the cerebellum hemisphere lobule VI, VII crus I, and VIII that contribute to optimize the intrinsic cerebellar computational model called the "internal model"[23], integrating spatial and temporal information and transmitting the signal to the hippocampus through the dentate nucleus.

Consolidation of the cerebellum-dependent spatio-temporal timing

To investigate whether cerebellum-dependent learning of spatio-temporal predictive timing is sensitive to the effects of sleep, similar to other types of learning, **Chapter 4** describes an experiment using the novel task from **Chapters 2** and **3** in a controlled sleep-study. Previous studies have shown that learning of explicit timing in auditory-paced motor timing is also sleep-dependent and that post-sleep cerebellar activations during the task are increased, compared with pre-sleep activation[24]. **Chapter 4** provides the first evidence on sleep-dependent consolidation of implicit timing. Furthermore, none of the participants in **Chapter 4** reported recognizing the difference in the fixed and randomized temporal sequences during their performances on the SISL task. Verbal reports support our notion that the temporal learning in our study was formed in the form of "implicit learning". Multiple studies have pointed out that implicit learning is an offline consolidation, i.e., spending time (with or without sleep) is essential for its consolidation[25,26]. This line of evidence, however, leaves room for doubt. One study suggests that implicit timing can be consolidated in a sleep-dependent fashion when the hippocampus is involved in the learning process[27]. Since **Chapter 2** clarified that the cerebellum interacts with the hippocampus during spatio-temporal predictive timing, and **Chapter 3** indicates that the cerebellum is a crucial region to establish the integration, the results obtained in **Chapter 4** lead to the conclusion that cerebellum-dependent learning of timing is consolidated by sleep, with the possible support of the hippocampus. A study of simultaneous EEG-fMRI during sleep supports this concept, i.e., the cerebellar-hippocampal activations evoked by stimulation during sleep positively correlated with the degree of the post-sleep memory retrieval[28]. Since only hippocampal activation during memory retrieval is observed in this study, a bidirectional interaction between the hippocampus and cerebellum may underlie sleep-dependent consolidation process in both hippocampal- and cerebellar-dependent learning.

Altogether, the cerebellum plays a critical role in the learning process of sequential timing through the spatial and temporal integration, which can be consolidated during sleep due to possible interactions with the hippocampus.

Multisensory integration during sleep: a role for the cerebellum?

As our aim was to investigate whether multisensory integration can in fact be established during sleep, we devised an experiment that attempted to modify the process of sleep-dependent consolidation of a visual detection task, by applying directionally selective stimulation during sleep. Crucially, this approach is not a targeted memory reactivation approach, as that would simply strengthen the consolidation process. Rather, the tactile stimuli administered during sleep were designed to modulate the consolidation process by biasing the performance in a particular direction.

Our results show that such a bias indeed occurred, seen as an improvement of visual perception in the opposite direction to the tactile motion stimulus direction. This result shows that visual-tactile integration happens during sleep. The mechanism of the cross-sleep directional facilitation of visual motion sensitivity fits with two current models: the reactivation model[29,30] and the synaptic homeostasis model[31–33]. In the reactivation model, the recurrence of the experience-specific neural activity patterns during sleep is thought to strengthen synaptic plasticity of the cortical system. The reactivation that occurs during the ongoing slow-wave sleep would in the present paradigm be biased towards the counterphase direction, as the tactile stimulation timelocked to the slow waves would cause a directional imbalance due to repeated stimulation that activates direction-sensitive neurons. The synaptic homeostasis model predicts that all synapses, including those used for the task performance during wakefulness, are “down-scaled”, with a relative sparing of the connections that were enhanced by the task. According to this theory, the relative synaptic sparing would occur preferentially for the synapses representing the counterphase direction, as these retain higher synaptic weight due to the ongoing and repeated stimulation, more than

synapses coding for other directions or not coding for task-related activity at all. Our findings agree with both models of sleep-dependent memory consolidation and necessitate future research to examine the synaptic activity of motion-sensitive neurons caused by the tactile motion stimulation during slow wave sleep.

Although in **Chapter 5** we could not determine which brain structures were crucially involved in the multisensory integration, due to the poor spatial resolution of the scalp EEG recording, we speculate that the cerebellum may be exquisitely suited to mediate the integration of tactile and visual information during sleep. We describe our reasoning in the below.

The cortical regions that predominately process visual and tactile information connect to the cerebellum. In the visual domain, the signal transmission in the visual motion network located in MT/MST (human MT+) receives the motion-selective inputs from the V1[34] and transmits this information to the cerebellum through the pons[35,36]. In the tactile domain, the primary somatosensory cortex (S1), the main region for tactile processing, also connects to the cerebellum via pons[37]. It is supported by the finding of electric stimulation in the somatosensory cortex (S1) evoking cerebellar cortical activation[38].

The cerebellum takes a role to integrate multiple sensory inputs and outputs. Recent evidence shows that the granule cells in crus I and II and paraflocculus in the cerebellar cortex received multimodal inputs through individual mossy fibers[39]. In addition, functional evidence from both human and non-human primate studies suggest that the cerebellum processes not only unimodal visual and tactile information[40–43], but also processes visual-tactile multisensory integration, i.e., the simultaneous perception of hand visual stimulation and hand tactile sensation[44], simultaneous visual and tactile motion discrimination[45], and the modulation of the proprioception by visual-tactile multisensory signals[46,47]. Notably, all these experiments were performed in the waking state, and it remains to be seen whether during sleep the cerebellum is still in a position to perform such integration.

The cerebellum acts to predict sensory outcome and to decrease somatosensory cortical activity in case of the predicted sensory stimulation[48]. The result can explain our findings in **Chapter 5** of decreased EEG power on the scalp overlying the somatosensory cortex during the tactile motion stimulations comparing with that during the random stimulations. It also may reflect the recalibration of the internal model of the visual motion perception from tactile sensory inputs[22,49–51].

In conclusion, we believe that converging past evidence in combination with our findings in **Chapter 5**, can be understood in the light of a possible contribution of the cerebellum to the tactile stimulation-induced directional bias in the visual detection skill acquired before sleep. In our working model, the cerebellum may synthesize direction-imbalanced inputs from the MT, MST, and somatosensory cortex to recalibrate the perceptive model for visual motion processing.

6.3 Conclusions and future perspectives

Through **Chapter 1-5**, we provide behavioral and neural evidence of spatio-temporal and multisensory integration with a particular emphasis on the cerebellum. The central conclusion of this thesis is that sleep contributes to cerebellar-dependent memory formation and the sleeping brain can form the new multisensory interaction that the cerebellum may cooperate with.

Yet, the studies described here represent only a first step and several follow-up studies will need to shed light on the neural mechanisms of this integration, and the possible contribution of the cerebellum in relation to other brain areas. For instance, we observed an interaction between cerebellum and hippocampus. Although it is known that the task-related reactivation occurs in the hippocampus when sleeping, may there be the reactivation in the cerebellum? In addition, does the synchronization of hippocampal and cerebellar reactivation exist? Together, as a future perspective, the EEG-fMRI recording for healthy participants, and the ECoG and depth electrodes in

patients with a clinical reason for invasive surgery such as detecting an epileptic focus and treating dystonia and ataxia[52–55] are ideal approaches to discover the synchronized reactivation of the cerebellum and hippocampus during post-task sleep period, which may positively correlate with the improvement of the temporal learning. Furthremore, such multimodal approaches can provide more beneficial supportive evidence of our interpretation from the results in **Chapter 5,** i.e., the adaptation effect on the cortical region and the cerebro-cerebellar network during the tactile stimulation in the sleep phase.

In addition, the behavioral results of the experiment 2 in **Chapter 5** indicate that the preprioceptive system contributes to the consolidation process. It was revealed that the position of the hand during sleep becomes the dominant reference frame, although the head and spatial coordinations may be dominant in the waking state, depending on the posture condition. Interestingly, the human brain is able to perform the intrinsic encoding of bodily sensations during sleep, and possibly of the dreaming experience, parallelling the physical bodily state. Although **Chapter 5** reports the dream contents after the repetitive tactile stimulation during sleep, we did not see common features about body information such as hand and posture movements in those dream reports. However, since the learning-related dreaming experience may boost the memory consolidation[56], it will become a highly interesting topic of investigation whether multisensory consolidation may arise from the aspect of the physical and dreamed body information.

References

1. Konkle, T., Wang, Q., Hayward, V. & Moore, C. I. Motion Aftereffects Transfer between Touch and Vision. *Current Biology* **19,** 745–750 (2009).
2. Bares, M. *et al.* Impaired predictive motor timing in patients with cerebellar disorders. *Experimental brain research* **180,** 355–65 (2007).
3. Bares, M. *et al.* The Neural Substrate of Predictive Motor Timing in Spinocerebellar Ataxia. *The Cerebellum* **10,** 233–244 (2011).
4. Aso, K., Hanakawa, T., Aso, T. & Fukuyama, H. Cerebro-cerebellar interactions underlying temporal information processing. *Journal of Cognitive Neuroscience* **22,** 2913–2925 (2010).
5. Spencer, R. M. C. & Ivry, R. B. in *Handbook of the Cerebellum and Cerebellar Disorders* (eds. Manto, M., Schmahmann, J. D., Rossi, F., Gruol, D. L. & Koibuchi, N.) 1201–1219 (Springer Netherlands, 2013).
6. Coull, J. T. & Nobre, A. C. Dissociating explicit timing from temporal expectation with fMRI. *Current Opinion in Neurobiology* **18,** 137–144 (2008).
7. Stefanescu, M. R. *et al.* Structural and functional MRI abnormalities of cerebellar cortex and nuclei in SCA3, SCA6 and Friedreich's ataxia. *Brain* **138,** 1182–1197 (2015).
8. Koekkoek, S. K. E. *et al.* Cerebellar LTD and Learning-Dependent Timing of Conditioned Eyelid Responses. *Science* **301,** 1736–1739 (2003).
9. Takehara, K., Kawahara, S. & Kirino, Y. Time-dependent reorganization of the brain components underlying memory retention in trace eyeblink conditioning. *The Journal of neuroscience : the official journal of the Society for Neuroscience* **23,** 9897–9905 (2003).
10. Hoffmann, L. C. & Berry, S. D. Cerebellar theta oscillations are synchronized during hippocampal theta-contingent trace conditioning. *Proceedings of the National Academy of Sciences of the United States of America* **106,** 21371–6 (2009).
11. Wikgren, J., Nokia, M. S. & Penttonen, M. Hippocampo-cerebellar theta band phase synchrony in rabbits. *Neuroscience* **165,** 1538–1545 (2010).
12. MacDonald, C. J., Lepage, K. Q., Eden, U. T. & Eichenbaum, H. Hippocampal "time cells" bridge the gap in memory for discontiguous events. *Neuron* **71,** 737–749 (2011).
13. Scelfo, B., Sacchetti, B. & Strata, P. Learning-related long-term potentiation of inhibitory synapses in the cerebellar cortex. *Proceedings of the National Academy of Sciences of the United States of America* **105,** 769–774 (2008).
14. Ruediger, S. *et al.* Learning-related feedforward inhibitory connectivity growth required for memory precision. *Nature* **473,** 514–518 (2011).
15. Burguière, E. *et al.* Spatial navigation impairment in mice lacking cerebellar LTD: a motor adaptation deficit? *Nature neuroscience* **8,** 1292–1294 (2005).
16. Rochefort, C. *et al.* Cerebellum Shapes Hippocampal Spatial Code. *Science* **311,** 385–390 (2011).
17. Iglói, K. *et al.* Interaction between hippocampus and cerebellum crus i in sequence-based but not place-based navigation. *Cerebral Cortex* **25,** 4146–4154 (2015).
18. Meck, W. H. Neuropharmacology of timing and time perception. *Cognitive Brain Research* **3,** 227–242 (1996).
19. Grossberg, S. & Merrill, J. W. L. The hippocampus and cerebellum in adaptively timed learning, recognition, and movement. *Journal of Cognitive Neuroscience* **8,** 257–277 (1996).
20. De Zeeuw, C. I. *et al.* Spatiotemporal firing patterns in the cerebellum. *Nature reviews. Neuroscience* **12,** 327–44 (2011).
21. Wolpert, D. M., Miall, R. C. & Kawato, M. Internal models in the cerebellum. *Trends in Cognitive Sciences* **2,** 338–347 (1998).
22. Roth, M. J., Synofzik, M. & Lindner, A. The cerebellum optimizes perceptual predictions about external sensory events. *Current Biology* **23,** 930–935 (2013).
23. Ito, M. Control of mental activities by internal models in the cerebellum. *Nature reviews neuroscience* **9,** 304–313 (2008).
24. Lewis, P. A., Couch, T. J. & Walker, M. P. Keeping time in your sleep: Overnight consolidation of temporal rhythm. *Neuropsychologia* **49,** 115–123 (2011).
25. Robertson, E. M., Pascual-Leone, A. & Press, D. Z. Awareness Modifies the Skill-Learning Benefits of Sleep. *Current Biology* **14,** 208–212 (2004).

26. Born, J. & Wagner, U. Awareness in memory: Being explicit about the role of sleep. *Trends in Cognitive Sciences* **8,** 242–244 (2004).
27. Spencer, R. M. C., Sunm, M. & Ivry, R. B. Sleep-Dependent Consolidation of Contextual Learning. *Current Biology* **16,** 1001–1005 (2006).
28. van Dongen, E. V. *et al.* Memory stabilization with targeted reactivation during human slow-wave sleep. *Proceedings of the National Academy of Sciences of the United States of America* **109,** 10575–10580 (2012).
29. Hasselmo, M. E. Neuromodulation: Acetylcholine and memory consolidation. *Trends in Cognitive Sciences* **3,** 351–359 (1999).
30. Oudiette, D. & Paller, K. A. Upgrading the sleeping brain with targeted memory reactivation. *Trends in Cognitive Sciences* **17,** 142–149 (2013).
31. Tononi, G. & Cirelli, C. Sleep function and synaptic homeostasis. *Sleep Medicine Reviews* **10,** 49–62 (2006).
32. Nere, A., Hashmi, A., Cirelli, C. & Tononi, G. Sleep-dependent synaptic down-selection (I): modeling the benefits of sleep on memory consolidation and integration. *Frontiers in neurology* **4,** 143 (2013).
33. Tononi, G. & Cirelli, C. Sleep and the Price of Plasticity: From Synaptic and Cellular Homeostasis to Memory Consolidation and Integration. *Neuron* **81,** 12–34 (2014).
34. Tootell, R. B. *et al.* Functional analysis of human MT and related visual cortical areas using magnetic resonance imaging. *The Journal of neuroscience : the official journal of the Society for Neuroscience* **15,** 3215–30 (1995).
35. Brodal, P. Further observations on the cerebellar projections from the pontine nuclei and the nucleus reticularis tegmenti pontis in the rhesus monkey. *Journal of Comparative Neurology* **204,** 44–55 (1982).
36. Distler, C. & Hoffmann, K. P. Cortical input to the nucleus of the optic tract and dorsal terminal nucleus (NOT-DTN) in macaques: a retrograde tracing study. *Cerebral cortex (New York, N.Y. : 1991)* **11,** 572–80 (2001).
37. Schmahmann, J. D. From movement to thought: Anatomic substrates of the cerebellar contribution to cognitive processing. *Human Brain Mapping* **4,** 174–198 (1996).
38. Matsui, T. *et al.* fMRI Activity in the Macaque Cerebellum Evoked by Intracortical Microstimulation of the Primary Somatosensory Cortex: Evidence for Polysynaptic Propagation. *PLoS ONE* **7,** (2012).
39. Ishikawa, T., Shimuta, M. & Häusser, M. Multimodal sensory integration in single cerebellar granule cells in vivo. *eLife* **4,** 1–10 (2015).
40. Händel, B., Thier, P. & Haarmeier, T. Visual motion perception deficits due to cerebellar lesions are paralleled by specific changes in cerebro-cortical activity. *The Journal of Neuroscience : the official journal of the Society for Neuroscience* **29,** 15126–15133 (2009).
41. Hagen, M. C. *et al.* Tactile motion activates the human middle temporal/V5 (MT/V5) complex. *European Journal of Neuroscience* **16,** 957–964 (2002).
42. Wacker, E., Spitzer, B., Lützkendorf, R., Bernarding, J. & Blankenburg, F. Tactile motion and pattern processing assessed with high-field fmRi. *PLoS ONE* **6,** (2011).
43. Van Kemenade, B. M. *et al.* Tactile and visual motion direction processing in hMT+/V5. *NeuroImage* **84,** 420–427 (2014).
44. Gentile, G., Petkova, V. I. & Ehrsson, H. H. Integration of visual and tactile signals from the hand in the human brain: an FMRI study. *Journal of Neurophysiology* **105,** 910–922 (2011).
45. Nakashita, S. *et al.* Tactile-visual integration in the posterior parietal cortex: A functional magnetic resonance imaging study. *Brain Research Bulletin* **75,** 513–525 (2008).
46. Ehrsson, H. H. That's My Hand! Activity in Premotor Cortex Reflects Feeling of Ownership of a Limb. *Science* **305,** 875–877 (2004).
47. Ehrsson, H. H. Touching a Rubber Hand: Feeling of Body Ownership Is Associated with Activity in Multisensory Brain Areas. *Journal of Neuroscience* **25,** 10564–10573 (2005).
48. Blakemore, S.-J., Wolpert, D. M. & Frith, C. D. The Cerebellum Contributes to Somatosensory Cortical Activity during Self-Produced Tactile Stimulation. *NeuroImage* **10,** 448–459 (1999).
49. Imamizu, H. *et al.* Human cerebellar activity reflecting an acquired internal model of a new tool. *Nature* **403,** 192–195 (2000).
50. Imamizu, H., Kuroda, T., Miyauchi, S., Yoshioka, T. & Kawato, M. Modular organization of internal models of tools in the human cerebellum. *Proceedings of the National Academy of Sciences of the United States of America* **100,** 5461–6 (2003).

51. Imamizu, H., Kawato, M. & Imamizu, H. Cerebellar internal models: Implications for the dexterous use of tools. in *Cerebellum* **11,** 325–335 (2012).
52. Teixeira, M. J. & Galhardoni, R. Deep brain stimulation of the dentate nucleus improves cerebellar ataxia after cerebellar stroke Clinical / Scientific Notes. (2015). doi:10.1212/WNL.0000000000002204
53. Kros, L., Rooda, O. H. J. E., Zeeuw, C. I. De & Hoebeek, F. E. Controlling Cerebellar Output to Treat Refractory Epilepsy. *Trends in Neurosciences* **38,** 787–799 (2015).
54. Dalal, S. S., Osipova, D., Bertrand, O. & Jerbi, K. Oscillatory activity of the human cerebellum: The intracranial electrocerebellogram revisited. *Neuroscience and Biobehavioral Reviews* **37,** 585–593 (2013).
55. Niedermeyer, E. & Uematsu, S. Electroencephalographic recordings from deep cerebellar structures in patients with uncontrolled epileptic seizures. *Electroencephalography and Clinical Neurophysiology* **37,** 355–365 (1974).
56. Wamsley, E. J., Tucker, M., Payne, J. D., Benavides, J. A. & Stickgold, R. Dreaming of a Learning Task Is Associated with Enhanced Sleep-Dependent Memory Consolidation. *Current Biology* **20,** 850–855 (2010).

List of abbreviations

BOLD	Blood oxygen level dependent
EEG	Electroencephalography
EMG	Electromyography
EOG	Electrooculography
LFP	Local field potential
fMRI	Functional magnetic resonance imaging
FWE	Family-wise error rate
NREM	Non-rapid eye movement
REM	Rapid eye movement
PCA	Principle component analysis
RBD	REM sleep behavior disorder
ROI	Region of interest
rTMS	Repetitive transcranial magnetic stimulation
SARA	Assessment and rating of ataxia
SCA6	Cerebellar ataxia type 6
SISL	Serial interception sequential learning
SMA	Supplementary motor area
SWS	Slow wave sleep

Summary

Does the cerebellum sleep? If so, does sleep contribute to cerebellar cognition? In this thesis, the sleep contribution to the consolidation process of spatial-temporal and multisensory integration was investigated in relation to the human cerebellum. Multiple experimental approaches were used to answer research questions addressed in the various chapters. Summarizing the evidence of the electrophysiology and neuroimaging studies, in Chapter 1 we present intriguing evidence that the cerebellum is involved in sleep physiology, and that cerebellar-dependent memory formation can be consolidated during sleep. In Chapter 2, using functional neuroimaging in healthy participants during various forms of the Serial interception sequential learning (SISL) task, i.e., predictive timing, motor coordination, and motor imagination, we assessed the cerebellar involvement in spatio-temporal predictive timing; and possible cerebellar interactions with other regions, most notably the hippocampus. In Chapter 3, we add to the findings of Chapter 2 that indicate the cerebellum and hippocampus are involved in the task, by showing that more than simply activated, the cerebellum is a necessary and responsible region for the establishment of the spatio-temporal prediction. This follows from the deficits in behavioral properties of the predictive and reactive timing in the cerebellar ataxia type 6 patients, using the modified version of the SISL task. In Chapter 4, we assessed the subsequent post-interval behavioral performances on the learning of the fixed and random timing sequences in the SISL task, comparing a sleep group and wake group in healthy participants. Our findings show that sleep consolidates the process of cerebellar-dependent spatio-temporal integration. In Chapter 5, we investigated the establishment of visual-tactile integration during sleep through the examination of tactile motion stimulation during sleep and showed that, subsequent to sleep, directional visual motion discrimination is biased depending on the direction of the stimulation during sleep. This effectively shows that sleep offers a window for crossmodal integration. In Chapter 6, we discussed the main findings on the consolidation of the cerebellum-dependent spatio-temporal timing and the new formation of the multisensory integration during sleep, in addition to the description of the methodological considerations and future perspectives.

Samenvating

Slaap het cerebellum? En indien ja, draagt de slaap dan bij aan cerebellaire cognitie? In dit proefschrift werd de slaapbijdrage aan het consolidatieproces van ruimtelijk-temporele en multisensorische integratie onderzocht in relatie tot het cerebellum in de mens. Verschillende experimentele benaderingen werden gebruikt om onderzoeksvragen te beantwoorden die in de verschillende hoofdstukken aan de orde kwamen. Hoofdstuk 1 vat het bewijs samen van elektrofysiologische en neuroimaging studies, resulterend in de intrigerende gedachte dat de kleine hersenen in de slaapfysiologie betrokken zijn, en dat cerebellair-afhankelijke geheugenprocessen tijdens de slaap geconsolideerd kunnen worden. In Hoofdstuk 2 hebben we met behulp van functionele neuroimaging bij gezonde deelnemers tijdens verschillende vormen van de Serial interception sequential learning (SISL) taak, d.w.z. timing van gedrag, motorcoördinatie en motor verbeelding, de betrokkenheid van het cerebellum in spatio-temporele voorspellende timing onderzocht; en mogelijke cerebellaire interacties met andere regio's, met name de hippocampus. In hoofdstuk 3 voegen we aan de bevindingen van hoofdstuk 2 die aangeven dat de kleine hersenen en de hippocampus bij de taak betrokken zijn, toe dat meer dan alleen geactiveerd het cerebellum een noodzakelijke en verantwoordelijke regio is voor het vaststellen van de spatio-temporele voorspelling. Dit volgt uit de tekortkomingen in gedragseigenschappen van de voorspellende en reactieve timing in de cerebellaire ataxie type 6-patiënten, met behulp van de gewijzigde versie van de SISL-taak. In hoofdstuk 4 hebben we de prestaties onderzocht bi na eeninterval volgend op het leren van de vaste en willekeurige timingsequenties in de SISL-taak, waarbij een slaapgroep en een wakkere groep gezonde deelnemers werden vergeleken. Onze bevindingen laten zien dat slaap het cerebellaire afhankelijke proces van spatio-temporele integratie consolideert. In Hoofdstuk 5 hebben we visuele-tactiele integratie tijdens de slaap onderzocht door het onderzoeken van tactiele bewegingsstimulatie tijdens de slaap en hebben we laten zien dat, na slaap, visuele bewegingsdiscriminatie in een bepaalde richting kan worden gestuurd, afhankelijk van de richting van de stimulatie tijdens de slaap. Dit toont aan dat slaap een venster biedt voor crossmodale integratie. In

hoofdstuk 6 bespraken we de belangrijkste bevindingen over de consolidatie van de cerebellum-afhankelijke spatio-temporele timing en de nieuwe vorming van de multisensorische integratie tijdens de slaap, naast de beschrijving van de methodologische overwegingen en het toekomstperspectief.

Curriculum vitae

Yoshiyuki Onuki was born on the 19th of October 1984 in Saitama prefecture, Japan. After he graduated from the Honjo East High School, he started to study psychology from 2003 at the Oklahoma State University, U.S. Under the supervision of Dr. Charles I. Abramson. From 2003 to 2007, he dedicated himself to study the history of psychology and comparative psychology. After he earned Psychology degree (B.S.), he entered the Nara Institute of Science and Technology, Japan. In 2010, he finished his master thesis titled as "The estimation of awake-sleep state using behavioral and physiological indices." In 2011, he was employed as Ph.D. student at the Netherlands Institute of Neuroscience (NIN). His projects were a part of the funded project called "the procedural memory formation during sleep" supervised by Prof. Chris I. De Zeeuw, Prof. Eus. J.W. Van Someren, and Dr. Ysbrand D. Van der Werf. First, he belonged to the Sleep and Cognition group where Prof. Eus. Van Someren worked as the department head and Dr. Van der Werf as a senior researcher. When Dr. Van der Werf became the department head of the Emotion and Cognition group from 2013, his affiliation was changed as well. After his employment contract was finished at the NIN, he has worked as a research resident from 2015 at Jichi Medical University, Japan. In the university, he has conducted multiple research projects: the multimodal analysis of the human hippocampus activity with fMRI and ECoG for the epileptic patients, the gene therapy for aromatic L-amino acid decarboxylase deficiency, and the deep brain stimulation on the subthalamic nucleus for the Parkinson's patients. Additionally, he performed the cognitive evaluation tests to pre-surgical patients with epilepsy, stroke, and brain tumors by analyzing the data of fMRI, functional near-infrared spectroscopy, and diffusion tensor imaging.

Academic certificates

2010 Master of Engineering
Field of Study: Computational neuroscience
Institution: Nara Institute of Science and Technology, Nara, Japan

2007 Bachelor of Science, Psychology
Field of Study: Comparative Psychology and History of Psychology
Institution: Oklahoma State University, Oklahoma, United States

Previous positions & affiliations

2016-2018 Research resident, Department of Neurosurgery, Jichi Medical University, Tochigi, Japan

2015-2016 Research resident, Functional Brain Laboratory, Jichi Medical University, Tochigi, Japan

2013-2015 PhD student, Emotion and Cognition Group, the Netherlands Institute for Neurosciences, Amsterdam, the Netherlands

2011-2013 PhD student, Sleep and Cognition Group, the Netherlands Institute for Neurosciences, Amsterdam, the Netherlands

2008-2010 Master student, Theoretical Life Science Laboratory, Graduate School of Information Science, Department of Bioinformatics and Genomics, Nara Institute of Science and Technology, Nara, Japan

2008-2010 Student intern, Department of Neuroinfomatics, Advanced Telecommunication Research Institute, Kyoto, Japan

2003-2007 Research assistant, Laboratory of Comparative Psychology and Behavioural Sciences

Relevant courses and training

2014 ABC advanced neuroimaing curriculum: pattern analysis and classification, organized by Amsterdam Brain and Cognition, Amsterdam, The Netherlands.

2013 Tool-kit of cognitive neurosciene: advanced topics in MR imaging of the brain, organized by Donders Institute in Nijmegen, the Netherlands.

2012 FreeSurfer tutorial and workshop organized by Department of Radiology, VU University Medical Center and MGH Martinos Center for Biomedical Imaging, Amsterdam, The Netherlands.

2011 A practical and theoretical introduction into FMRI: 3-days course on Statistical Parametric Mapping (SPM) organized by the Rudolf Magnus Institute of Neuroscience /University Medical Center Utrecht and Helmholz Institute/Utrecht University.

2011 Tool-kit of cognitive neuroscience: 5-days course on essentials of major neuroimaging techniques (EEG, MEG, fMRI, PET, TMS) organized by Donders Institute in Nijmegen, the Netherlands.

2011 The eight BCI2000 workshop: 2-day course on using a software system for brain-computer interface research (BCI2000) organized by Rudolf Magnus Institute for Neuroscience and the BCI 2000 project, Utrecht, The Netherlands.

Publications

Canto, C. B*., Onuki, Y*., Bruinsma, B., Van der Werf, Y. D., & De Zeeuw, C. I. (2017). The Sleeping Cerebellum. *Trends in Neurosciences, 40*(5),309-323.

Broersen, R., Onuki, Y., Abdelgabar, A. R., Owens, C. B., Picard, S., Willems, J., Boele H-J., Gazzola V., Van der Werf, Y. D., & De Zeeuw, C. I. (2016). Impaired spatio-temporal predictive motor timing associated with spinocerebellar ataxia type 6. *PLOS one*, *11*(8), e0162042.

Verweij, I. M*., Onuki, Y*., Van Someren, E. J., & Van der Werf, Y. D. (2016). Sleep to the beat: A nap favours consolidation of timing. *Behavioral neuroscience*, *130*(3), 298.

Onuki, Y., Van Someren, E. J., De Zeeuw, C. I., & Van der Werf, Y. D. (2013). Hippocampal–cerebellar interaction during spatio-temporal prediction. *Cerebral cortex*, *25*(2), 313-321.

Onuki, Y., & Abramson, C.I. (2004). The process of creating the website "The Guide to the History of Japanese Psychology," advantage and problems to introduce the history on the Internet. *History of Psychology and Psychological Studies*, 6, 33-43.

Onuki, Y., Lakbila-Kamal, O., Scheffer, B., Van Someren, E. J. W., & Van der Werf, Y. D. (2018). Tactile sensation during sleep biased the enhancement of visual learning. In Submission.

Onuki,Y., De Zeeuw, C.I., & Van der Werf, Y. D. (2018). Keeping track of time: hippocampal activations during temporal estimation. In Preparation.

Onuki, Y., Ono, S., Nakajima, T., Kojima, K., Kato, M., Miyauchi, A., Taga, N., Osaka, J., Hirai, M., Sato, T., Kawai, K., Muramatsu, S., & Yamagata, T. (2018). Gene therapy for aromatic L-amino acid decarboxylase deficiency induces the longitudinal gene expression and structural development in the adolescent brain. In Submission.

Miyata, S., Tominaga K., Sakashita, E., Urabe, M., Onuki, Y., Gomi, A., Yamaguchi, T., Mizukami, H., Kume, A., Ozawa, K., Watanabe, E., Kawai, K., & Endo, H. (2018). Comprehensive metabolomic analysis of *IDH1*^{R132H} clinical glioma samples reveals suppression of β-oxidation due to carnitine deficiency. Under Review.

* These authors contributed equally.

Acknowledgements

During the period that I worked as a Ph.D. Student at the Netherlands Institute for Neuroscience (NIN), countless people supported my research projects and daily life directly and indirectly in the Netherlands. Without their sincere and heartwarming supports, it was impossible to finalize this thesis. I sincerely express my gratitude to some people who deserve special mention for making this thesis come true.

First, I would like to thank my supervisors, **Ysbrand**, **Eus**, and **Chris**. This thesis could not be achieved without their energetic and inspirable supervisions.

Ysbrand, I do not know how to express my appreciation to you. Your decision to employ me changed my life dramatically into something over what I dreamed about. I learned a lot from your project management skills and kind attitude toward your colleagues. I could not finalize without your continued warm support even after I left the NIN. I am missing the time that we sat together in front of our desk and had the discussion about our results.

Eus, I really appreciate your warm welcome to your laboratory. You provided me with innumerable opportunities and your insightful advice to achieve my research projects that were published in this thesis. What I learned and experienced during my sleep research in your laboratory is the wealth of my career as a sleep neuroscientist.

Chris, it is my pleasure and great fortune to work with you. Your feedbacks based on your profound insights and knowledge about the cerebellum and related subjects always encouraged me to challenge technical and scientific difficulties in my research project. You are my role model as a brilliant neuroscientist, and your support has been invaluable in my career.

I also would like to express my deep appreciation to the Members of the Thesis Committee for spending your precious time and energy to review this thesis. I am very honored by your presence at my Ph.D. defense.

I consider myself fortunate to conduct research with brilliant colleagues in the extraordinal scientific environment at NIN. **Ilse**, it was a lot of fun to be able to bring out research results together. I enjoyed a lot of our chats during lunchtimes. Please also say hello to your children! **Frank**, I always enjoy our conversations about our interests (spacecraft and funny Japanese topics). Best wishes for your success in the Ph.D. program at Austria! **Johan**, (polite bowing) thank you so much for always having a good time. It was a pleasant memory for me to participate in the simultaneous EEG-fMRI experiment. **Jennifer**, I'm grateful for your countless support and beneficial advice in my sleep research. I could not manage my research projects without your devoted assistance. Thank you very much! **Giovanni**, thank you very much for discussing my research and other scientific topics. Your sincere attitude to science and talented analytical skills is a great example to me. **German**, I really appreciate your technical assistance in the server maintenance and EEG preprocessing analysis. **Diederick**, thank you very much for your help in the server maintenance and analysis of structural and functional MRI data. **Jeroen**, thank you for your heartwarming birthday party and Christmas mails! Your tasty tomato soup is one of my favorites. **Sarah**, I learned a lot from your creditable efforts to the statistics. Best wishes for your career ahead. **Rebecca**, I would like to thank you for the kind and welcoming thoughts with Giovanni, Sarah, Ilse when I first joined in the Sleep and Cognition group. **Nico**, you are the person who has the talent to brighten the surroundings in the laboratory. Thank you very much! **Filippo**, I'm missing your warm greeting with your smile and powerful handshakes. I never forget your dedicated attitude to science. **Rick**, I still remember your admirable efforts to develop your device by trial and error late into the night. I wish your successful career in Australia. **Michele**, I really appreciate your advice for EEG analysis on the sleep data. Thank you very much! **Yvon**, I learn a lot from your attitude of kindness to patients, which served as my best reference on how to communicate with patients. **Yi-Shu**, thanks for your advice about the EEG data analysis. Good luck with your thesis. **Jacob**, your fluent Japanese skills made me feel like being in Japan. Thanks a lot! **Marco**, it was really fun time to be your colleague during your stay. **Fantastic team Bakiwi (Bart, Kim, Wisse)**, thank you so much for always welcoming me. I am grateful that I could work in an amicable workplace. I really appreciate your heart-touching friendship even I left the NIN. When I stay

in Japan, your birthday email really encouraged me to finalize my thesis. Doumo Arigatou! For the research assistance, I would like to thank **Anne**, **Inger**, **Verena**, **Oti**, **Bo, Yvonne**, **Sophie**, and **Konstantinos** who joined in and helping our projects as intern students. I also would like to thank **Joris** for his effort to create the MR-compatible tactile device. Without their remarkable cooperation, I could not make progress in many research projects. I hope all of you enjoyed my souvenir cookies imported from Japan.

I also would like to express my gratitude to **Robin** and **Cathrin** in De Zeeuw group. Robin and Cathrin, it was my enjoyable time to write manuscripts, communicating with you via email and Skype beyond the time difference between the Netherlands and Japan. I could not achieve this thesis without your great contributions. Furthermore, I really appreciate your presences as my paranymph and opponent in my Ph.D. defense.

I thank **Christian** and **Valeria** for their helpful comments on our start-up project and SCA6 project. Also, I am excited to collaborate with you on our ECoG projects. I'm really looking forward to making our achievements.

My special thanks go to **Heidi**, **Ernita**, **Bart**, and **Marcia** for supporting my daily life and research activities in the Netherlands, accompanying heartwarming smiles.

I also would like to thank my friends for their cheering support and sharing me with their scientific interests. It was really a fortune that I got acquited with **Atsuko**, **Makiko**, and **Tomoko** in the Netherlands. Thank you very much for having fun times in Nijmegen and providing helpful comments on my research. It was my unforgettable experience shared with **Takashi**, **Chisato**, and **Manabu** for having dinners in Amsterdam and Utrecht and taking a trip to Norway together. I'm looking forward to our future collaboration in clinical neuroimaging research. **Yumi** and **Daniel**, I am super lucky to have good friends who love video games, dinner, and drinks together! Your house is a place for relaxation and refreshment in my research life. You are the best comrade who survive many virtual

battlefields together, Daniel. I appreciate your kindness for accepting my offer to be my paranymph with an immediate reply, Yumi.

Many thanks to **colleagues in the Functional Brain Laboratory, the Department of Neurosurgery, and the Division of Neurology at Jichi Medical University**. I appreciate having opportunities to involve in advanced clinical research projects such as the electrocorticography in epilepsy patients, the deep brain stimulation to Parkinson's disease patients, and the gene therapy to children with AADC deficiency.

Finally, I'm grateful to **my family**, **relatives**, and **Charmy** for their heartwarming and encouraging supports.